

Supporting Information for

Voltage imaging with a NIR-absorbing phosphine oxide rhodamine voltage reporter

Monica A. Gonzalez,^{*,†} Alison S. Walker,^{*,††} Kevin J. Cao,[§] Julia R. Lazzari-Dean,[‡] Nicholas S. Settineri,[‡] Eui Ju Kong,[‡] Richard H. Kramer,^{§†} and Evan W. Miller^{†§†*}

Departments of [†]Chemistry and [§]Molecular & Cell Biology and [‡]Helen Wills Neuroscience Institute. University of California, Berkeley, California 94720, United States.

DOI: **10.1021/jacs.0c11382**

Contents

Contents	1
Supplementary Figures and Tables.	4
Table S1. Tabulated Spectroscopic Properties of poRhoVR and poRhodamine isomers	4
Figure S1. Chemical characterization of isomers of phosphine oxide rhodamine dyes.	4
Figure S2. Quantification of poRhoVR brightness in HEK cells.	5
Figure S3. Absorption/Emission Spectra and Voltage sensitivity of poRhoVR dyes.....	6
Figure S4. Voltage imaging in dissociated hippocampal neurons with poRhoVR 13.....	7
Figure S5. Quantification of brightness, voltage sensitivity and signal to noise of poRhoVR 13 and 14 in neurons	8
Figure S6. Photostability comparison between poRhoVR 14 and BeRST.	9
Figure S7. Internalization of poRhoVR 14 in HEK293T cells.	10
Figure S8. Toxicity of poRhoVR 14 in HEK 293T cells.	12
Figure S9. All-optical electrophysiology using poRhoVR 14 and ChR2.	14
Figure S10. Compatibility of poRhoVR 14 with OGB Ca ²⁺ imaging in rat hippocampal neurons...	15
Figure S11. Quantification of evoked activity in neurons using poRhoVR 14 and Oregon Green BAPTA	16
Figure S12. Characterization of cellular uptake of poRhoVR (14).....	17
Figure S13. poRhodamine 9- <i>cis</i> does not display photobleaching under prolonged illumination.	18
Figure S14. Spatial evolution of voltage signals in <i>rd1</i> mouse retina, monitored by poRhoVR	19
Supporting Information Methods	20
HEK293T cell culture information	20
Preparation of primary neuron cultures.....	20
General Imaging Parameters	20
Image Analysis	20
Table S2. Concentration of poRhoVR used in experiments	26
Photophysical Characterization.....	27
General Synthesis and Characterization Information	27
Scheme S1. Synthesis of sulfonated phosphine-oxide rhodamines and rhodamine voltage reporters (poRhoVRs)	30

Synthesis of methyldiphenylphosphine oxide, 2:	30
Synthesis of methylbis(3-nitrophenyl)phosphine oxide, 3:.....	31
Synthesis of bis(3-aminophenyl)(methyl)phosphine oxide, 4:	31
Synthesis of bis(3-(diethylamino)phenyl)(methyl)phosphine oxide, 5:	31
Synthesis of m-bromo tetraethylphosphorous rhodamine (mBrTEPR), 8:	32
Synthesis of p-bromo tetraethylphosphorous rhodamine (pBrTEPR), 9:	33
Synthesis of 12:.....	34
Synthesis of 13:.....	35
Synthesis of 14:.....	36
Synthesis of 15:.....	37
Supplemental Spectra.....	39
Spectrum S1. ¹ H NMR methyldiphenylphosphine oxide, 2.....	39
Spectrum S2. ¹ H NMR methylbis(3-nitrophenyl)phosphine oxide, 3	40
Spectrum S3. ¹ H NMR bis(3-aminophenyl)(methyl)phosphine oxide, 4	41
Spectrum S4. ¹ H NMR bis(3-(diethylamino)phenyl)(methyl)phosphine oxide, 5	42
Spectrum S5. ¹ H NMR m-bromosulfo-phosphine oxide rhodamine (cis), 8.....	43
Spectrum S6. ³¹ P NMR m-bromosulfo-phosphine oxide rhodamine (cis), 8	43
Spectrum S7. LC/MS traces m-bromosulfo-phosphine oxide rhodamine (cis), 8.....	43
Spectrum S8. ¹ H NMR m-bromosulfo-phosphine oxide rhodamine (trans), 8	46
Spectrum S9. ³¹ P NMR m-bromosulfo-phosphine oxide rhodamine (trans), 8	46
Spectrum S10. LC/MS traces m-bromosulfo-phosphine oxide rhodamine (trans), 8	47
Spectrum S11. ¹ H NMR p-bromosulfo-phosphine oxide rhodamine (cis), 9.....	48
Spectrum S12. ³¹ P NMR p-bromosulfo-phosphine oxide rhodamine (cis), 9	48
Spectrum S13. LC/MS traces p-bromosulfo-phosphine oxide rhodamine (cis), 9.....	49
Spectrum S14. ¹ H NMR p-bromosulfo-phosphine oxide rhodamine (trans), 9	51
Spectrum S15. ³¹ P NMR p-bromosulfo-phosphine oxide rhodamine (trans), 9.....	51
Spectrum S16. LC/MS traces p-bromosulfo-phosphine oxide rhodamine (trans), 9	52
Spectrum S17. ¹ H NMR poRhoVR (cis), 12.....	54
Spectrum S18. ³¹ P NMR poRhoVR (cis), 12.....	54
Spectrum S19. LC/MS traces poRhoVR (cis), 12.....	55
Spectrum S20. ¹ H NMR poRhoVR (cis), 13.....	57
Spectrum S21. ³¹ P NMR poRhoVR (cis), 13.....	57
Spectrum S22. LC/MS traces poRhoVR (cis), 13.....	58
Spectrum S23. ¹ H NMR poRhoVR (trans), 13	60
Spectrum S24. ³¹ P NMR poRhoVR (trans), 13	60
Spectrum S25. LC/MS traces poRhoVR (trans), 13	61
Spectrum S26. ¹ H NMR poRhoVR (cis), 14.....	63

Spectrum S27. ^{31}P NMR poRhoVR (cis), 14.....	63
Spectrum S28. LC/MS traces poRhoVR (cis), 14.....	64
Spectrum S29. ^1H NMR poRhoVR (cis),15.....	66
Spectrum S30. ^{31}P NMR poRhoVR (cis),15.....	66
Spectrum S31. LC/MS traces poRhoVR (cis),15.....	66

Supplementary Figures and Tables.

Table S1. Tabulated Spectroscopic Properties of poRhoVR and poRhodamine isomers
NMR Chemical Shift (ppm)

	Compound	^{31}P	$^1\text{H}_a$	$^1\text{H}_b$	$^1\text{H}_c$
Major (<i>cis</i>)	9 – <i>cis</i>	20.32	2.01	7.19	7.82
	8 – <i>cis</i>	20.37	2.02	7.48	---
	13 – <i>cis</i>	20.20	2.00	6.25	---
Minor (<i>trans</i>)	9 – <i>trans</i>	18.22	1.95	7.23	7.80
	8 – <i>trans</i>	18.39	1.97	7.55	---
	13 – <i>trans</i>	18.21	2.01	6.26	---

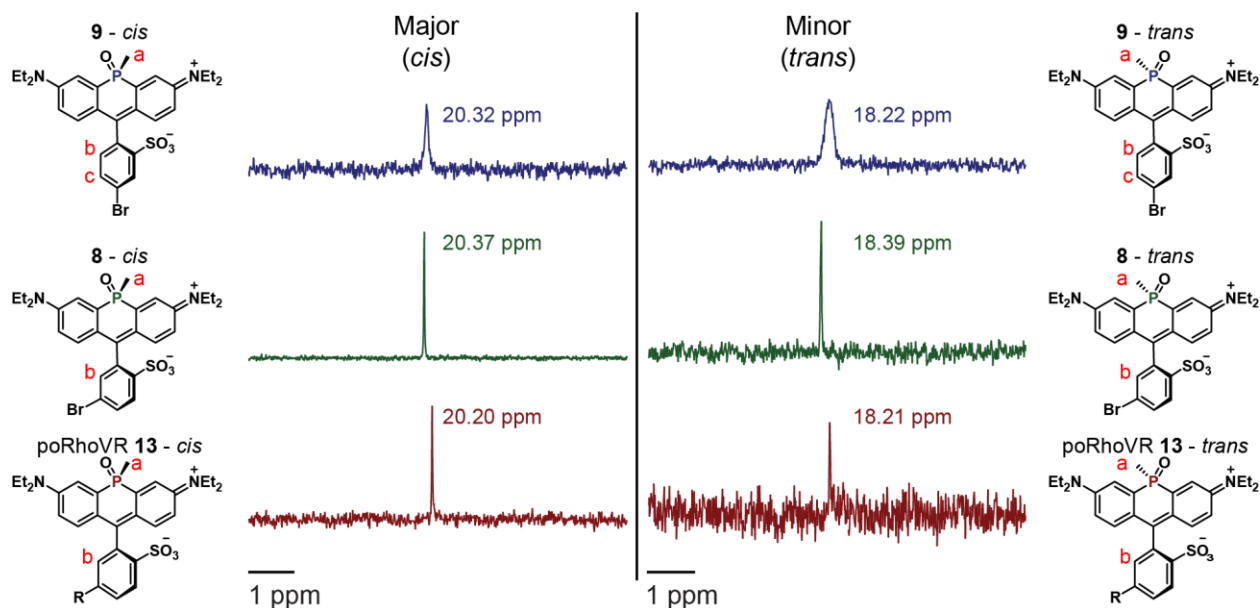


Figure S1. Chemical characterization of isomers of phosphine oxide rhodamine dyes.
(center) Decoupled ^{31}P spectra the *trans*- and *cis*- isomers of po-rhodamines **8** and **9** and for poRhoVR **13**.
(sides) Proposed structures of **8**, **9**, and **13**. The structure of **8** – *cis* and **9** – *cis* were confirmed by x-ray crystallography (**Figure 1b** and **c**). The structure of the major isomer of **13** is assumed to be the *cis* isomer, based on similarities in the ^{31}P NMR. ^1H labels on the structures (a, b, and c) refer to the indicated chemical shifts in **Table S1**.

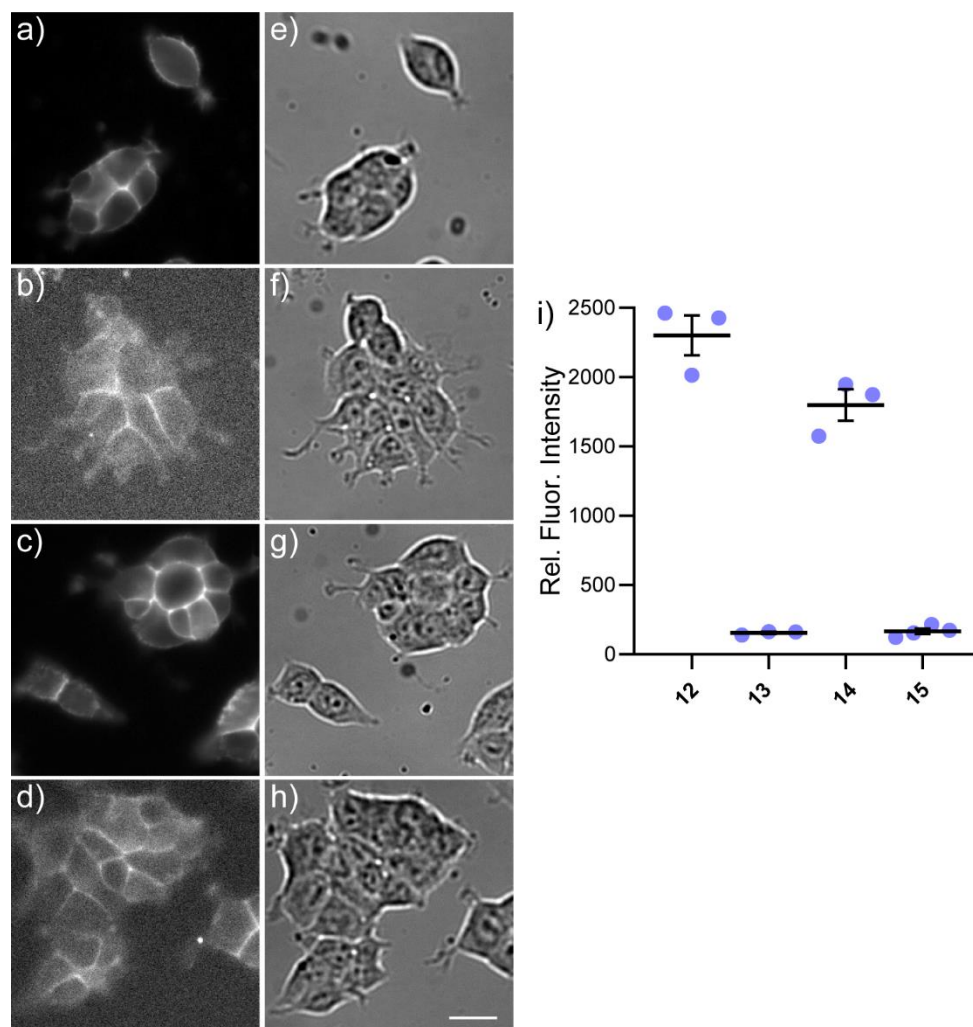


Figure S2. Quantification of poRhoVR brightness in HEK cells.

(a-d) Widefield epifluorescence images and (e-h) differential interference contrast (DIC) images of poRhoVR indicators in HEK cells (2 μ M); a,e) poRhoVR 12, b,f) poRhoVR 13, c,g) poRhoVR 14, and d,h) poRhoVR 15. Scale bar for (a-h) is 20 μ m. i) Plot of fluorescence intensity of HEK cells stained with 2 μ M poRhoVR dyes (12 – 15). Bars represent mean fluorescence intensity for n = 3 independent coverslips of HEK cells. The average value for a coverslip of HEK cells stained with poRhoVR is shown as a blue dot. Each coverslip contained 30 to 60 individual cells/regions of interest (ROIs) that were used to determine the mean fluorescence. Error bars depict standard deviation (n = 3).

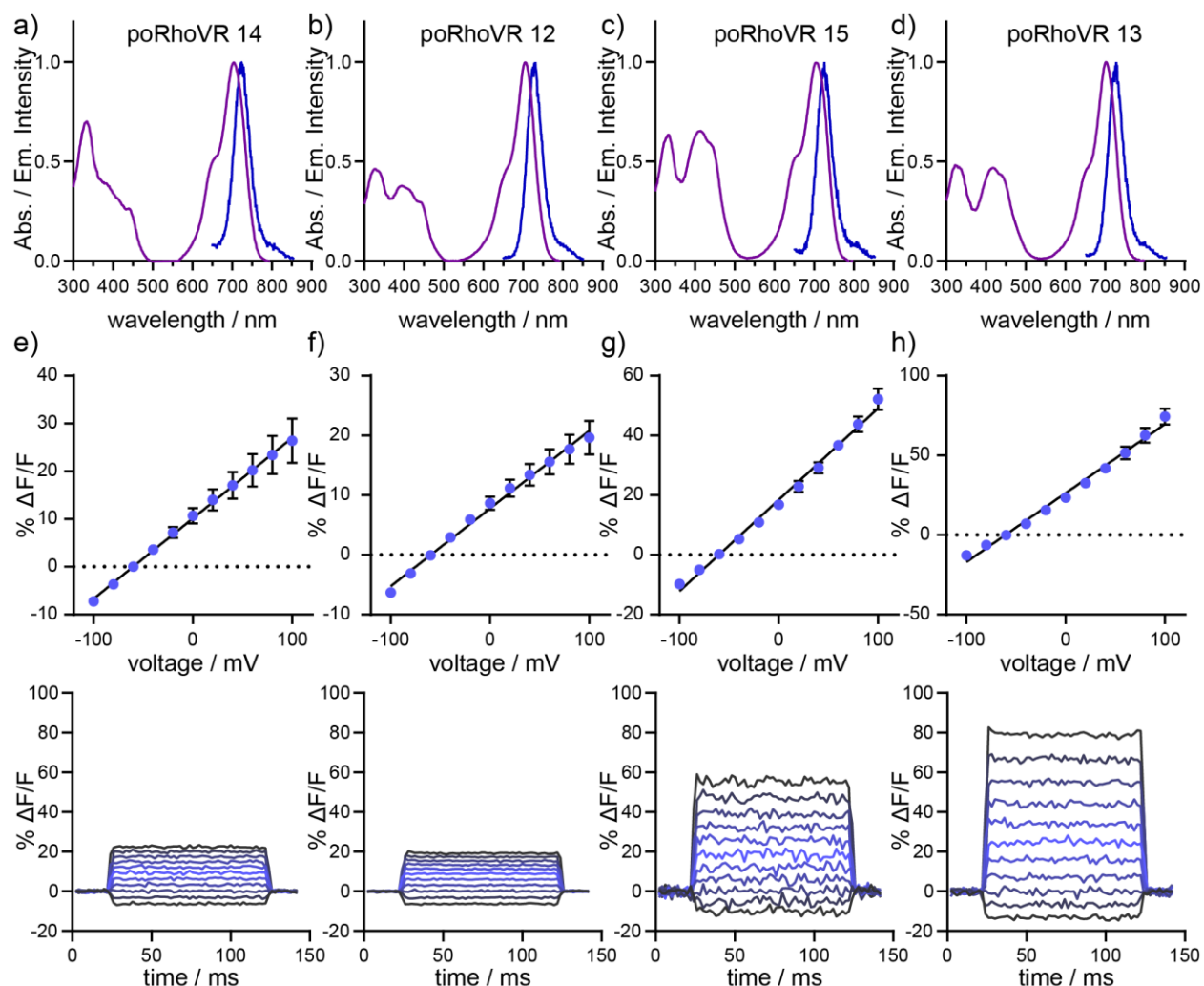


Figure S3. Absorption/Emission Spectra and Voltage sensitivity of poRhoVR dyes.

Plot of normalized absorption (purple) and emission (blue) for poRhoVR dyes **a) 14**, **b) 12**, **c) 15**, and **d) 13**. Spectra were acquired at 1 μM (0.1 % DMSO) in PBS buffer. For emission spectrum, excitation was provided at 625 nm. Voltage sensitivity plots for poRhoVR dyes **e) 14**, **f) 12**, **g) 15**, and **h) 13**. Upper row depicts plots of $\Delta F/F$ vs. final membrane potential (mV) in HEK cells loaded with 1 μM poRhoVR dye and subjected to whole-cell voltage-clamp conditions. Error bars represent standard deviation for $n = 6, 5, 5,$ and 4 cells, respectively. Lower row depicts plots of $\Delta F/F$ (%) vs time for HEK cells loaded with 1 μM poRhoVR and held at -60 mV under whole-cell voltage-clamp and stepped to hyper- and depolarizing potentials in increments of 20 mV (± 100 mV).

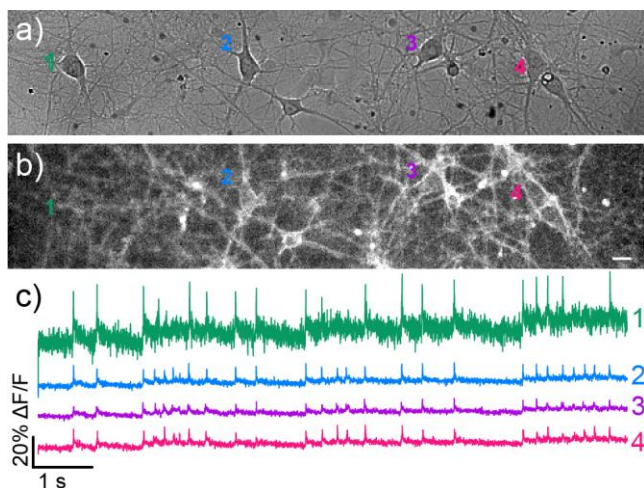


Figure S4. Voltage imaging in dissociated hippocampal neurons with poRhoVR 13. Transmitted light image of neurons loaded with **a)** poRhoVR 13 (500 nM). **b)** Epifluorescence image of neurons showing poRhoVR 13 staining. Scale bars are 20 μm . **c)** Plot of fractional change in poRhoVR 13 fluorescence ($\Delta F/F$) vs time emanating from cells 1-4 in image (**b**). Optical sampling rate is 500 Hz.

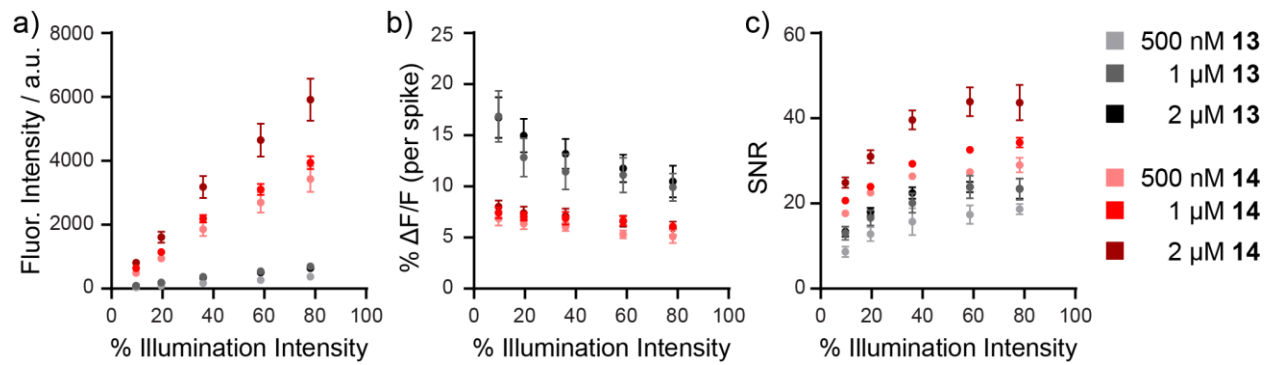


Figure S5. Quantification of brightness, voltage sensitivity and signal to noise of poRhoVR 13 and 14 in neurons

Plots of **a)** fluorescence intensity, **b)** fractional change in fluorescence in response to evoked action potentials ($\Delta F/F$), and **c)** and signal-to-noise ratios (SNR) for these action potentials vs. illumination intensity in neurons. Hippocampal rat neurons were stained with poRhoVR **13** (grey) or **14** (red) at concentrations of 500 nM (light red/light grey), 1 μ M (red/grey), or 2 μ M (dark red/dark grey) poRhoVR dye and imaged at 500 Hz. Data represent mean values \pm S.E.M. for $n = 4$ images, comprising approximately 10-20 neurons per image.

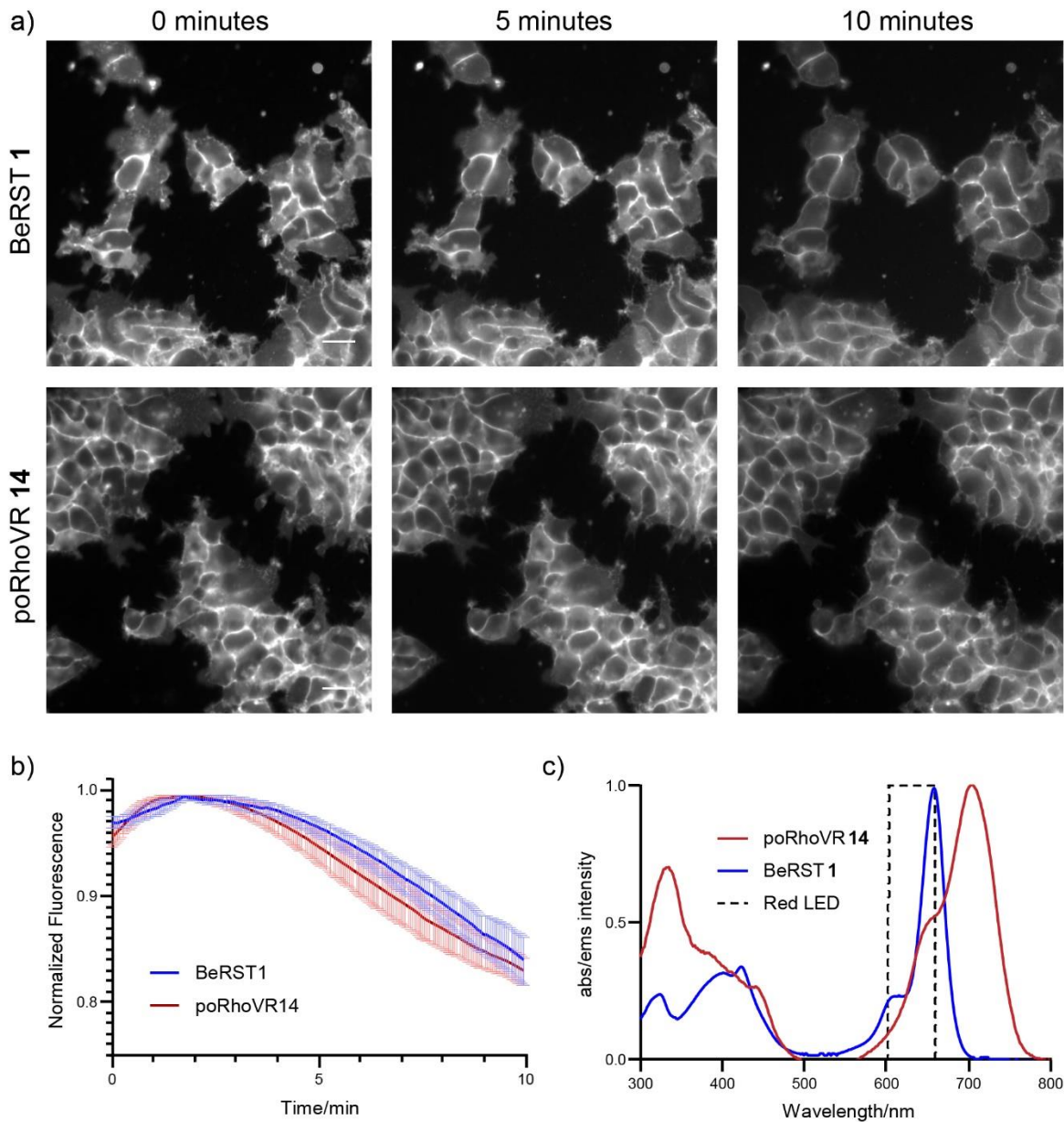


Figure S6. Photostability comparison between poRhoVR 14 and BeRST.

a) Widefield fluorescence images of HEK293T stained with 300 nM BeRST **1** and 500 nM poRhoVR **14** at timepoints 0, 5, 10 minutes of continuous illumination with a red LED (78.6 mW/mm²). Scale bar is 20 μ m. **b)** Plot of photobleaching curve of BeRST**1** (blue) and poRhoVR **14** (red). The bold line represents the background subtracted average cellular fluorescence at each time point (6 coverslips each) and the error bars represent the standard error of the mean. **c)** Absorption spectra for poRhoVR **14** (solvent: dPBS with 1% DMSO) and BeRST **1** (solvent: solvent: dPBS with 0.1% sodium dodecyl sulfate). To account for differences in absorption of light from the red LED used to illuminate the cells, the absorbances of the dyes were matched at 631nm. As a result, cells were stained with either 300 nM BeRST **1** or 500 nM poRhoVR **14**.

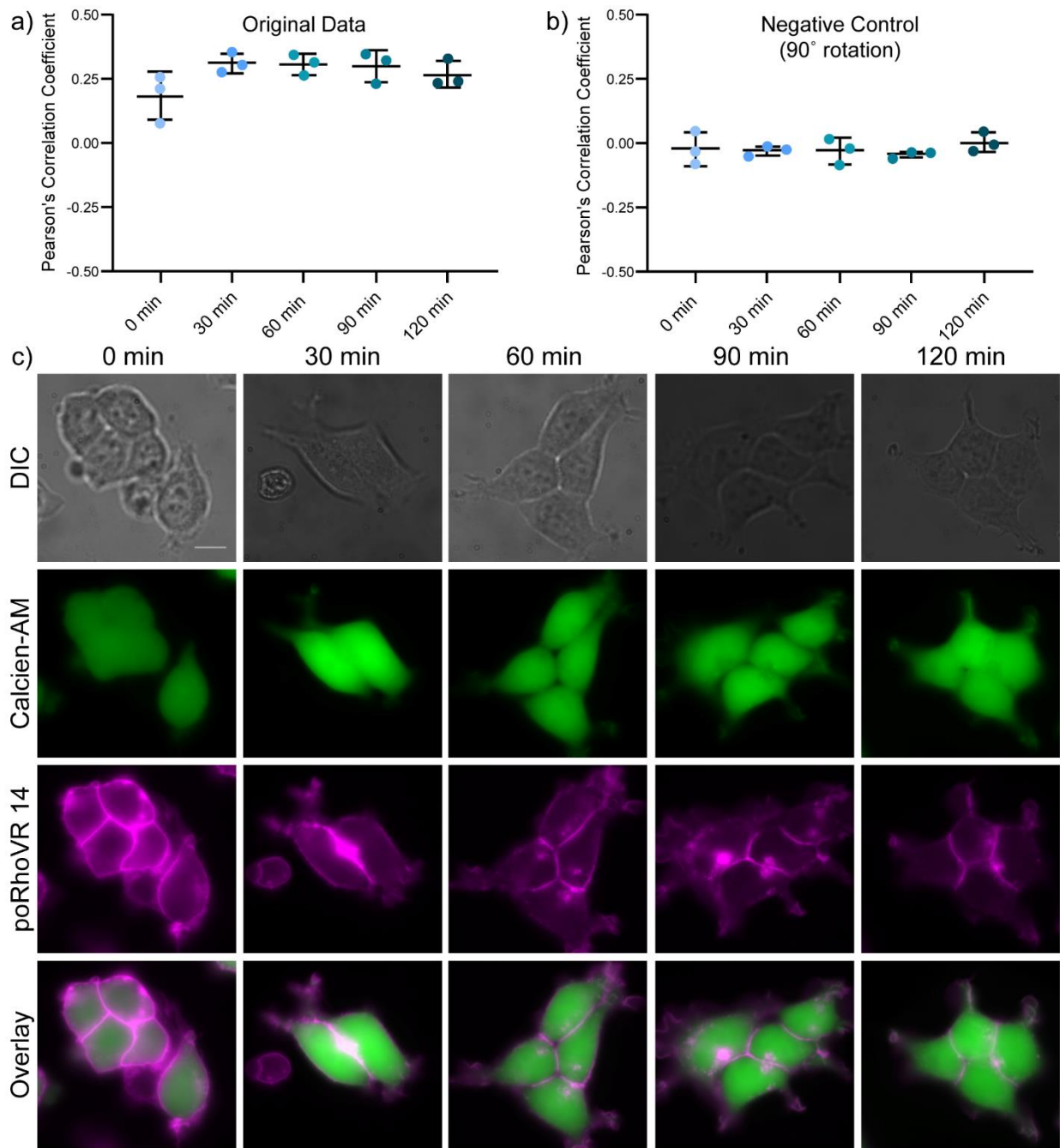


Figure S7. Internalization of poRhoVR 14 in HEK293T cells.

a) Graph of the average Pearson's correlation coefficient (PCC) per timepoint. Error bars show standard deviation. Each point represents an independent replicate (a coverslip). The PCC for each coverslip was calculated as the average PCC of 4 imaged areas per coverslip. The PCC for each area was calculated as the average PCC for all ROIs in the area imaged. Dunnett's multiple comparisons test of 0 min versus all other time points gave the following P-values: 0.0772 (0 vs. 30 min), 0.0894 (0 vs. 60 min), 0.1138 (0 vs. 90 min), 0.3039 (0 vs. 120 min). A P-value below 0.05 is considered statistically significant. b) Graph of the average PCC for the negative control. Data points were calculated in the same manner as in a). The negative control values were obtained by rotating the Calcein-AM image 90° and rerunning the analysis. Dunnett's multiple comparisons test of 0 min versus all other time points gave the following P-values: 0.9981

(0 vs. 30 min), 0.9979(0 vs. 60 min), 0.9118 (0 vs. 90 min), 0.8743 (0 vs. 120 min). c) Representative images at each time point displaying the poRhoVR 14 and Calcein-AM staining. Scale bar is 10 μ m.

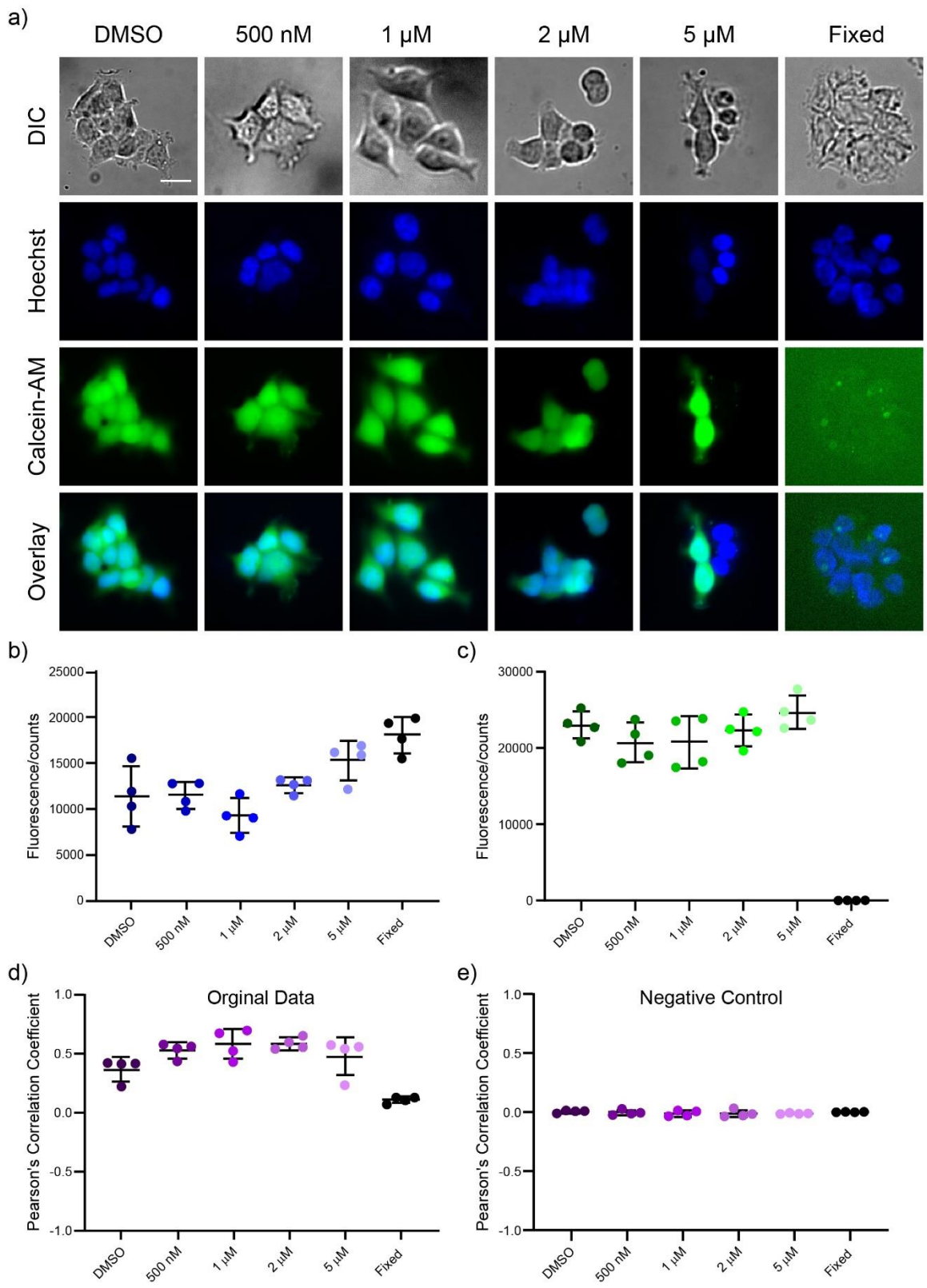


Figure S8. Toxicity of poRhovR 14 in HEK 293T cells.

a) Images of HEK 293T cells that have been loaded DMSO or with varying concentrations of poRhoVR **14** or fixed with formaldehyde and then stained with Hoechst 33342 and Calcein-AM. Scale bar 20 μM . **b)** Background subtracted Hoechst 33342 fluorescence. Each data point represents a single coverslip. A total of four coverslips were imaged per condition (the value of each coverslip was determined from 4 distinct areas that had approximately 20 to 50 cellular regions of interest). The error bars represent the standard deviation. Dunnett's multiple comparisons test of DMSO, the positive control, versus poRhoVR **14** treated and fixed cells gave the following P-values: 0.9999 (DMSO vs. 500 nM), 0.4617 (DMSO vs. 1 μM), 0.8729 (DMSO vs. 2 μM), 0.0600 (DMSO vs. 5 μM) and 0.0010 (DMSO vs. Fixed). A P-value below 0.05 constitutes a statistically significant difference. **c)** Background subtracted Calcein-AM fluorescence. Each data point represents an area of a coverslip. The error bars represent the standard deviation. Dunnett's multiple comparisons test of DMSO versus poRhoVR **14** treated and fixed cells gave the following P-values: 0.4672 (DMSO vs. 500 nM), 0.5116 (DMSO vs. 1 μM), 0.9852 (DMSO vs. 2 μM), 0.7441 (DMSO vs. 5 μM) and <0.0001 (DMSO vs. Fixed). **d)** Pearson's correlation coefficient for Hoechst 3332 and Calcein-AM fluorescence for each area. The error bars represent the standard deviation. Dunnett's multiple comparisons test of DMSO versus poRhoVR **14** treated and fixed cells gave the following P-values: 0.1231 (DMSO vs. 500 nM), 0.0298 (DMSO vs. 1 μM), 0.0261 (DMSO vs. 2 μM), 0.4247 (DMSO vs. 5 μM) and 0.0071 (DMSO vs. Fixed). **e)** Pearson's correlation coefficient for Hoechst 3332 and Calcein-AM fluorescence, rotated 90° for each area. The error bars represent the standard deviation. Dunnett's multiple comparisons test of DMSO versus poRhoVR **14** treated and fixed cells gave the following P-values: 0.9752 (DMSO vs. 500 nM), 0.7539 (DMSO vs. 1 μM), 0.7280 (DMSO vs. 2 μM), 0.7544 (DMSO vs. 5 μM) and 0.9986 (DMSO vs. Fixed).

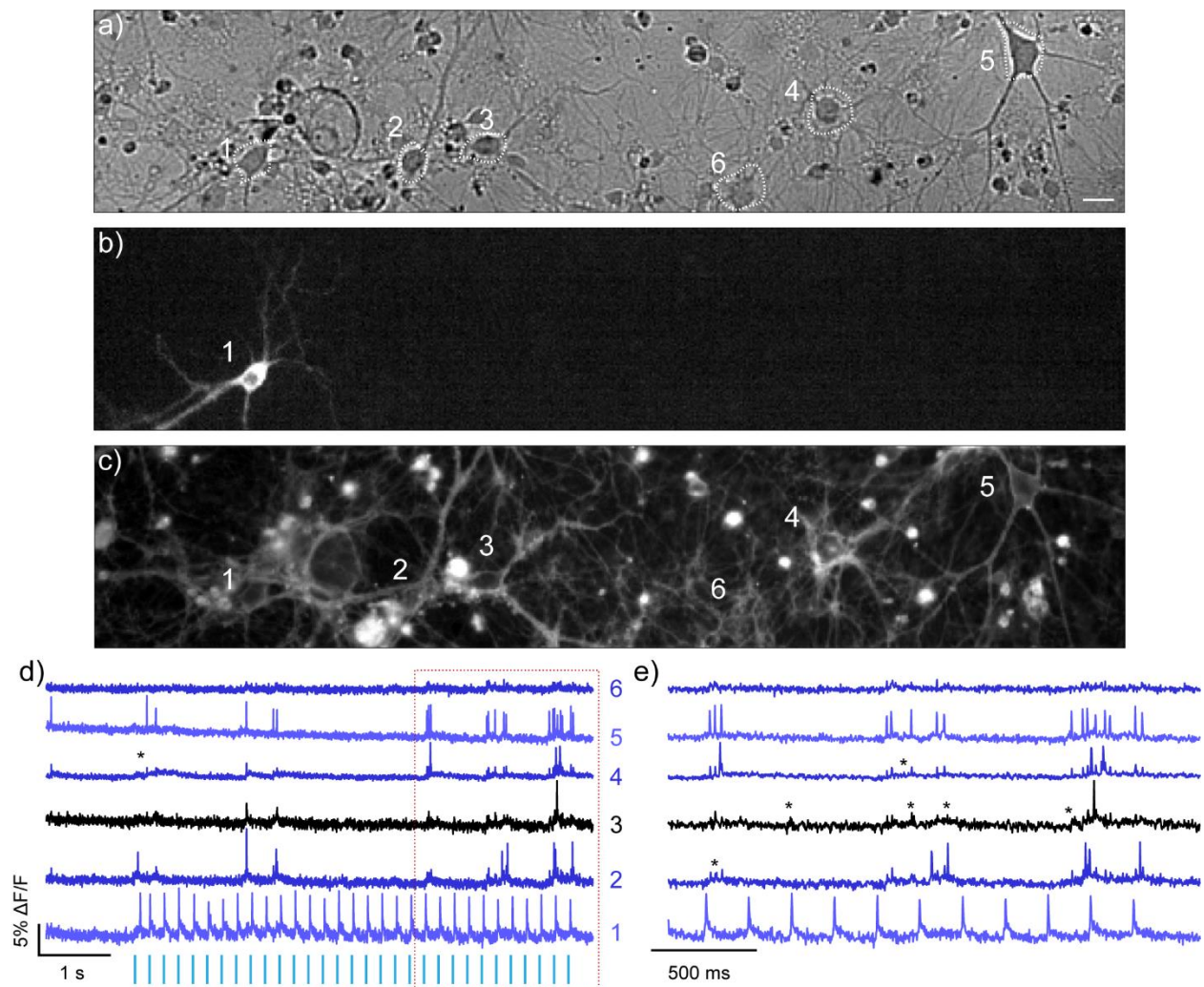


Figure S9. All-optical electrophysiology using poRhoVR 14 and ChR2.

a) Transmitted light image of dissociated rat hippocampal neurons stained with poRhoVR 14 (500 nM). Scale bar is 20 μm . **b)** Epifluorescence image of neuron displaying YFP genetic marker for ChR2. **c)** Epifluorescence image of neurons stained with poRhoVR 14. **d)** Recording of $\Delta F/F$ from the cell bodies of neurons indicated in panels **a-c**. **e)** Expanded time base recording of activity within the red, dashed box in panel **d**. Optical sampling rate was 500 Hz. ChR2 (+) cell 1 was stimulated optically with flashes of cyan light (475 nm, 5 ms, 1.92 mW/mm^2) as indicated by the cyan bars below the blue optical recording in panel **d**. Notably, there is no visible cyan light excitation of poRhoVR 14 (see for example, $\Delta F/F$ plot of cell 6, in panels **d** and **e**).

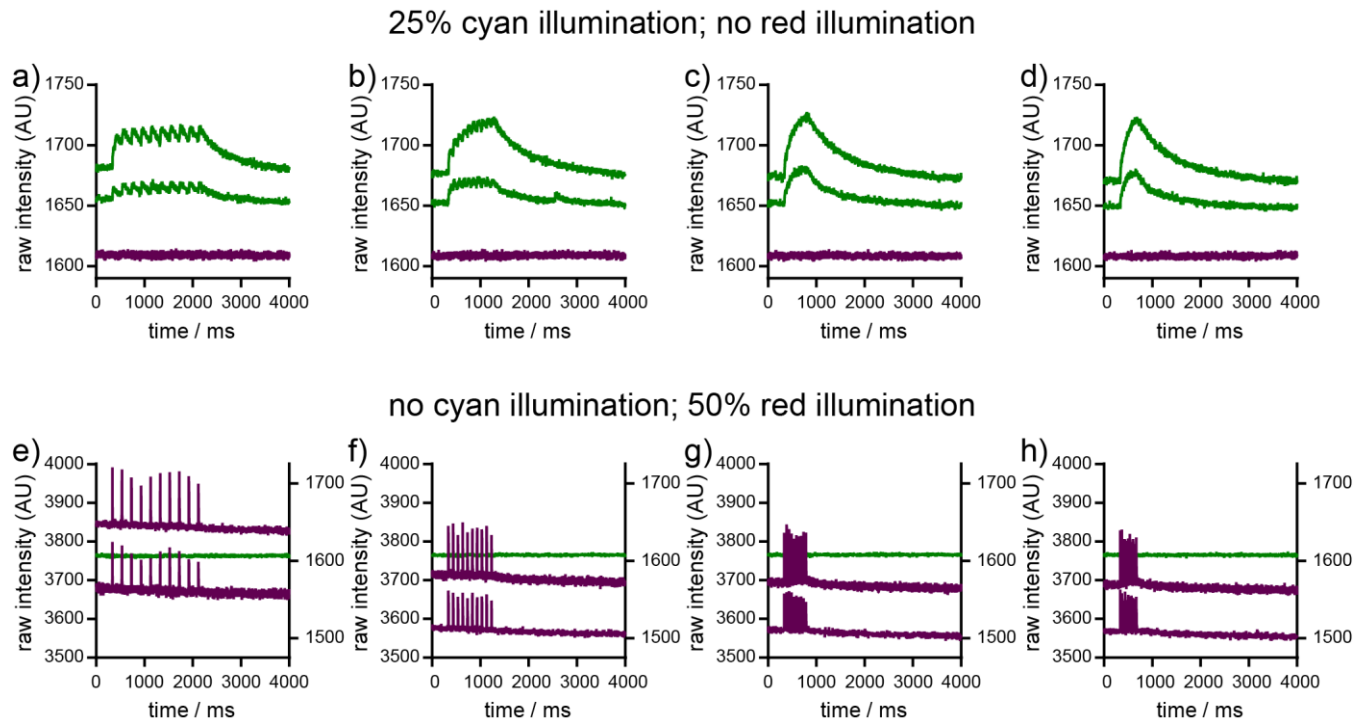


Figure S10. Compatibility of poRhoVR 14 with OGB Ca^{2+} imaging in rat hippocampal neurons.

Rat hippocampal neurons with stained with poRhoVR 14 (1 μM) and OGB (1 μM) and imaged using an image-splitter to enable acquisition of simultaneous NIR (poRhoVR) and green (OGB) fluorescence, as in **Figure 5** (main text). **a-d**) Plots of fluorescence intensity vs. time for OGB (green traces) and poRhoVR 14 (magenta traces) vs. time (ms) with cyan illumination only (17.6 mW/mm^2). Under single wavelength (cyan) illumination, field stimulation was provided at **a**) 5, **b**) 10, **c**) 20, and **d**) 30 Hz. **e-h**) Plots of fluorescence intensity vs. time for poRhoVR 14 (magenta traces) and OGB (green traces) vs. time with red illumination only (50%, 49.7 mW/mm^2). Under single wavelength (red) illumination, field stimulation was provided at **e**) 5, **f**) 10, **g**) 20, and **h**) 30 Hz. Each plot shows the responses of two neurons (recorded simultaneously in red and green channels).

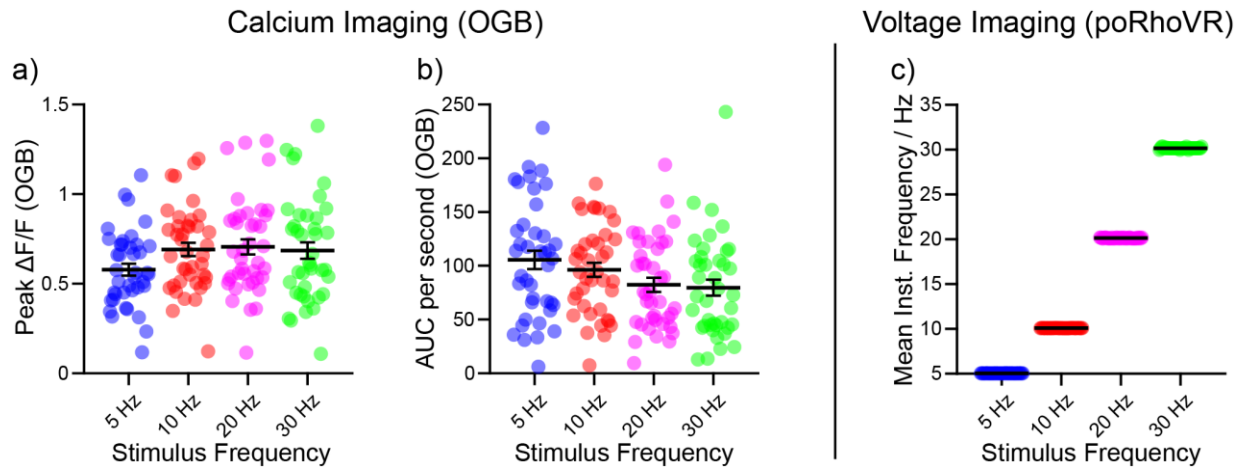


Figure S11. Quantification of evoked activity in neurons using poRhoVR 14 and Oregon Green BAPTA

Analysis of data presented in **Figure 5** of main text. Ca^{2+} imaging data with OGB was quantified as **a)** peak $\Delta F/F$ or **b)** integrated area under the curve per second vs stimulus frequency, in Hz. For Ca^{2+} imaging data, black bars represent the mean \pm S.E.M. for n = 40 cells. Data points represent individual cells. There are no statistically-significant differences between stimulus frequency when analyzing peak $\Delta F/F$ or AUC per second (one-way ANOVA + Tukeys comparisons). Voltage imaging data with poRhoVR **14** was quantified as **c)** the mean instantaneous frequency (Mean Inst. Frequency), in Hz, vs stimulus frequency, in Hz. For voltage imaging data, black bars represent the mean \pm S.E.M. for n = 40 cells. Data points represent the mean instantaneous frequency between spikes for each analyzed cell (10 spikes, 9 intra-spike intervals). For voltage imaging, all of the differences between stimulus frequencies are significant ($p < 0.0001$, one-way ANOVA Kruskal-Wallis test + Dunns comparison).

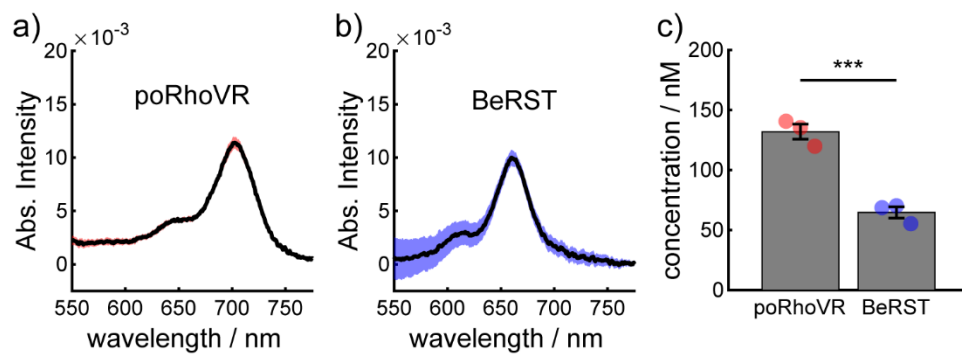


Figure S12. Characterization of cellular uptake of poRhoVR (14).

Plot of absorbance intensity vs. wavelength for **a)** poRhoVR (14) or **b)** BeRST 1 in a suspension of HEK cells. Data are mean (black line) \pm S.E.M. (shaded region) for $n = 3$ independent determinations. **c)** Dye concentration in HEK cell membranes for poRhoVR (14) or BeRST. Data are mean values \pm S.E.M. for $n = 3$ independent determinations. Data represent the concentration estimated using ϵ values of $86,000 \text{ M}^{-1} \text{ cm}^{-1}$ for poRhoVR (this work) and $150,000 \text{ M}^{-1} \text{ cm}^{-1}$ for BeRST. *** ($p = 0.001$, t-test, two tailed, equal variance).

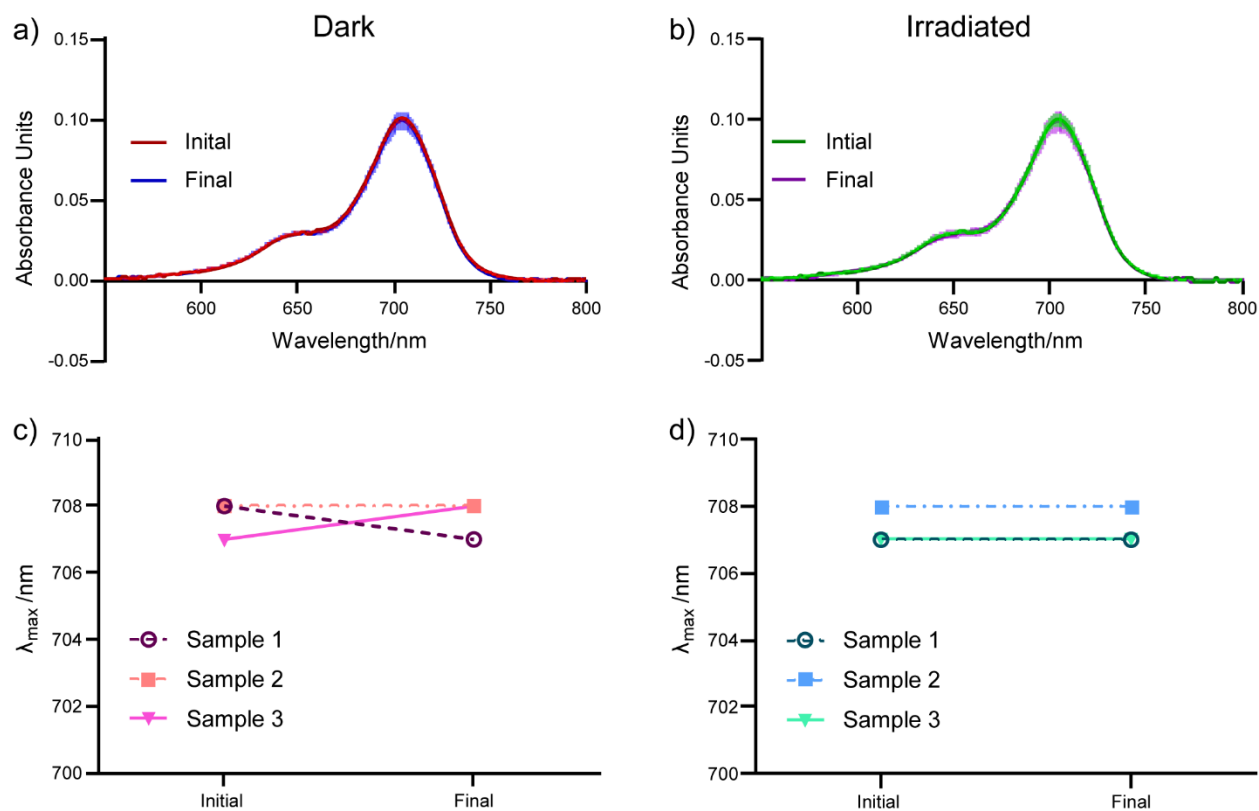


Figure S13. poRhodamine 9-cis does not display photobleaching under prolonged illumination.

Plot of absorbance of 9-cis vs wavelength after **a)** storage in the dark for one hour or **b)** irradiation with a red LED (78.6 mW/mm²) using a 20x/1.0 NA water objective for one hour. Data are mean of three separate experiments. Error bars are standard deviation.

The maximum absorbance (λ_{max}) before and after treatment is plotted for each condition, either **c)** storage in the dark, or **d)** irradiation for one hour. Although control samples (“dark”) shift slightly, there is no change in λ_{max} for irradiated samples.

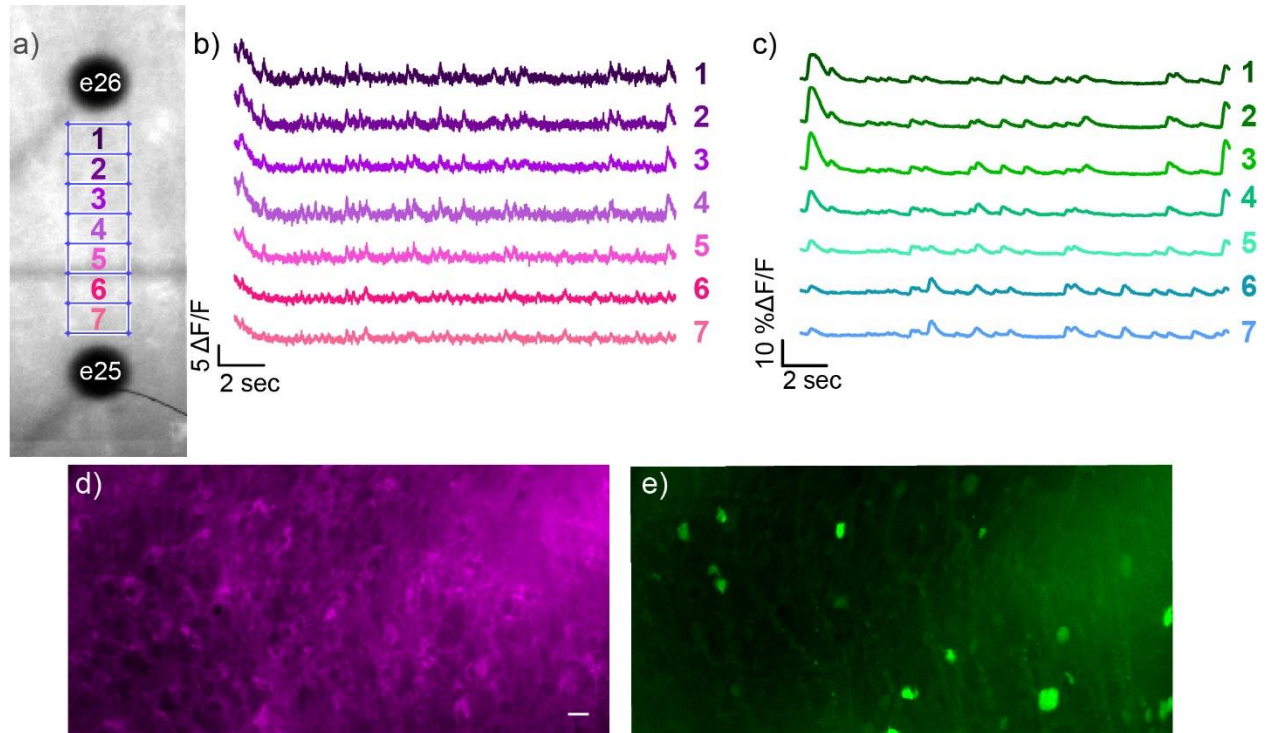


Figure S14. Spatial evolution of voltage signals in *rd1* mouse retina, monitored by poRhoVR
a) Widefield, epifluorescence image of *rd1* mouse retina stained with poRhoVR **14**. Black circles are the electrodes, labeled “e25” and “e26”. Rectangles indicate regions of interest. Plots of relative change in fluorescence (arbitrary units) from either **b)** poRhoVR **14** or **c)** GCaMP6 vs time for the ROIs indicated in panel **(a)**. Higher resolution, widefield, epifluorescence image of *rd1* mouse retina stained with **d)** poRhoVR **14** and expressing **e)** GCaMP6.

Supporting Information Methods

HEK293T cell culture information

HEK293T cells were obtained from the UC Berkeley Cell Culture Facility. Cells were passaged and plated onto 12 mm glass coverslips coated with Poly-D-Lysine (PDL; 1 mg/mL; Sigma-Aldrich) to a confluency of approximately 15% and 50% for electrophysiology and imaging, respectively. HEK293T cells were plated and maintained in Dulbecco's modified eagle medium (DMEM) supplemented with 4.5 g/L D-glucose, 10% fetal bovine serum (FBS), and 1% Glutamax. Cells were maintained at 37 °C in a humidified incubator with 5 % CO₂.

Preparation of primary neuron cultures

Hippocampi were dissected from embryonic day 19 Sprague Dawley rats (Charles River Laboratory) in cold sterile HBSS (zero Ca²⁺, zero Mg²⁺). Hippocampal tissue was treated with trypsin (2.5%) for 15 min at 37 °C. The tissue was triturated using fire polished Pasteur pipettes, in minimum essential media (MEM) supplemented with 5% FBS, 2% B-27, 2% 1M dextrose and 1% GlutaMax. The dissociated cells were plated onto 12 mm diameter coverslips (Fisher Scientific) pre-treated with PDL at a density of 25,000-30,000 cells per coverslip in MEM supplemented media (as above). Neurons were maintained at 37 °C in a humidified incubator with 5 % CO₂. After 1 day in vitro (DIV) half of the MEM supplemented media was removed and replaced with Neurobasal media containing 2% B-27 supplement and 1% GlutaMax. Functional imaging was performed on mature neurons 13-20 DIV.

General Imaging Parameters

Imaging experiments were performed on either an upright or an inverted epifluorescence microscope, AxioExaminer Z-1 (Zeiss), equipped with a Spectra-X Light engine LED light (Lumencor), and an OrcaFlash4.0 sCMOS camera (Hamamatsu). The following LED light sources were used; red (631/28 nm bandpass), teal LED (510/25 nm bandpass), cyan (475/34 nm bandpass), violet (390/22 nm bandpass). The microscope was controlled via Slidebook (v6, Intelligent Imaging Innovations) or MicroManager (Studio Version 1.4.22). Imaging was done with a W-Plan-Apo 20x/1.0 objective (20x; Zeiss) or a W-Plan-Apo 63x/1.0 objective (63x; Zeiss). The QUAD emission filter set, a quadruple dichroic mirror (432/38, 509/22, 586/40, 654 nm LP) combined with a quadruple emission filter (430/32 nm, 508/14 nm, 586/30 nm, 708/98 nm), was routinely used. For experiments with simultaneous voltage and calcium imaging a Dual View emission splitter (Optical Insights) was used. The Dual-View contained a 585dcxr dichroic and two emission filters (520/28 nm and 723/68 nm) which separated the calcium (GCaMP or Oregon Green BAPTA-AM) and poRhoVR fluorescence signals.

Image Analysis

Analysis of voltage sensitivity in HEK cells was performed using custom MATLAB routines in which a region of interest (ROI) was automatically selected based on changes in fluorescence intensity. The ROI is then applied as a mask to all frames in the image stack. Fluorescence intensity values were calculated at known baseline and voltage step epochs and used to calculate a percent change in baseline fluorescence (% $\Delta F/F$) per 100 mV change in membrane potential.

Optical traces of neuronal calcium and voltage activity were obtained by drawing ROIs around the cell bodies of neurons, transfected with GCaMP6s or stained with poRhoVR or OGB-AM, in ImageJ and extracting the mean cellular fluorescence from each frame in the image stack. The mean background fluorescence was subtracted from the mean cellular fluorescence of each frame. $\Delta F/F$ values were

calculated by first subtracting a mean background value from all raw fluorescence frames to give a background subtracted trace (bkgsb). A baseline fluorescence value (F_{base}) is calculated by averaging the fluorescence of 10 to 20 frames that show no activity. F_{base} was subtracted from each timepoint of the bkgsb trace to yield a ΔF trace. The ΔF was then divided by F_{base} to give $\Delta F/F$ traces.

A custom ImageJ macro aligned and split the image stack into two, one for the GCaMP6s signal and the other for the poRhoVR **14** signal. Custom MATLAB routines were used to extract raw fluorescence traces of retinal activity. Either ring-shaped ROIs 16 pixels (20.8 μm) wide or a series of 7 rectangular ROIs each 16 pixels (20.8 μm) by 32 pixels (41.6 μm) were drawn around or between the electrodes. These ROIs were applied as masks to all frames in the image stack. poRhoVR **14** traces were bleach corrected by approximating the bleach curve via asymmetric least squares and subtracting the resulting curve from the raw poRhoVR **14** signal. A baseline fluorescence value (F_{base}) is calculated by averaging the fluorescence of 10 to 20 frames that show no activity. F_{base} was subtracted from each timepoint of the the bleach corrected poRhoVR **14** traces or the raw GCaMP6s traces to yield a ΔF trace. The ΔF was then divided by F_{base} to give $\Delta F/F$ traces.

Figure 2. Cellular characterization of pRhoVR indicators in HEK cells

Multi-color imaging (Figure 2 a-h)

HEK293T cells were incubated at 37 °C for 20 minutes in an HBSS solution containing the following dyes at 1 μM concentrations: poRhoVR, Rhodamine 123 and Hoechst 33342. Images were taken using W-Plan-Apo 63x/1.0 objective (Zeiss) on an upright epifluorescence microscope. poRhoVR was imaged using a red LED (Neutral Density Setting, ND, 75; 30.8 mW/mm^2) as the excitation source and 100 ms exposure. Emission was collected with a single emission filter (723/68 nm) after passing through a quadruple dichroic mirror (432/38, 509/22, 586/40, 654 nm LP). Rhodamine 123 was imaged using a cyan LED (ND 75, 51.5 mW/mm^2) and 100 ms exposure. Emission was collected with a single emission filter (540/50 nm) after passing through a dichroic mirror (510 nm LP). Hoechst 33342 was imaged using a violet LED (ND 75, 6.7 mW/mm^2) and 100 ms exposure. Emission was collected using a triple emission filter (473/22 nm, 543/19 nm, 648/98 nm) after passing through a triple dichroic mirror (475/30 nm, 540/25 nm, 642/96 nm).

Voltage sensitivity measurements (Figure 2 i-j)

HEK293T cells were incubated at 37 °C for 20 minutes in an HBSS solution containing 1 μM poRhoVRs. Voltage sensitivity data was acquired using a 20X water immersion objective on an upright epifluorescence microscope. Recordings were binned 4X4 and recorded at an optical sampling rate of 500 Hz. poRhoVRs were imaged with a red LED (ND 75, 30.8 mW/mm^2) and emission was collected with the QUAD filter set (see *General Imaging Parameters*). For electrophysiological experiments in HEK293T cells, pipettes were pulled from borosilicate glass (Sutter Instruments, BF150-86-10), with a resistance of 4–7 $\text{M}\Omega$, and were filled with an internal solution; 125 mM potassium gluconate, 1 mM EGTA, 10 mM HEPES, 5 mM NaCl, 10 mM KCl, 2 mM ATP disodium salt, 0.3 mM GTP trisodium salt (pH 7.25, 285 mOsm). Recordings were made with an Axopatch 200B amplifier (Molecular Devices) at room temperature. The signals were digitized with a Digidata 1440A, sampled at 50 kHz and recorded with pCLAMP 10 software (Molecular Devices) on a PC. Fast capacitance was compensated in the on-cell configuration. Recordings were only pursued if series resistance in voltage clamp was less than 30 $\text{M}\Omega$. Cells were held at -60 mV and hyper- and depolarizing steps applied from +100 to -100 mV in 20 mV increments. Analysis of voltage sensitivity in HEK cells was performed using custom MATLAB routines in which a region of interest (ROI) was automatically selected based on changes in fluorescence intensity. The ROI is then applied as a mask to all frames in the image stack. Fluorescence intensity values were calculated at known baseline and voltage step epochs and used to calculate a percent change in baseline fluorescence ($\% \Delta F/F$) per 100 mV change in membrane potential.

Figure 3. Voltage imaging in dissociated rat hippocampal neurons with poRhoVR 14

Dissociated rat hippocampal neurons were incubated at 37 °C for 20 min in an HBSS solution containing 500 nM poRhoVR **14**. Spontaneous neuronal activity was monitored using a 20X water immersion objective on an upright epifluorescence microscope. The field of view was binned 4X4 and recorded at an optical sampling rate of 500 Hz. poRhoVR **14** was imaged using a red LED (ND 50, 21.2 mW/mm²). Emission was collected with the QUAD filter set (see *General Imaging Parameters*).

Figure 4. and Figure S6. All-optical electrophysiology using poRhoVR 14 and ChR2

Dissociated rat hippocampal neurons previously transfected with Channelrhodopsin-2-YFP (ChR2-YFP) were incubated at 37 °C for 20 minutes in an HBSS solution containing 500 nM poRhoVR **14**. ChR2 positive cells were identified by locating YFP expressing neurons using a teal LED (50% max power, 9.2 mW/mm²). YFP emission was collected via a triple emission filter (473/22 nm, 543/19 nm, 648/98 nm) after passing through a triple dichroic mirror (475/30 nm, 540/25 nm, 642/96 nm). ChR2 was activated by 5 ms pulses of cyan light (2% of max power, 1.92 mW/mm²). poRhoVR **14** was imaged with a red LED (100% of max power, 78.5 mW/mm²) and emission was collected with the QUAD filter set (see *General Imaging Parameters*). The field of view was binned 4X4 and recorded at an optical sampling rate of 500 Hz using a 20X water immersion objective on an upright epifluorescence microscope.

Figure 5. Simultaneous voltage and calcium imaging with poRhoVR 14

Dissociated rat hippocampal neurons previously transfected with GCaMP6s were incubated at 37 °C for 20 minutes in an HBSS solution containing 500 nM poRhoVR **14**. Separately, neurons were loaded with 1 μM OGB-AM and 500 nM poRhoVR with 0.01% pluronic. A red LED (50% of max power, 49.7 mW/mm²) was the source of excitation light for poRhoVR **14** and a cyan LED was used for GCaMP6s (10% of max power, 7.9 mW/mm²). Emission from GCaMP6s or OGB-AM and poRhoVR **14** was collected simultaneously with the QUAD filter set and a Dual-View emission splitter (see *General Imaging Parameters*). Extracellular field stimulation was delivered by a Grass Stimulator connected to a recording chamber containing two platinum electrodes (Warner), with triggering provided through a Digidata 1440A digitizer and pCLAMP 10 software (Molecular Devices). Action potentials were triggered by 1 ms 80 V field potentials delivered at 5 Hz. To prevent recurrent activity the HBS bath solution was supplemented with synaptic blockers 10 μM 2,3-Dioxo-6-nitro-1,2,3,4-tetrahydrobenzo[f]quinoxaline-7-sulfonamide (NBQX; Santa Cruz Biotechnology) and 25 μM DL-2-Amino-5-phosphonopentanoic acid (APV; Sigma-Aldrich).

Figure 6. and Figure S9. Simultaneous mapping of electrical and Ca²⁺ activity using poRhoVR, GCaMP6s and multi-electrode 370arrays (MEA) in ex vivo retinas from rd1 mice

Retinas were dissected from 3-month-old heterozygous rd1-GCaMP6f mouse in artificial cerebral spinal fluid (ACSF). ACSF was prepared with the following: NaCl (119 mM), KCl (2.5 mM), MgCl₂ (1.3 mM), CaCl₂ (2.5), NaHCO₃ (26.2 mM), D-glucose (20 mM) and KH₂PO₄ (1 mM). GCaMP6f was expressed under a synapsin promotor. Each retina was cut into four pieces and placed into an ACSF solution of 5 μM poRhoVR **14**. The solution was bubbled continuously for approximately 2 hours at room temperature with carbogen (95% O₂ and 5% CO₂). A piece of retina was placed on to an MEA chip (Multichannel Systems 60 pin ThinMEA chip, 200 μm interelectrode distance, 30 μm electrode diameter, 180 μm thickness) with the RGC layer in direct contact with the electrodes. The electrode pins on the MEA chip are made of titanium nitride (TiN) and the chip itself is made of indium tin oxide (ITO). Electrical data from the MEA was recorded on a Multichannel Systems USB-64 system at a sampling rate of 20kHz. The retina was imaged on an inverted

epifluorescence microscope equipped with an OracFlash4.0 sCMOS camera (Hamamatsu) via a 20X air objective. The field of view was binned 4X4 and recorded at an optical sampling rate of 500 Hz. A red LED (20% of max power, 8.85 mW/mm²) was used as the excitation source for poRhoVR **14** and a cyan LED (20% of max power, 8.77 mW/mm²) was used for GCaMP6f. Emission from GCaMP6f and poRhoVR **14** was collected simultaneously with the QUAD filter set alongside a Dual-View emission splitter (Optical Insights). The Dual-View contained a 585dcxr dichroic and two emission filters (520/28 nm and 723/68 nm) which separated the GCaMP6f and poRhoVR **14** fluorescence signals. After a few initial recordings the ACSF solution was replaced by a solution of synaptic blockers. The solution of synaptic blockers was prepared in ACSF with the following: DNQX (40 μM), D-AP5 (30 μM), Curare (50 μM), Strychnine (10 μM), TPMPA (50 μM), Gabazine (10 μM) and L-AP4 (10 μM). Recordings of pharmacologically isolated ganglion cells were taken approximately 10-15 minutes after blocker treatment.

Figure S2. Quantification of poRhoVR staining in HEK cells.

HEK 293T cells were incubated in a 2 μM HBSS solution of one of poRhoVRs **12-15** for 20 min at 37 °C. A mixture of *cis* and *trans* poRhoVR **13** isomers was used. Images were taken using 20x water immersion objective on an upright epifluorescence microscope. poRhoVRs were imaged using a red LED (ND 75, 30.8 mW/mm²) as the excitation source and 50 ms exposure. Emission was collected with the QUAD filter set (see *General Imaging Parameters*). The median fluorescence of cell ROIs were compared across all four dyes.

Figure S6. Photobleaching.

Due to differences in absorption spectra the absorbances of poRhoVR **14** (λ_{\max} = 703 nm) and BeRST **1** (λ_{\max} = 658 nm) were matched at 631 nm (central emission wavelength of red LED used for imaging). As a result, HEK293T cells, seeded at 75,000 cells per 12 mm coverslip, were incubated at 37 °C in either a 500 nM HBSS solution of poRhoVR or a 300 nM HBSS solution of BeRST **1**. The cells were imaged using a 20X water objective on an upright epifluorescence microscope. Cells were continuously illuminated with a red LED (78.6 mW/mm²) for 10 minutes and images were taking at 3 second intervals with 50 milliseconds exposure. Emission was collected using a long pass filter (732/68 nm).

For each 10-minute time-lapse three cellular ROIs and a background ROI were circled. The average fluorescence intensity from each ROI was plotted for each frame. The background fluorescence trace was subtracted from each cellular ROI fluorescence trace. The resulting background subtracted trace was normalized by dividing each value by the largest fluorescence value. In order to determine the photobleaching curve for each coverslip, the normalized background subtracted traces for each ROI were averaged. The final graphical representation of the data is the average of the six coverslips analyzed for each dye.

Figure S7. Endocytosis.

Extent of endocytosis in HEK293T cells procedure

A 1 μM solution of poRhoVR **14** in HBSS was bath applied to HEK293T cells for 20 minutes at 37 °C. The poRhoVR **14** solution was removed and replaced with a 250 nM Calcein-AM solution with 0.1% pluronic in HBSS. The cells were incubated at 37 °C for one of the following times 30, 60, 90 or 120 minutes. For the 0-minute time point poRhoVR **14** and Calcein-AM were coloaded together for 20 minutes. Four areas were imaged for each coverslip. Cells were imaged using a 63X water objective on an upright epifluorescence microscope. Cells were illuminated with a red LED (1.22 mW/mm²) or a cyan LED (0.82 mW/mm²). Images were taken at 100 ms exposure setting. Emission was filtered with a QUAD dichroic.

Analysis of endocytosis in HEK293T cells procedure

For each coverslip, a total of four images were taken. Each image was analyzed by circling ROIs on the poRhoVR **14** image. The ROIs included only live cells as was determined by the presence of cytosolic Calcein-AM fluorescence. The Pearson's correlation coefficient (PCC) for each ROI in the poRhoVR**14** Calcein-AM images were calculated via MATLAB. As a negative control the Calcein-AM image was rotated 90°, the same ROIs were applied to the rotated image and the PCCs were calculated for each ROI in the unrotated poRhoVR **14** image and the rotated Calcein-AM image. The average PCC for each image was calculated by averaging the PCCs of all the ROIs in the image. The average PCC for each coverslip was calculated by averaging all of the areas imaged for each of the coverslips. Dunnett's multiple comparisons test was performed to determine if the differences between the means of the 0-minute time point, and other time points were statistically significant. If the P-values of the pairwise comparisons were less than 0.05 the difference between the means was considered statistically significant. One-way ANOVA followed by Dunnett's multiple comparisons test was performed in GraphPad Prism version 8.4.3. for Windows, GraphPad Software, San Diego, California USA, www.graphpad.com.

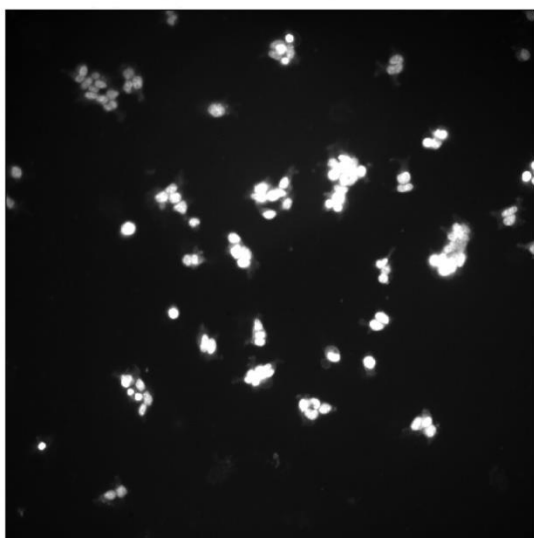
Figure S8. Toxicity.

poRhoVR 14 Toxicity assay procedure

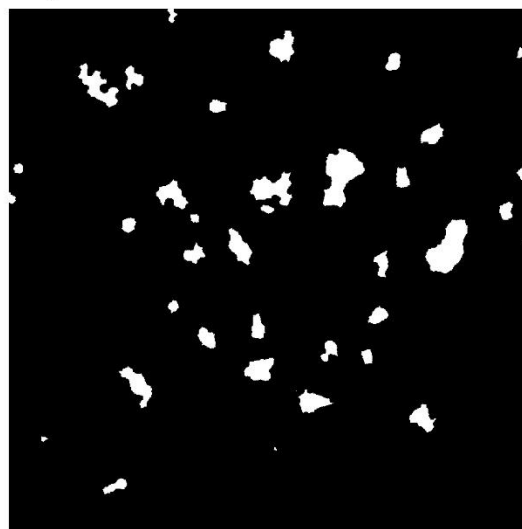
A solution of poRhoVR **14**, concentrations ranged from 500 nM to 5 μ M, in HBSS was bath applied to HEK293T cells for 20 minutes at 37 °C. Cells were incubated in 0.25% v/v DMSO HBSS solution as a positive control. The first solution was removed and replaced with an HBSS solution of 250 nM Calcein-AM with 0.1% pluronic in HBSS and 1 μ M Hoechst 33342. The cells were incubated at 37 °C for an additional 20 minutes. As a negative control cells were fixed with 4% formaldehyde for 20 minutes and then permeabilized with 0.1% TritonX-100 for 5 minutes. Cells were then stained with Hoechst 33342 and Calcein-AM in the same manner as the other conditions. Four areas were imaged for each coverslip. A total of 4 coverslips were imaged per condition. Cells were imaged using a 20X water objective on an upright epifluorescence microscope. Cells were illuminated with a violet LED (6.68 mW/mm²) or a cyan LED (7.87 mW/mm²). Images were taken at 100 ms exposure setting. Emission was filtered with a QUAD dichroic.

poRhoVR 14 Toxicity assay analysis procedure

1. Use Hoechst 33342 fluorescence to create a binary mask

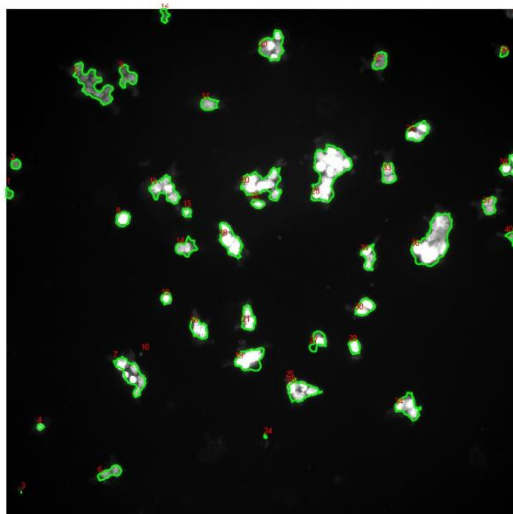


Hoechst 33342 fluorescence image

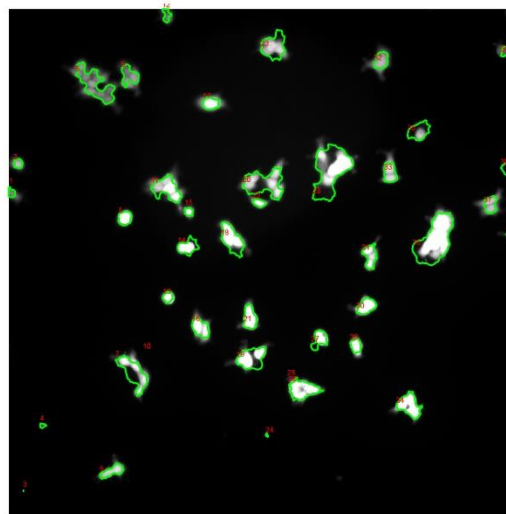


Binary mask generated from Hoechst 33342 image

2. Use the binary mask to generate ROIs that are applied to Hoechst 33342 and Calcein-AM images. The background subtracted fluorescence and PCC coefficient are determined and averaged for each image.



Hoechst 33342 image with ROIs



Calcein-AM image with ROIs

Figure S15. ROI selection for poRhoVR 14 toxicity assay.

ROIs were selected as described in Figure S8. For each ROI the background subtracted fluorescence was calculated for Hoechst 33342 and Calcein-AM images. The PCC value for Hoechst 33342 and Calcein-AM images were also calculated for each ROI. In live cells Hoechst 33342 and Calcein-AM fluorescence overlaps and a PCC of 1 is expected. In dead cells, Hoechst 33342 fluorescence is still visible, but Calcein-AM fluorescence is not present, and this inverse correlation would lead to an expected PCC value of -1. As a negative control, where a PCC of 0 indicates no correlation, the Calcein-AM image was rotated 90° and PCC values were recalculated for each ROI. ROIs that were smaller than 10 pixels were excluded from the analysis as well as those that did not appear to encompass a nucleus as determined visually. The remaining

ROIs were averaged for each image to generate a single value for background subtracted fluorescences and PCC values. Dunnett's multiple comparisons test was performed to determine if the differences between the mean of the control, DMSO treated cells, and the mean of poRhoVR **14** treated cells or fixed cells are statistically significant. If the P-values of the pairwise comparison were less than 0.05 the difference between the means was considered statistically significant. One-way ANOVA followed by Dunnett's multiple comparisons test was performed in GraphPad Prism version 8.4.3. for Windows, GraphPad Software, San Diego, California USA, www.graphpad.com.

Procedure for Figure S12 (cellular uptake)

HEK cells from a 10 cm dish (~70% confluency) were resuspended using 0.05% trypsin. After incubating for about 30 seconds at 37 °C, 3 mL of DMEM were added to quench the trypsin. Cells were spun down on a benchtop centrifuge for 10 minutes at 13,000 rpm. The pellets were washed once with HBSS before being resuspended in 1.5 mL of HBSS. Cells were counted using a hemocytometer and diluted to 500,000 cells per mL. To three 2 mL Eppendorf tubes, 1 μ L of 1 mM BeRST1 in DMSO was added to 1 mL of the diluted cell suspension. Three separate solutions were prepared in the same manner using a 1 mM stock solution of poRhoVR **14**. Two tubes were filled with 1 mL of the diluted cell suspension but were not labeled with dye. All 8 tubes were placed on a shaker set to 37 °C and 500 rpm for 20 minutes. The cells were spun down again on a benchtop centrifuge for 10 minutes at 13,000 rpm. The pellets were washed once with HBSS and resuspended in 1.0 mL of HBSS. The absorbances of the solutions were measured from 200 to 800 nm.

All the traces were corrected so that their baseline absorption at 800 nm was zero. The traces of the unlabeled cell suspension were averaged and subtracted from the traces of cells labeled with dye. The concentration of dye in cells was estimated using the corrected absorbances at each of the dye's maximum absorption wavelengths in aqueous buffer and their extinction coefficients (ϵ). Reported ϵ for BeRST 1 in Tris-Buffered Saline (TBS) is 150,000 $M^{-1}cm^{-1}$ at 658 nm and for the phosphine oxide rhodamine, **9-cis**, it is 86,000 $M^{-1}cm^{-1}$ at 702 nm in HBSS.

Procedure for Figure S13 (photobleuing)

For each sample, a fresh solution of 11 μ M **9-cis**, 600 μ L, was prepared in dPBS, pH = 7.38. Initial absorbance measurements were taken in a Quartz cuvetted by diluting 100 μ L of initial solution into 900 μ L of dPBS. A 100 μ L droplet of the undiluted solution was placed into two separated 3 cm imaging dishes. One dish was covered in foil and placed in a drawer. A 20X water objective was placed into the droplet on the second dish on an upright epifluorescence microscope. This second dish was illuminated with a red LED (78.6 mW/mm²) for one hour. The droplet covered the entire lens of the objective. The droplets of solution in the imaging dishes were diluted with 900 μ L dPBS, transferred to quartz cuvettes and final absorbance measurements were taken.

Table S2. Concentration of poRhoVR used in experiments

System	Study	Figure	[Dye]
HEK cells	co-localization	Figure 2a-h	1 μ M
HEK cells	membrane localization	Figure S2	2 μ M

HEK cells	voltage sensitivity	Figure 2i-j; Figure S3	1 μ M
rat hippocampal neurons	spontaneous activity imaging	Figure 3 Figure S4	500 nM
rat hippocampal neurons	all-optical electrophysiology	Figure 4 Figure S9	500 nM
rat hippocampal neurons	concentration screen / evoked activity	Figure S5	500 nM / 1 μ M / 2 μ M
rat hippocampal neurons	dual Ca ²⁺ and voltage imaging	Figure 5 Figure S10 Figure S11	1 μ M
mouse retina	dual Ca ²⁺ and voltage imaging	Figure 6 Figure S12	5 μ M

Photophysical Characterization

Absorbance and emission spectra were collected using a Shimadzu 2501 Spectrophotometer (Shimadzu) and a Quantmaster Master 4 L-format scanning spectrofluorometer (Photon Technologies International). The fluorometer excitation source is an LPS-220B 75-W xenon lamp. The fluorometer is equipped with a power supply, A-1010B lamp housing with integrated igniter, switchable 814 photon-counting/analog photomultiplier detection unit, and MD5020 motor driver. Samples were measured in 1-cm path length quartz cuvettes (Starna Cells).

Relative quantum yields (ϕ_F) were measured via comparison to Cy5.5 ($\phi_{\text{standard}} = 0.23$ in PBS).^{1, 2} DMSO stocks of fluorophores **8-9** and poRhoVRs **12-15** were diluted in PBS with 0.1% sodium dodecyl sulfate (SDS) until the max absorbance was less than 0.1 absorbance units. Serial dilutions were made from the initial dilution into PBS with 0.1% SDS. The absorbance at 625 nm versus the total area under the fluorescence curve from 635-855 nm were plotted. The slope of the resulting linear plot was calculated for each compound and for the standard. The slope was put into the equation below where; x represents the compound being analyzed, st represents the standard, ϕ_x is the ϕ_F for compound x and η is the refractive index of the solvent in which the measurements were made. The absorbance and fluorescence measurements for fluorophores **8** and **9** were made in PBS and in PBS with 0.1% SDS for poRhoVRs **12-15**. For both solutions the refractive index was approximated to the refractive index of water ($\eta = 1.33$).

$$\phi_x = \phi_{st} \left(\frac{\text{Slope}_x}{\text{Slope}_{st}} \right) \left(\frac{\eta_x^2}{\eta_{st}^2} \right)$$

General Synthesis and Characterization Information

Chemical reagents and solvents were purchased from commercial sources and used without further purification. Flash column chromatography was performed using Silicycle Silica Flash F60 (230–400 Mesh).

Preparative Thin Layer Chromatography (PTLC) purification was done using glass plates coated with a layer of silica gel (Silicycle, F254, 1000 μm). Preparative High Performance Liquid Chromatography (Prep-HPLC) was done using a Waters Acquity Autopurification system equipped with a Waters XBridge BEH 5 μm C18 column (19 mm I.D. x 250 mm) with a flow rate of 30.0 mL/min, made available by the Catalysis Facility of Lawrence Berkeley National Laboratory (Berkeley, CA). The mobile phases were MiliQ (MQ-H₂O) with 0.05% formic acid (FA) and HPLC grade acetonitrile (MeCN) with 0.05% FA. Absorbance was monitored at 350 nm over 200 min with a gradient of 10-100% of MeCN with 0.05% FA. NMR spectra were collected on one of the following instruments; Bruker AVB-400 MHz, AVQ-400 MHz, Bruker AV-600 MHz. Chemical shifts are reported in parts per million (ppm) and couplings constants are reported in Hertz (Hz). Characterization of purity and identity was also done via High Performance Liquid Chromatography (HPLC) and low resolution ESI mass spectrometry on an Agilent Infinity 1200 analytical instrument coupled to an Advion CMS-L ESI mass spectrometer. The column used for the analytical HPLC was Phenomenex Luna 5 μm C18(2) (4.6 mm I.D. x 75 mm) with a flow rate of 1.0 mL/min. The mobile phases were MQ-H₂O with 0.05% formic acid (FA) and HPLC grade MeCN with 0.05% FA. Absorbance was monitored at 254, 280, 350 and 690 nm over 10 min with a gradient of 10-100% of MeCN with 0.05% FA.

Crystallization of 8- and 9- *cis*

Crystals were grown through vapor diffusion. The compound was dissolved in a mixture of 90% 1,2-dichloroethane, 5% ethanol, 5% methanol by volume. The resulting solution was filtered with a 0.45 μm PTFE filter into a 60 mm test tube. The tube was placed into a 20 mL vial containing 7 mL of hexanes and capped with lid (foil inner lining). The vial was kept at room temperature away from light.

Single-crystal X-ray diffraction experiments were performed at the UC Berkeley CHEXRAY crystallographic facility. Measurements of all compounds were performed on a Bruker Quazar SMART APEX-II using Mo K α radiation ($\lambda = 0.71073 \text{ \AA}$). Crystals were kept at 100(2) K throughout collection. Data collection was performed with Bruker APEX2 software (v. 2014.11). Data refinement and reduction were performed with Bruker SAINT (V8.34A). All structures were solved with SHELXT.53. Structures were refined with SHELXL-2016. Molecular graphics were computed with Mercury 4.0. All non-hydrogen atoms were refined anisotropically, and hydrogen atoms were included at the geometrically calculated positions and refined using a riding model.

	8	9
Chemical formula	C ₃₀ H ₄₄ BrN ₂ O ₈ PS	C ₃₀ H ₃₇ BrCl ₂ N ₂ O _{4.55} PS
Formula weight	703.61	712.27
Color, habit	Blue, plate	Blue, plate
Temperature (K)	100(2)	100(2)
Crystal system	Triclinic	Monoclinic
Space group	P -1	C 2/c
a (\AA)	10.4009(5)	34.703(3)
b (\AA)	12.1497(5)	10.3808(7)
c (\AA)	15.2206(7)	24.3311(18)
α ($^\circ$)	100.379(3)	90
β ($^\circ$)	107.814(3)	133.946(6)
γ ($^\circ$)	110.872(2)	90
V (\AA^3)	1618.10(13)	6310.9(9)
Z	2	8
Density (Mg m ⁻³)	1.444	1.499
F(000)	736	2939
Radiation Type	MoK α	MoK α
μ (mm ⁻¹)	1.435	1.629

Crystal size (mm ³)	0.19 x 0.075 x 0.20 x 0.06 x 0.03	
	0.035	
Meas. Refl.	28286	47710
Indep. Refl.	5937	5767
R(int)	0.0739	0.0327
Final R indices [I >	R = 0.0494	R = 0.0332
2σ(I)]	R _w = 0.0973	R _w = 0.0859
Goodness-of-fit	1.028	1.050
Δρ _{max} , Δρ _{min} (e Å ⁻³)	1.198, -1.003	0.569, -0.481

NMR Abbreviations

s = singlet

d = doublet

dd = doublet of doublets

t = triplet

dt = doublet of triplets

td = triplet of doublets

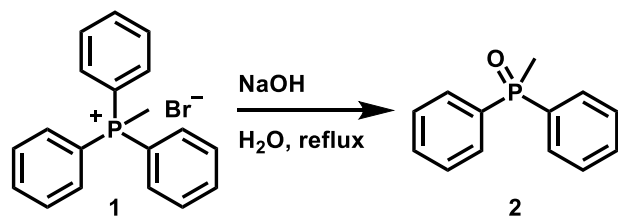
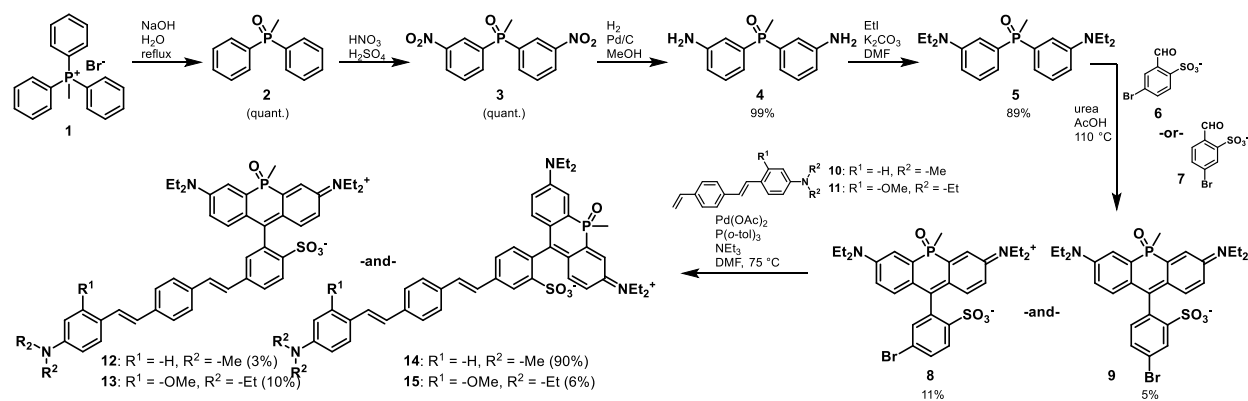
q = quartet

qnt = quintet

dqnt = doublet of quintets

m = multiplet

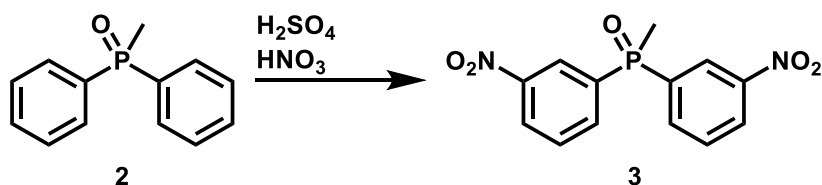
Scheme S1. Synthesis of sulfonated phosphine-oxide rhodamines and rhodamine voltage reporters (poRhoVRs)



Synthesis of methyl diphenyl phosphine oxide, 2:

Added 50 mL of H₂O to **1** (5.00 g, 14.0 mmol). Refluxed the solution for 30 minutes. Made a separate solution of NaOH (2.80 g, 70.0 mmol) in 25 mL of H₂O. The solution of NaOH was added to the solution of **1** and the reaction mixture became cloudy and opaque. The mixture was refluxed for an additional 2 hours. Once the mixture cooled to room temperature it was extracted with CHCl₃ (3X). The organic layer was washed with H₂O (3X), collected and dried with anhydrous Na₂SO₄. The solvent was removed by rotary evaporation. Collected 3.02 g of a white solid (quantitative yield).

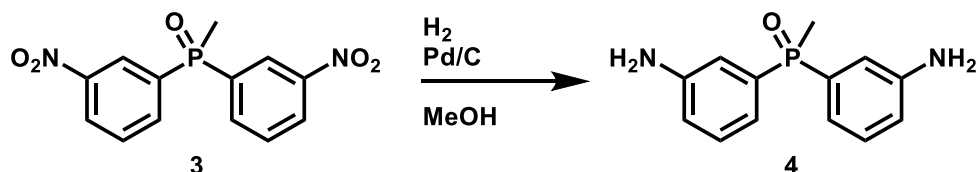
¹H NMR (400 MHz, CDCl₃) δ7.754-7.700 (m, 4 H); δ7.528-7.445 (m, 6 H); δ2.041-2.008 (d, J=13.2, 3 H).



Synthesis of methylbis(3-nitrophenyl)phosphine oxide, 3:

Dissolved **2** (1.00 g, 4.63 mmol) in 5.2 mL of concentrated H_2SO_4 . The solution was cooled to $0\text{ }^\circ\text{C}$. A separate solution of concentrated H_2SO_4 (1.8 mL) and HNO_3 (1.0 mL) was made while on ice. The acid mixture was added dropwise to the solution of **2**. After addition was complete the reaction mixture changed from clear to yellow. The reaction was stirred at $0\text{ }^\circ\text{C}$ for two hours and then for an additional 3 hours at room temperature. The mixture was poured over ice and extracted with CHCl_3 . The organic layer was collected and washed with a saturated NaHCO_3 solution (3X) and brine (1X). The organic layer was dried over anhydrous Na_2SO_4 and the solvent removed by rotary evaporation. Collected 1.40 g of a pale yellow solid (quantitative yield).

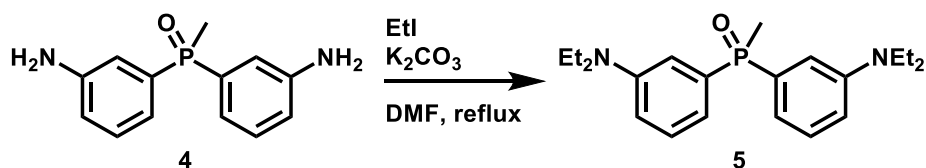
$^1\text{H NMR}$ (400 MHz, CDCl_3) δ 8.577-8.538 (dt, $J=1.8\text{ Hz}$, $J=12.2\text{ Hz}$, 2 H); δ 8.441-8.414 (dqnt, $J=1.1\text{ Hz}$, $J=8.2\text{ Hz}$, 2H); δ 8.154-8.107 (m, 2 H); δ 7.777-7.731 (td, $J=2.72\text{ Hz}$, $J=7.9\text{ Hz}$, 2 H); δ 2.221-2.188 (d, $J=13.4\text{ Hz}$, 3 H).



Synthesis of bis(3-aminophenyl)(methyl)phosphine oxide, 4:

Added **3** (0.25 g, 0.82 mmol) and 5% Pd/C (0.025 g, 10% wt) to a Schlenk flask. Evacuated the flask and backfilled using a balloon filled with H_2 . Added 10 mL of MeOH and stirred at room temperature for 12 hours. The reaction mixture was filtered through a pad of Celite. The pad was washed with acetone and the filtrate collected. The solvent was removed by rotary evaporation. Collected 0.20 g of crude product, 99% yield.

$^1\text{H NMR}$ (400 MHz, MeOD) δ 7.245-7.197 (td, $J=3.8\text{ Hz}$, $J=7.7\text{ Hz}$, 2 H); δ 7.016-6.936 (m, 4H); δ 6.876-6.856 (dqnt, $J=1.1\text{ Hz}$, $J=8.1\text{ Hz}$, 2 H); δ 2.221-2.188 (d, $J=13.4\text{ Hz}$, 3 H).

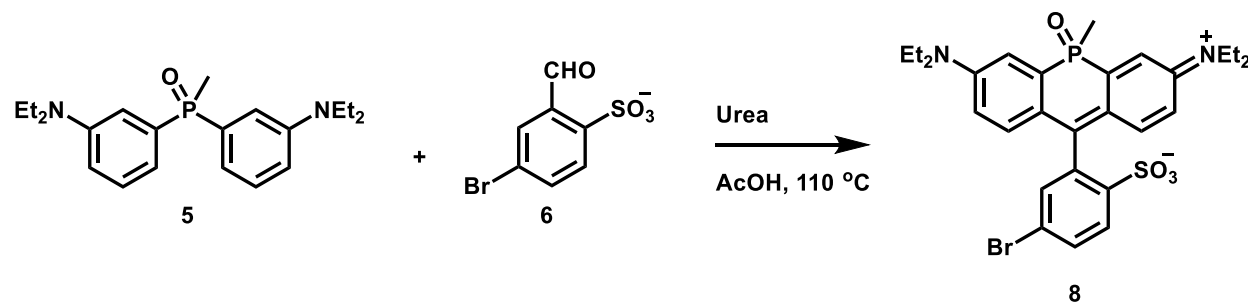


Synthesis of bis(3-(diethylamino)phenyl)(methyl)phosphine oxide, 5:

To **4** (5.83 g, 23.7 mmol) added 10 mL of dry DMF, EtI (10.0 mL, 124.4 mmol) and K_2CO_3 (16.4 g, 118.7 mmol). Refluxed for 12 hours. Removed DMF from reaction mixture by rotary evaporation. The remaining solid was redissolved in H_2O and extracted with DCM (3X). The organics layer was dried over Na_2SO_4 and

the solvent removed by rotary evaporation. The resulting residue was purified via flash column chromatography using silica as the stationary phase and 3% MeOH in DCM as the mobile phase. Collected 7.6 g of a golden oil (89% yield).

$^1\text{H NMR}$ (400 MHz, CDCl_3) δ 7.260-7.217 (m, 2 H); δ 7.108-7.073 (dm, $J=13.9$ Hz, 2 H); δ 6.880-6.833 (m, 2 H); δ 6.772-6.746 (dm, $J=8.3$ Hz, 2H); δ 3.378-3.326 (q, $J=7.1$ Hz, 8 H); δ 1.973-1.940 (d, $J=13.1$ Hz, 3 H); δ 1.143-1.108 (t, $J=7.0$ Hz, 12 H).



Synthesis of *m*-bromo tetraethylphosphorous rhodamine (*mBrTEPR*), **8**:

Dissolved **5** (0.100 g, 0.280 mmol), **6** (0.067 g, 0.25 mmol) and urea (0.030 g, 0.50 mmol) in 2 mL of glacial acetic acid. Stirred at 110 °C for 24 hours. The reaction mixture changed from clear yellow to a dark blue green. Once the mixture had cooled to room temperature the acetic acid was removed by rotary evaporation. The blue green residue was redissolved in saturated NaHCO_3 and extracted with 2:1 DCM:IPA (3X). The organic layer was collected and dried over Na_2SO_4 and the solvent removed by rotary evaporation. The product was obtained by purifying first with a silica column using a gradient from 2-20% MeOH in DCM, followed by a basic alumina column using a gradient from 0-2% MeOH in DCM. The first blue green band to elute was collected which corresponds to the *cis* isomer of **8**. The second blue green band to elute was also collected and contained the *trans* isomer of **8** but required further purification. The *trans* isomer was obtained using reverse phase HPLC using a gradient from 0-100% MeCN in H_2O with 0.05% formic acid. Collected 0.015 g of the major *cis* isomer as a black blue solid (10 % yield) and 1.6 mg of the minor *trans* isomer (1.1% yield).

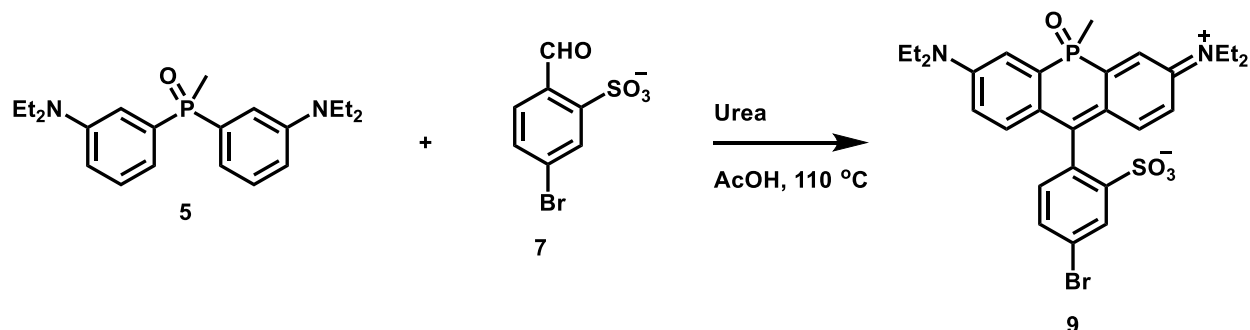
8 (*cis*) $^1\text{H NMR}$ (400 MHz, MeOD) δ 8.041-8.020 (d, $J=8.4$ Hz, 1 H); δ 7.868-7.842 (dd $J=2.0$ Hz, $J=8.4$ Hz, 1 H); δ 7.686-7.639 (dd $J=2.8$ Hz, $J=16.0$ Hz, 2 H); δ 7.478-7.473 (d $J=2.0$ Hz, 1 H); δ 7.111-7.073 (m, 2 H); δ 6.930-6.889 (dd $J=2.8$ Hz, $J=9.6$ Hz, 2 H); δ 3.838-3.722 (m, 8 H); δ 2.018-1.983 (d, $J=14.0$ Hz, 3 H); δ 1.355-1.319 (t, $J=7.2$ Hz, 12 H).

$^{31}\text{P NMR}$ (400 MHz, MeOD) δ 20.375.

8 (*trans*) $^1\text{H NMR}$ (400 MHz, MeOD) δ 8.057-8.036 (d, $J=8.4$ Hz, 1 H); δ 7.863-7.837 (dd $J=2.0$ Hz, $J=8.4$ Hz, 1 H); δ 7.677-7.630 (dd $J=2.8$ Hz, $J=16.0$ Hz, 2 H); δ 7.545-7.540 (d $J=2.0$ Hz, 1 H); δ 7.127-7.088 (m, 2 H); δ 6.915-6.884 (dd $J=2.8$ Hz, $J=9.6$ Hz, 2 H); δ 3.845-3.641 (m, 8 H); δ 1.963-1.929 (d, $J=13.6$ Hz, 3 H); δ 1.354-1.318 (t, $J=7.2$ Hz, 12 H).

$^{31}\text{P NMR}$ (400 MHz, MeOD) δ 18.389.

ESI MS, calculated for $[\text{M}]^+$, $\text{C}_{28}\text{H}_{33}\text{BrN}_2\text{O}_4\text{PS}^+$, 603.11; found: 603.1. HR-ESI-MS, calculated for $[\text{M}]^+$, $\text{C}_{28}\text{H}_{33}\text{BrN}_2\text{O}_4\text{PS}^+$, 603.1077, found 603.1075.



Synthesis of p-bromo tetraethylphosphorous rhodamine (pBrTEPR), 9:

Dissolved **5** (0.100 g, 0.280 mmol), **7** (0.067 g, 0.25 mmol) and urea (0.030 g, 0.50 mmol) in 2 mL of glacial acetic acid. Stirred at 110 °C for 24 hours. The reaction mixture changed from clear yellow to a dark blue green. Once the mixture had cooled to room temperature the acetic acid was removed by rotary evaporation. The blue green residue was redissolved in saturated NaHCO₃ and extracted with 2:1 DCM:IPA (3X). The organic layer was collected and dried over Na₂SO₄ and the solvent removed by rotary evaporation. The product was obtained by purifying first with a silica column using a gradient from 2-20% MeOH in DCM, followed by a basic alumina column using a gradient from 0-2% MeOH in DCM. The first blue green band to elute was collected which corresponds to the *trans* isomer of **9**. Collected 0.007 g of the *cis* isomer as a black blue solid (5 % yield). The second blue green band to elute contained the minor *trans* isomer with an impurity that had a mass corresponding to the dibrominated product. The *trans* isomer further purified via reverse phase HPLC using a gradient from 0-100% MeCN in H₂O with 0.05% formic acid. Collected 0.7 mg of the minor *trans* isomer (0.46 % yield).

9 (*cis*) ¹H NMR (400 MHz, MeOD) δ8.268-8.264 (d, J=2.0 Hz, 1 H); δ7.825-7.805 (dd, J=2.0Hz, J=8.1 Hz, 1 H); δ7.678-7.640 (dd, J=2.7 Hz, J=15.9 Hz, 2 H); δ7.194-7.177 (d, J=8.1 Hz, 1 H); δ7.102-7.072 (m, 2 H); δ6.914-6.890 (dd, J=2.5 Hz, J=9.6 Hz, 2 H); δ3.797-3.725 (m, 8 H); δ2.015-1.987 (d, J=14.0 Hz, 3 H); δ 1.345-1.317 (t, J=6.9 Hz, 12 H).

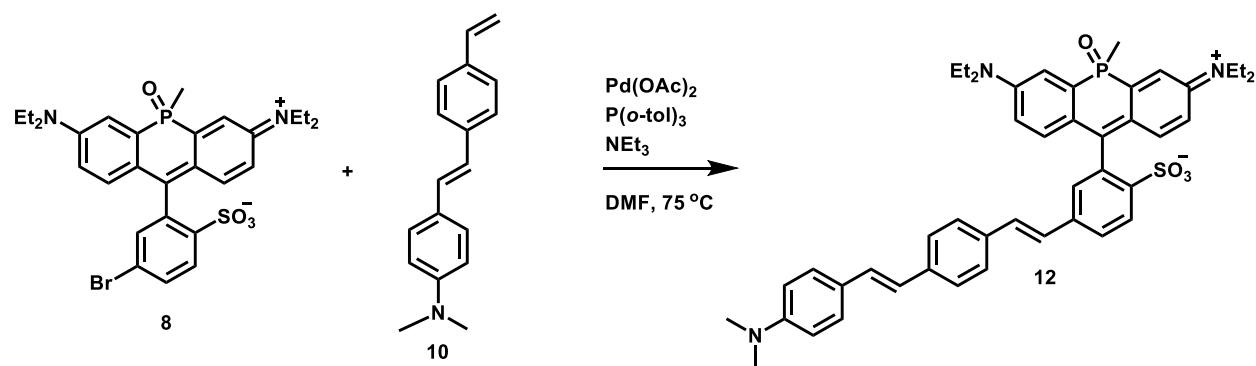
³¹P NMR (400 MHz, MeOD) δ20.325.

ε₇₀₂ (HBSS) = 86,000 M⁻¹ cm⁻¹

9 (*trans*) ¹H NMR (400 MHz, MeOD) δ8.286-8.281 (d, J=2.0 Hz, 1 H); δ7.800-7.775 (dd, J=2.0 Hz, J=8.2Hz, 2 H); δ7.673-7.627 (dd, J=2.6 Hz, J=16 Hz, 2 H); δ7.232-7.212 (d, J=8.2Hz, 1 H); δ7.124-7.085 (m, 2 H); δ 6.905-6.875 (dd, J=2.6 Hz, J=9.6 Hz); δ3.841-3.687 (m, 8 H); δ 1.948-1.914 (d, J=13.5 Hz); δ1.349-1.313 (t, J=7.0 Hz, 12 H).

³¹P NMR (400 MHz, MeOD) δ18.217.

ESI MS, calculated for [M]⁺, C₂₈H₃₃BrN₂O₄PS⁺, 603.11; found: 603.1. HR-ESI-MS, calculated for [M]⁺, C₂₈H₃₃BrN₂O₄PS⁺, 603.1077; found 603.1079, calculated for [M-H+Na]⁺, C₂₈H₃₂BrN₂O₄PSNa⁺, 625.0896; found 625.0899.



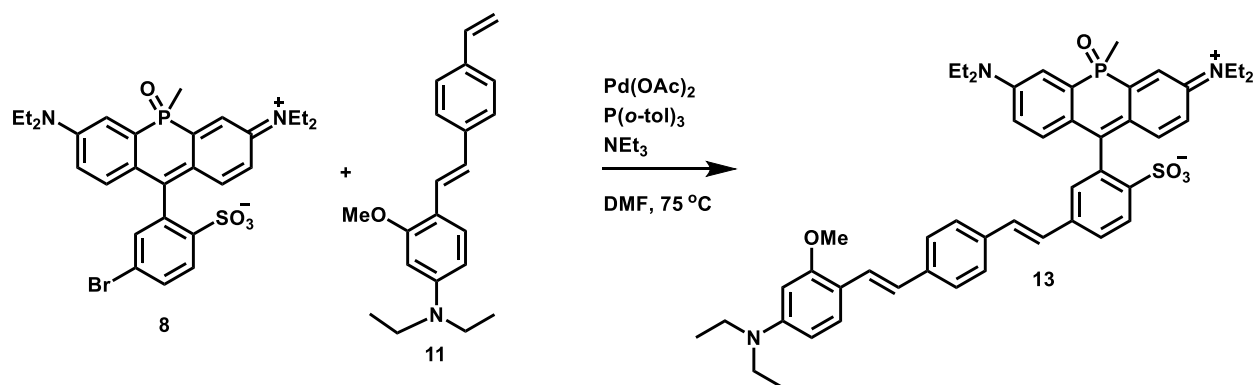
Synthesis of 12:

In an oven-dried flask added **8** (25 mg, 0.042 mmol), **10** (10 mg, 0.042 mmol), Pd(OAc)₂ (2.4 mg, 0.011 mmol) and P(o-tol)₃ (6.4 mg, 0.029 mmol). Evacuated and back-filled the flask with N₂ (3X). Dissolved the solids in 0.4 mL of dry DMSO and added dry NEt₃ (0.12 mL). Stirred at 75 °C for 18 hours. Once the reaction mixture cooled it was diluted with DCM and washed with H₂O (3X). The organic layer was washed with brine (1X) and dried over Na₂SO₄. The solvent was removed by rotary evaporation and the resulting residue was purified via prep TLC using 10% MeOH in DCM as the mobile phase. Further purified via reverse phase HPLC using a gradient from 0-100% MeCN in H₂O with 0.05% formic acid. Collected 1.1 mg of product (3.0 % yield).

¹H NMR (400 MHz, MeOD) δ 8.110-8.092 (d, J=8.3 Hz, 1 H); δ 7.874-7.851 (dd, J=1.4 Hz, J=8.3 Hz, 1 H); δ 7.682-7.651 (dd, J=2.7 Hz, J=15.8 Hz, 2 H); δ 7.543-7.529 (d, J=8.3 Hz, 2 H); δ 7.489-7.475 (d, J=8.3 Hz, 2 H); δ 7.422-7.408 (m, 3 H); δ 7.347-7.319 (d, J=16.4 Hz, 1 H); δ 7.243-7.189 (m, 3 H); δ 7.116-7.089 (d, J=16.3 Hz, 1 H); δ 6.946-6.891 (m, 3 H); δ 6.767-6.752 (d, J=8.9 Hz, 2 H); δ 3.794-3.729 (m, 8 H); δ 2.966 (s, 3.6 H); δ 2.031-2.008 (d, J=14 Hz, 3 H); δ 1.353-1.336 (t, J=6.9 Hz, 10 H).

ESI MS, calculated for [M+H]²⁺, C₄₆H₅₂N₃O₄PS²⁺, 386.67; found: 386.6.

HR-ESI-MS, calculated for [M]⁺, C₄₆H₅₁N₃O₄PS⁺, 772.3332; found 772.3321, calculated for [M-H+Na]⁺, C₄₆H₅₀N₃O₄PSNa⁺, 794.3152; found 794.3149,



Synthesis of 13:

In an oven-dried flask added **8** (14.3 mg, 0.0237 mmol), **11** (7.3 mg, 0.024 mmol), Pd(OAc)₂ (2.7 mg, 0.012 mmol) and P(*o*-tol)₃ (7.2 mg, 0.024 mmol). Evacuated and back-filled the flask with N₂ (3X). Dissolved the solids in 1 mL of dry DMF and added NEt₃ (0.13 mL). Stirred at 75 °C for 2 hours before adding another 2.7 mg of Pd(OAc)₂. After the second addition of catalyst allowed the reaction to stir for an additional 12 hours. The product was obtained by purifying the reaction mixture via prep TLC using 10% MeOH in DCM as the mobile phase. Collected a green solid that was a mixture of isomers (9.8 mg, 50% yield). To separate the two isomers further purification was required. The solvent was removed from the reaction mixture and the remaining residue was first purified on an alumina column using 0-5% MeOH in DCM as the mobile phase. Two green solids were collected and are further purified via reverse phase HPLC with 0-100% MeCN in H₂O with 0.05% formic acid. Collected 1.8 mg of the major *cis* product (9.0 % yield) and 0.2 mg of the minor *trans* product (1.0 % yield).

13 (*cis*) ¹H NMR (400 MHz, MeOD) δ8.054-8.033 (d, J=8.3 Hz, 1 H); δ7.766-7.740 (dd, J=1.76 Hz, J=8.3 Hz, 1 H); δ7.652-7.605 (dd, J=2.7 Hz, J=15.9 Hz, 2 H); δ7.459-7.344 (m, 7 H); δ7.266-7.226 (d, J=16.3 Hz, 1 H); δ7.163-7.100 (m, 3 H); δ6.902-6.861 (d, J=16.4 Hz, 1 H); δ6.822-6.791 (dd, J=2.7 Hz, J=9.7 Hz, 2 H); δ6.345-6.317 (dd, J=2.4 Hz, J=8.8 Hz, 1 H); δ6.253-6.247 (d, J=2.4 Hz, 1 H); δ3.873 (s, 3 H); δ3.757-3.722 (m, 8 H); δ3.444-3.392 (q, J=7.0 Hz, 4 H); δ2.002-1.967 (d, J=14.0, 3 H); δ1.339-1.303 (t, J=7.0 Hz, 12 H); δ1.205-1.170 (t, J=7.0 Hz, 6 H).

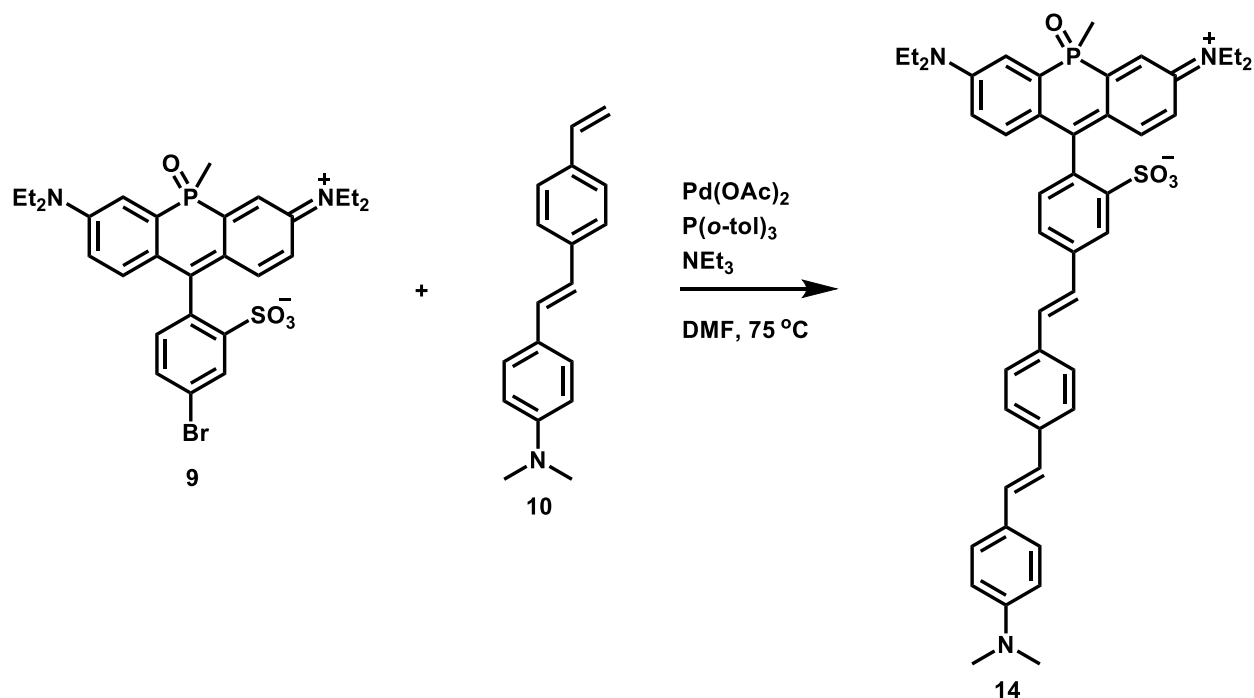
³¹P NMR (400 MHz, MeOD) δ20.204.

13 (*trans*) ¹H NMR (400 MHz, MeOD) δ8.437 (s, 4 H); δ8.129-8.108 (d, J=8.2 Hz, 1 H); δ7.873-7.848 (dd, J=1.7 Hz, J=8.2 Hz, 1 H); δ7.687-7.640 (dd, J=2.8 Hz, J=16.0 Hz, 2 H); δ7.528-7.507 (d, J=8.4 Hz, 2 H); δ7.459-7.320 (m, 6 H); δ7.244-7.188 (m, 3 H); δ6.930-6.884 (m, 3 H); δ6.345-6.317 (dd, J=2.4 Hz, J=8.7 Hz, 1 H); δ6.256-6.250 (d, J=2.4 Hz, 1 H); δ3.874 (s, 3 H); δ3.843-3.691 (m, 8 H); δ3.446-3.394 (q, J=7.04 Hz, 4 H); δ 2.006-1.972 (d, J=13.5 Hz, 3 H); δ1.354-1.319 (t, J=6.9 Hz, 12 H); δ1.205-1.170 (t, J=7.0 Hz, 6 H).

³¹P NMR (400 MHz, MeOD) δ18.209.

ESI MS, calculated for [M]⁺, C₄₉H₅₇N₃O₅PS⁺, 830.38; found 830.4; [M+H]²⁺, C₄₉H₅₈N₃O₅PS²⁺, 415.69; found: 415.7.

HR-ESI-MS, calculated for [M]⁺, C₄₉H₅₇N₃O₅PS⁺, 830.3751; found 830.3732, calculated for [M-H+Na]⁺, C₄₉H₅₆N₃O₅PSNa⁺, 852.3571; found 852.3570.



Synthesis of 14:

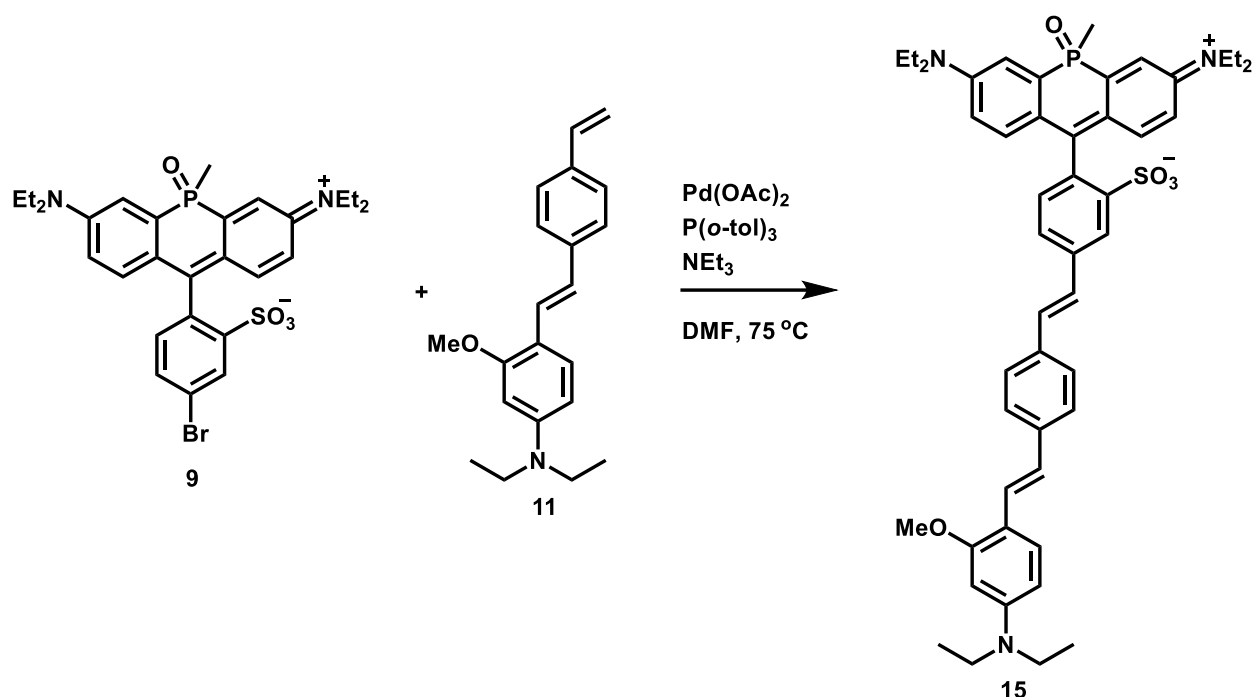
In an oven-dried flask added **9** (5.8 mg, 0.0096 mmol), **10** (2.5 mg, 0.0096 mmol), Pd(OAc)₂ (1.1 mg, 0.0048 mmol) and P(*o*-tol)₃ (2.9 mg, 0.0038 mmol). Evacuated and back-filled the flask with N₂ (3X). Dissolved the solids in 1 mL of dry DMF and added NEt₃ (0.05 mL). Stirred at 75 °C for 2 hours. The product was obtained by purifying the reaction mixture via prep TLC using 10% MeOH in DCM as the mobile phase. Collected 6.7 mg of a green solid (90% yield).

¹H NMR (600 MHz, MeOD) δ 8.550 (s, 1 H, formate); δ 8.313-8.311 (d, J=0.8 Hz, 1 H); δ 7.833-7.818 (dd, J=0.9 Hz, J=8.8 Hz, 1 H); δ 7.672-7.642 (dd, J=2.5 Hz, J=15.8 Hz, 2 H); δ 7.607-7.593 (d, J=8.2 Hz, 2 H); δ 7.537-7.524 (d, J=8.2 Hz, 2 H); δ 7.440-7.426 (d, J=8.7 Hz, 2 H); δ 7.409-7.381 (d, J=16.4 Hz, 1 H); δ 7.346-7.319 (d, J=16.4 Hz, 1 H); δ 7.223-7.173 (m, 3 H); δ 7.147-7.120 (d, J=16.3 Hz, 1 H); δ 6.976-6.949 (d, J=16.3 Hz, 1 H); δ 6.906-6.885 (dd, J=2.6 Hz, J=9.7 Hz, 2 H); δ 6.776-6.762 (d, J=8.7 Hz, 2 H); δ 3.813-3.716 (m, 8 H); δ 2.030-2.007 (d, J=13.9 Hz, 3 H); δ 1.343-1.321 (t, J=6.5 Hz, 12 H).

³¹P NMR (400 MHz, MeOD) δ 20.359.

ESI MS, calculated for [M+]⁺, C₄₆H₅₁N₃O₄PS⁺, 772.33; found 772.3; [M+H]²⁺, C₄₆H₅₂N₃O₄PS²⁺, 386.67; found: 386.7.

HR-ESI-MS, calculated for [M+]⁺, C₄₆H₅₁N₃O₄PS⁺, 772.3332; found 772.3344, calculated for [M+H]²⁺, C₄₆H₅₂N₃O₄PS²⁺, 386.6703; found 386.6707, calculated for [M+H+Na]²⁺, C₄₆H₅₁N₃O₄PSNa²⁺, 397.6612; found 397.6617.



Synthesis of 15:

In an oven-dried flask added **9** (50 mg, 0.083 mmol), **11** (26 mg, 0.083 mmol), Pd(OAc)₂ (4.7 mg, 0.021 mmol) and P(o-tol)₃ (12.8 mg, 0.042 mmol). Evacuated and back-filled the flask with N₂ (3X). Dissolved the solids in 0.5 mL of dry DMF and added dry NEt₃ (0.02 mL). Stirred at 75 °C for 12 hours. The product was obtained by purifying the reaction mixture via prep TLC using 10% MeOH in DCM as the mobile phase. further purified via reverse phase HPLC using a gradient from 0-100% MeCN in H₂O with 0.05% formic acid. Collected 4.5 mg of a green solid (6.5% yield).

¹H NMR (600 MHz, MeOD) δ 8.305 (s, 1 H); δ 7.809-7.796 (d, J=7.92 Hz, 1 H); δ 7.665-7.635 (dd, J=2.34 Hz, J=15.78 Hz, 2 H); δ 7.573-7.560 (d, J=8.1 Hz, 2 H); δ 7.485-7.472 (d, J=8.1 Hz, 2 H); δ 7.448-7.406 (m, 2 H); δ 7.387-7.360 (d, J=16.3 Hz, 1 H); δ 7.318-7.291 (d, J=16.3 Hz, 1 H); δ 7.203-7.167 (m, 3 H); δ 6.948-6.921 (d, J=16.4 Hz, 1 H); δ 6.891-6.870 (dd, J=2.5 Hz, J=12.2 Hz, 2 H); δ 6.351-6.334 (dd, J=1.3 Hz, J=8.7 Hz, 1 H); δ 6.266-6.264 (d, J=1.5 Hz, 1 H); δ 3.801-3.709 (m, 8 H); δ 3.442-3.407 (q, J=7.0 Hz, 4 H); δ 3.887 (s, 3 H); δ 2.026-2.002 (d, J=14.0 Hz, 3 H); δ 1.339-1.316 (t, J=6.8 Hz, 12 H); δ 1.206-1.83 (t, J=7.0 Hz, 6 H).

³¹P NMR (400 MHz, MeOD) δ 20.322. ESI MS, calculated for [M+H]²⁺, C₄₉H₅₈N₃O₅PS²⁺, 415.69; found: 415.7. HR-ESI-MS, calculated for [M]⁺, C₄₉H₅₇N₃O₅PS⁺, 830.3751; found 830.3729, calculated for [M+Na]⁺, C₄₉H₅₆N₃O₅PSNa⁺, 852.3571; found 852.3570,

Synthesis of 6, 7, 10 & 11:

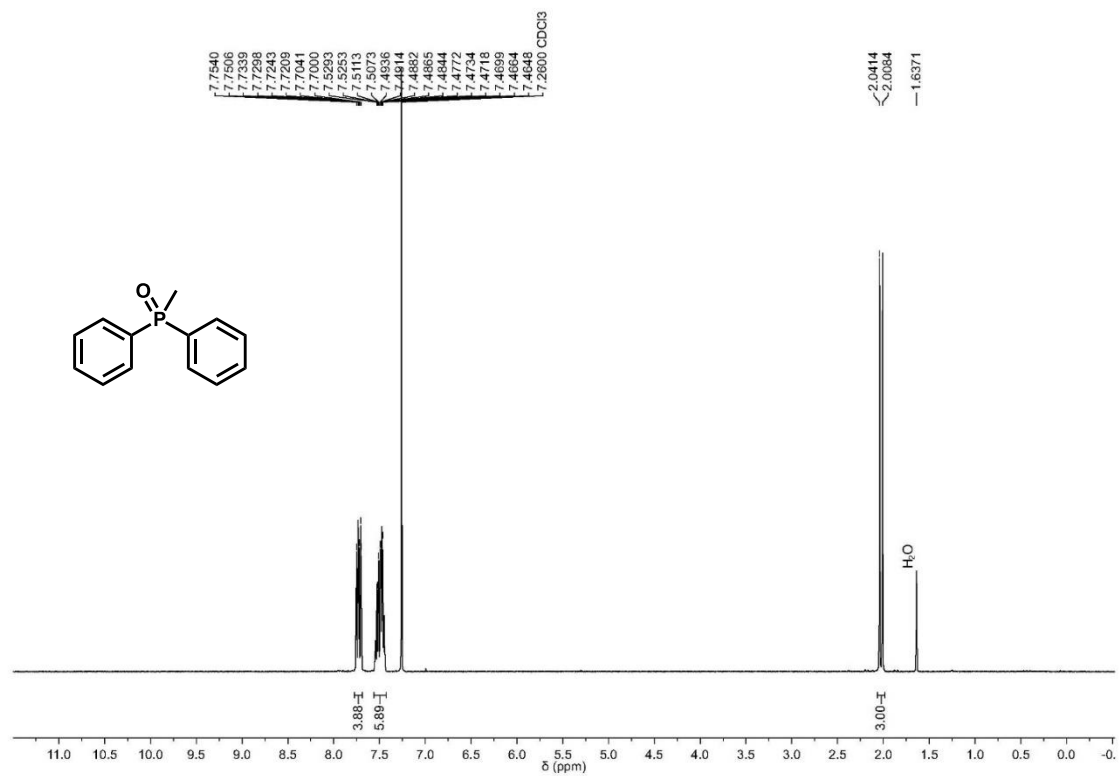
Synthesis of these compounds can be found in Kulkarni, R.U.; Yin, H.; Pourmandi, N.; James, F.; Adil, M.M.; Schaffer, D.V.; Wang, Y.; Miller, E.W.; ACS Chem. Biol. **12**, 407–413 (2017)

References

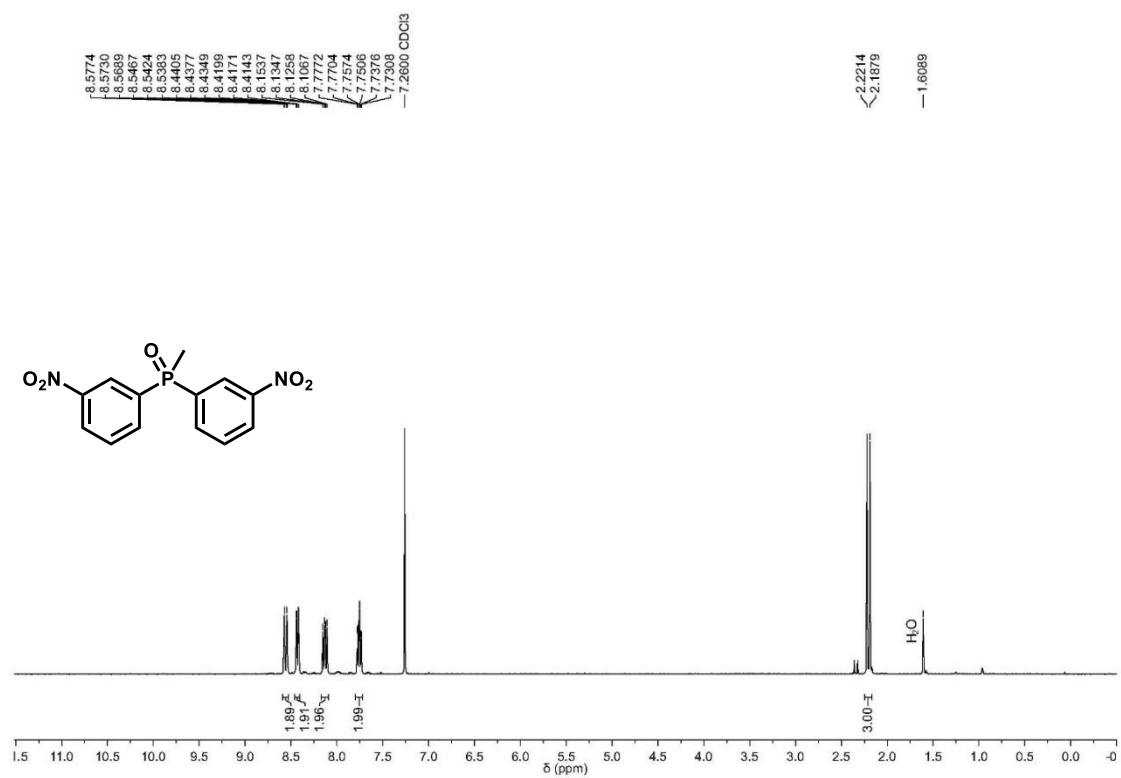
1. Chai, X.; Cui, X.; Wang, B.; Yang, F.; Cai, Y.; Wu, Q.; Wang, T., Near-Infrared Phosphorus-Substituted Rhodamine with Emission Wavelength above 700 nm for Bioimaging. *Chemistry – A European Journal* **2015**, *21* (47), 16754-16758.
2. Fery-Forgues, S.; Lavabre, D., Are Fluorescence Quantum Yields So Tricky to Measure? A Demonstration Using Familiar Stationery Products. *J Chem Educ* **1999**, *76*, 1260-1264.

Supplemental Spectra

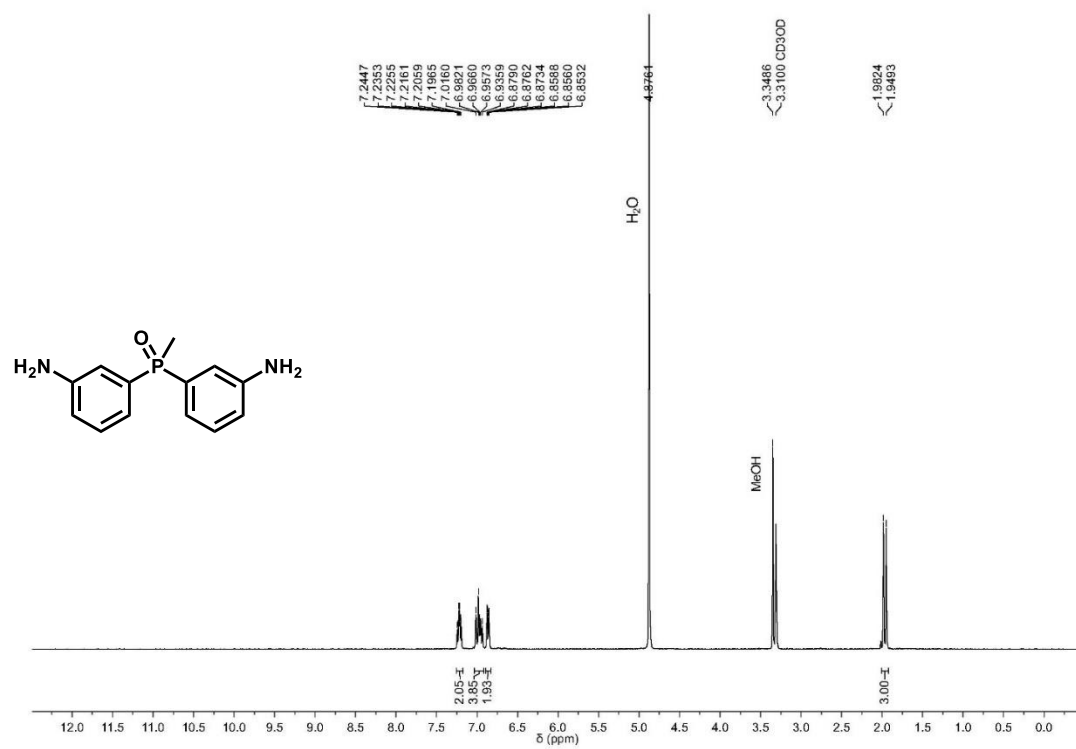
Spectrum S1. ¹H NMR methylphenylphosphine oxide, **2**



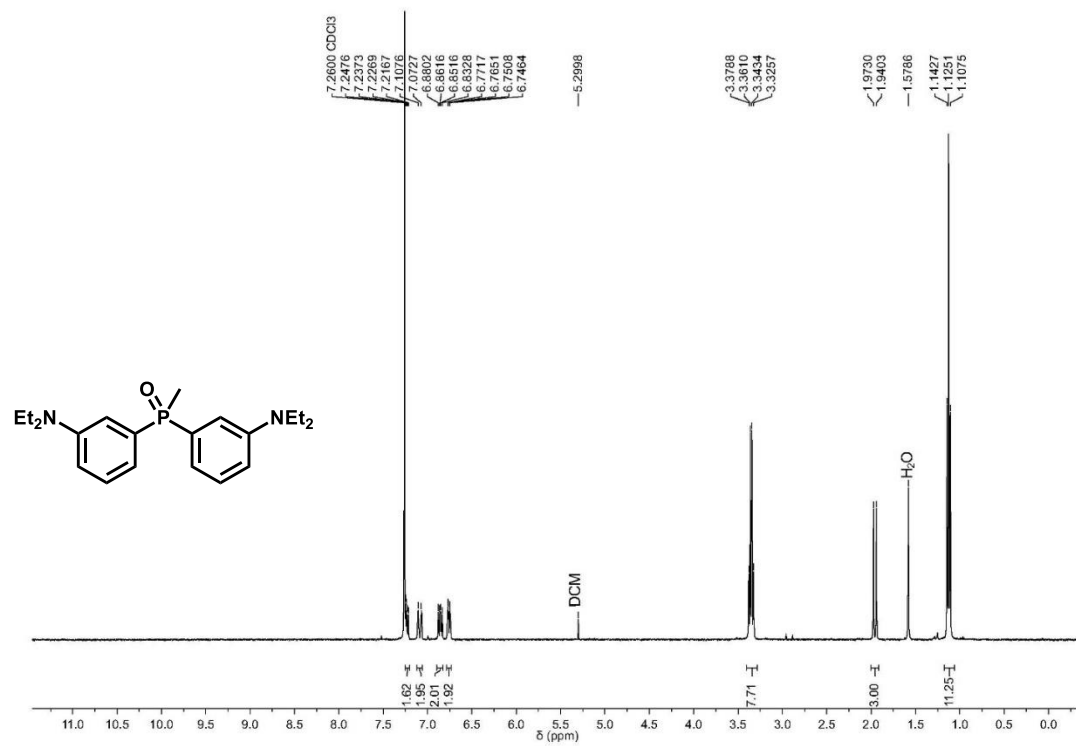
Spectrum S2. ¹H NMR methylbis(3-nitrophenyl)phosphine oxide, **3**



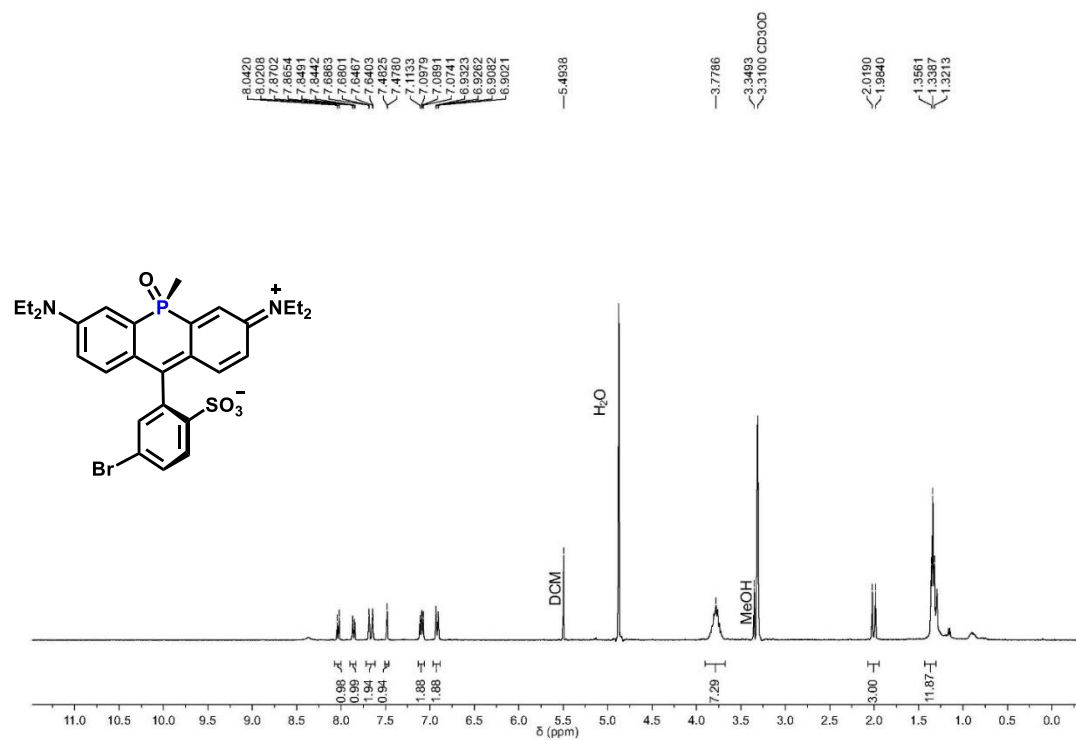
Spectrum S3. ¹H NMR bis(3-aminophenyl)(methyl)phosphine oxide, **4**



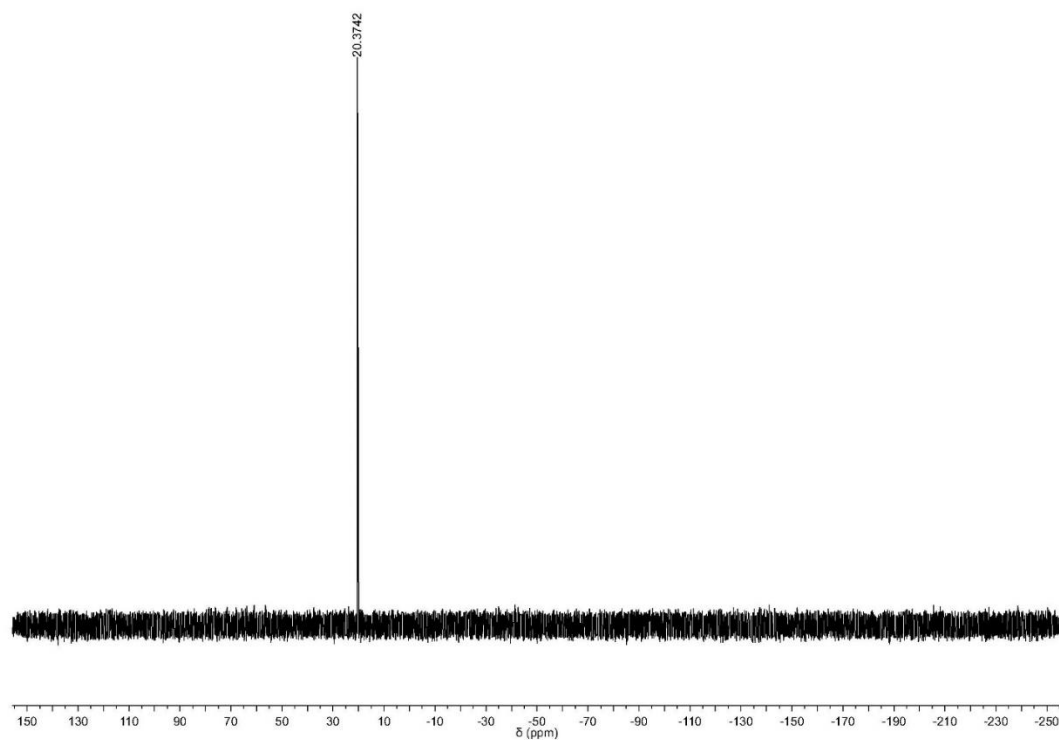
Spectrum S4. ¹H NMR bis(3-(diethylamino)phenyl)(methyl)phosphine oxide, **5**



Spectrum S5. ^1H NMR *m*-bromosulfo-phosphine oxide rhodamine (*cis*), **8**

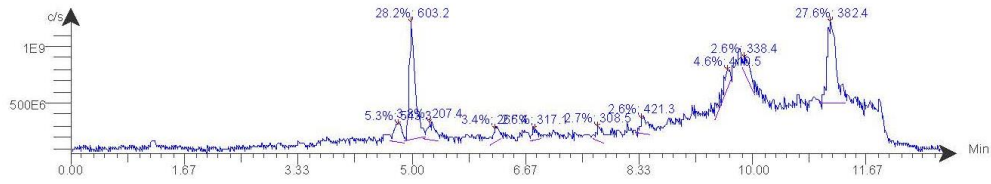


Spectrum S6. ^{31}P NMR *m*-bromosulfo-phosphine oxide rhodamine (*cis*), **8**

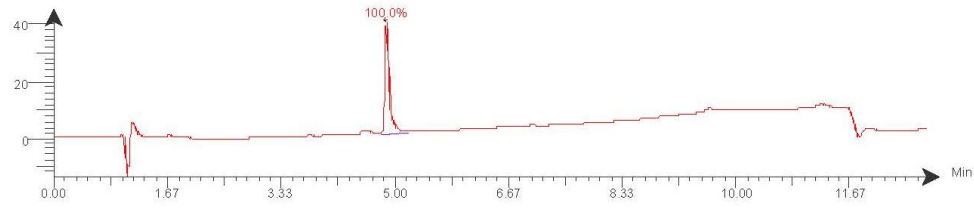


Spectrum S7. LC/MS traces *m*-bromosulfo-phosphine oxide rhodamine (*cis*), **8**

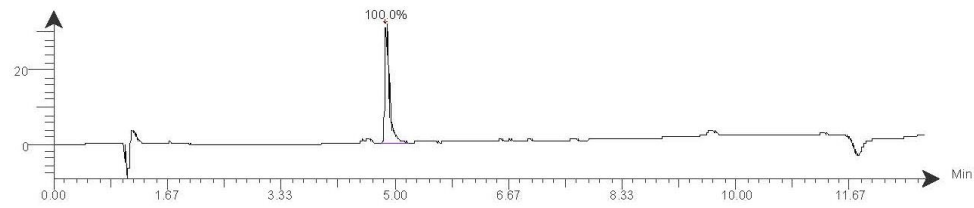
TIC
mBrPRmajor_1.dabx 2019.07.03 20:10:44 ;
ESI +



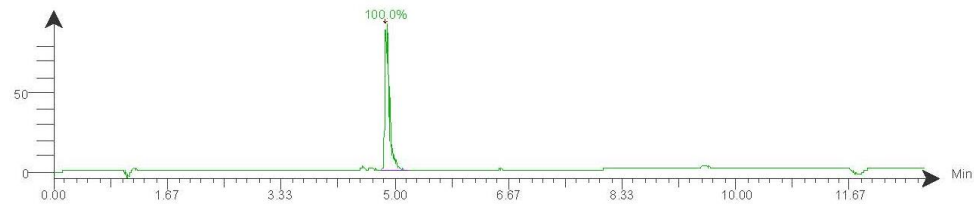
DAD: Signal B, 254 nm/Bw 4 nm
mBrPRmajor_1.dabx 2019.07.03 20:10:44 ;



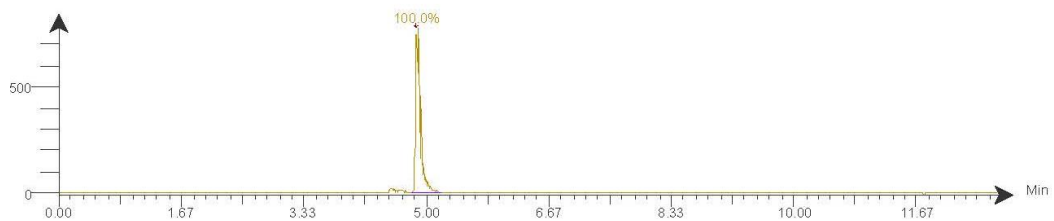
DAD: Signal C, 280 nm/Bw 4 nm
mBrPRmajor_1.dabx 2019.07.03 20:10:44 ;



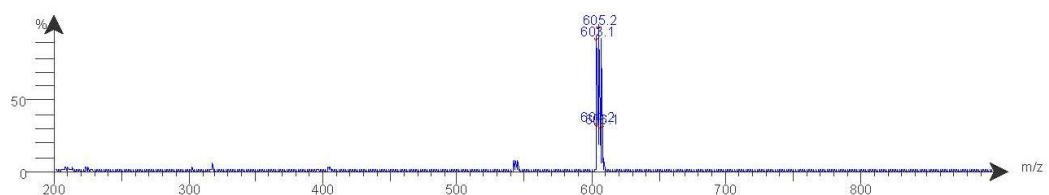
DAD: Signal D, 350 nm/Bw 4 nm
mBrPRmajor_1.dabx 2019.07.03 20:10:44 ;



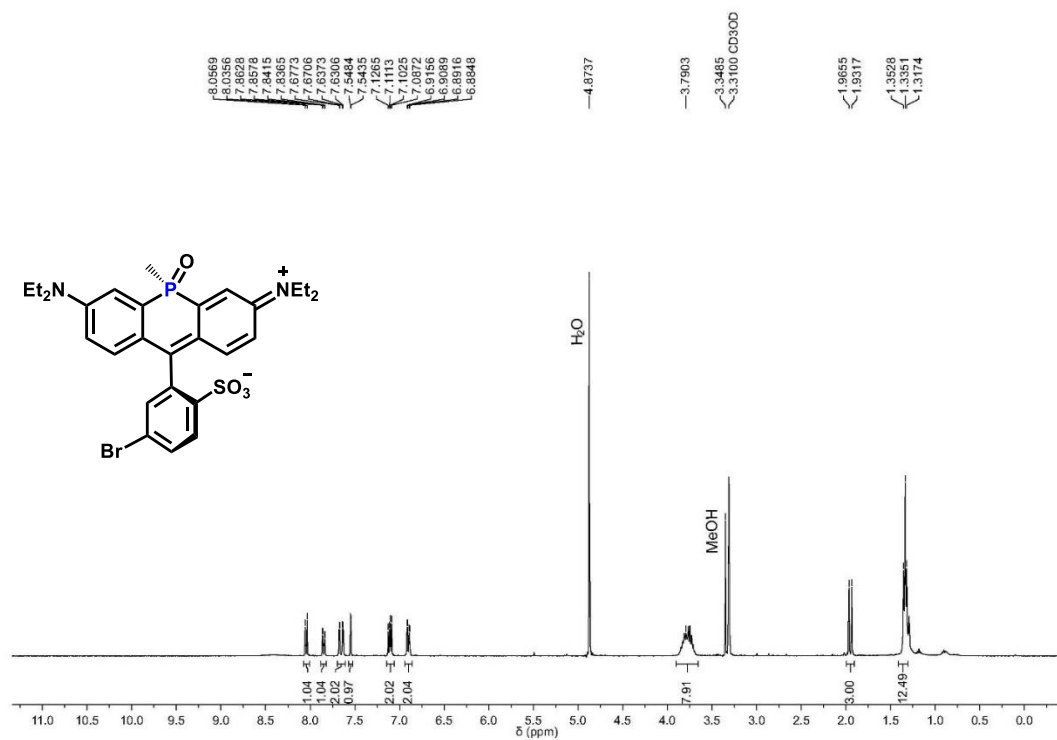
Intensity DAD: Signal E, 690 nm/Bw:4 nm
mBrPRmajor_1.datx 2019.07.03 20:10:44 ;



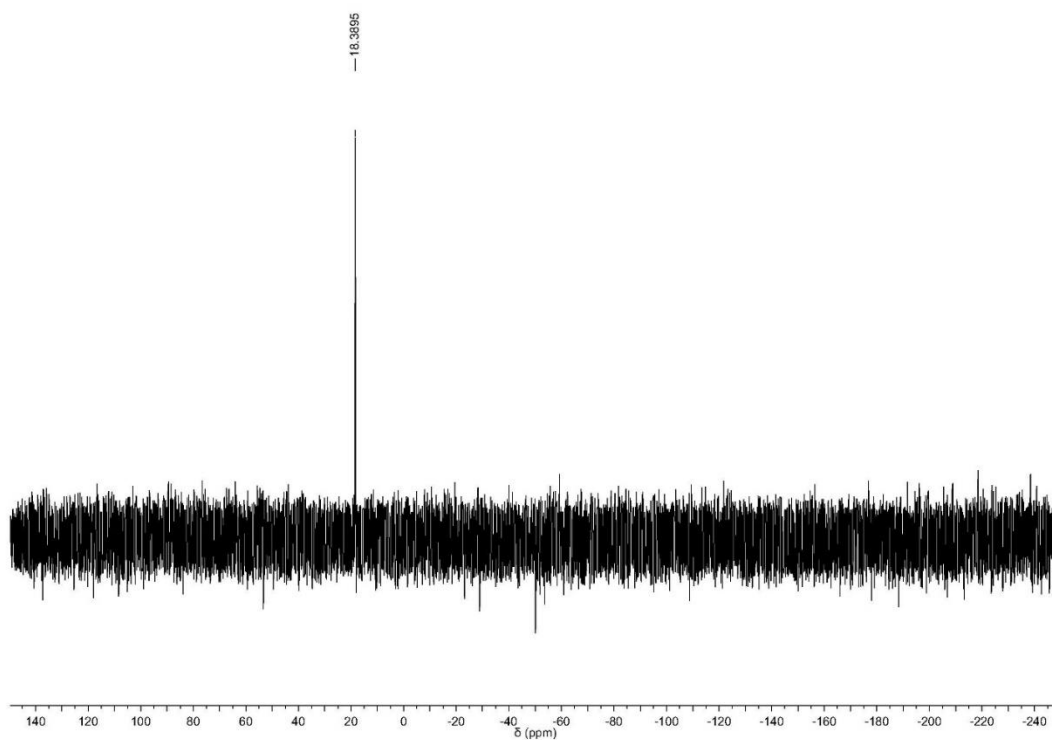
Intensity Spectrum RT 4.81 - 5.17 (63 scans)
mBrPRmajor_1.datx 2019.07.03 20:10:44 ;
ESI + Max: 7.3E6



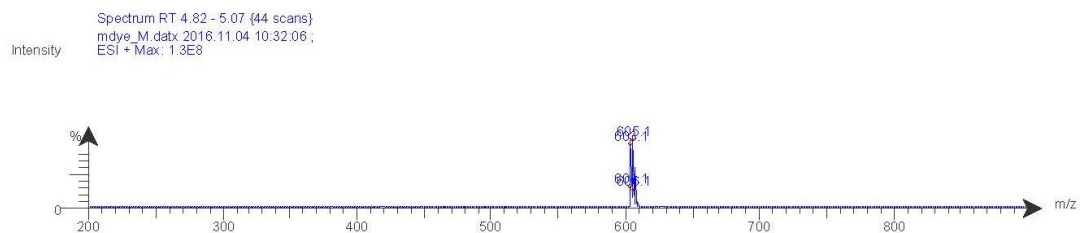
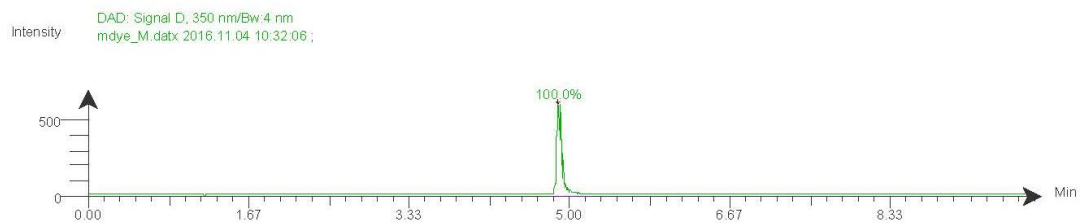
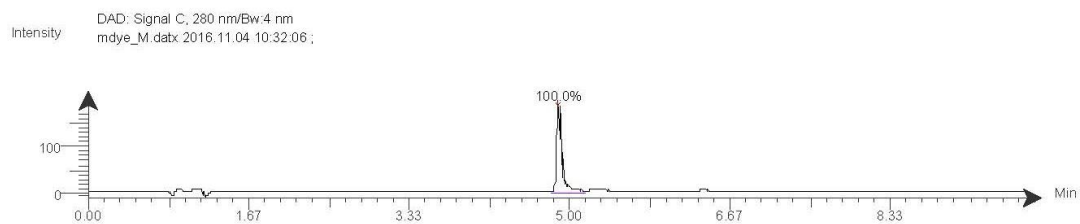
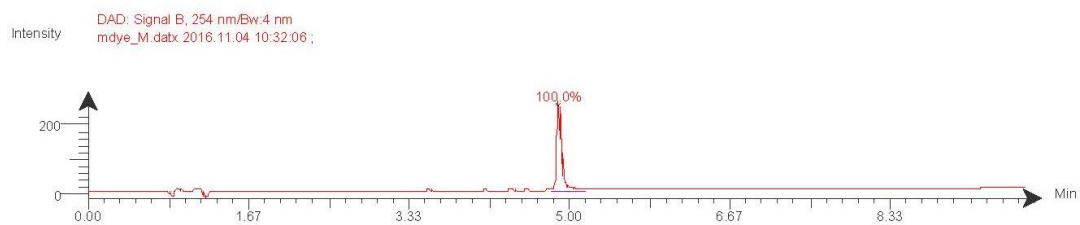
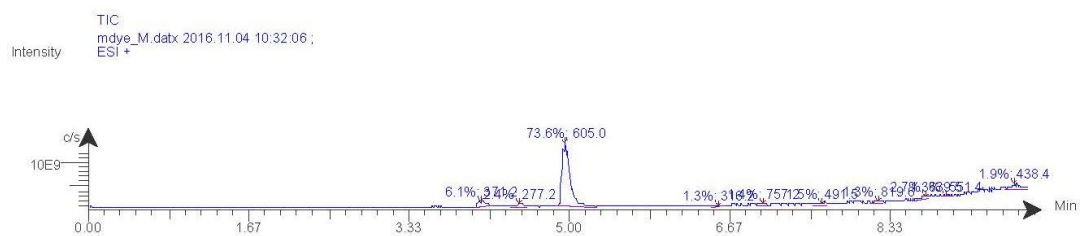
Spectrum S8. ¹H NMR *m*-bromosulfo-phosphine oxide rhodamine (*trans*), **8**



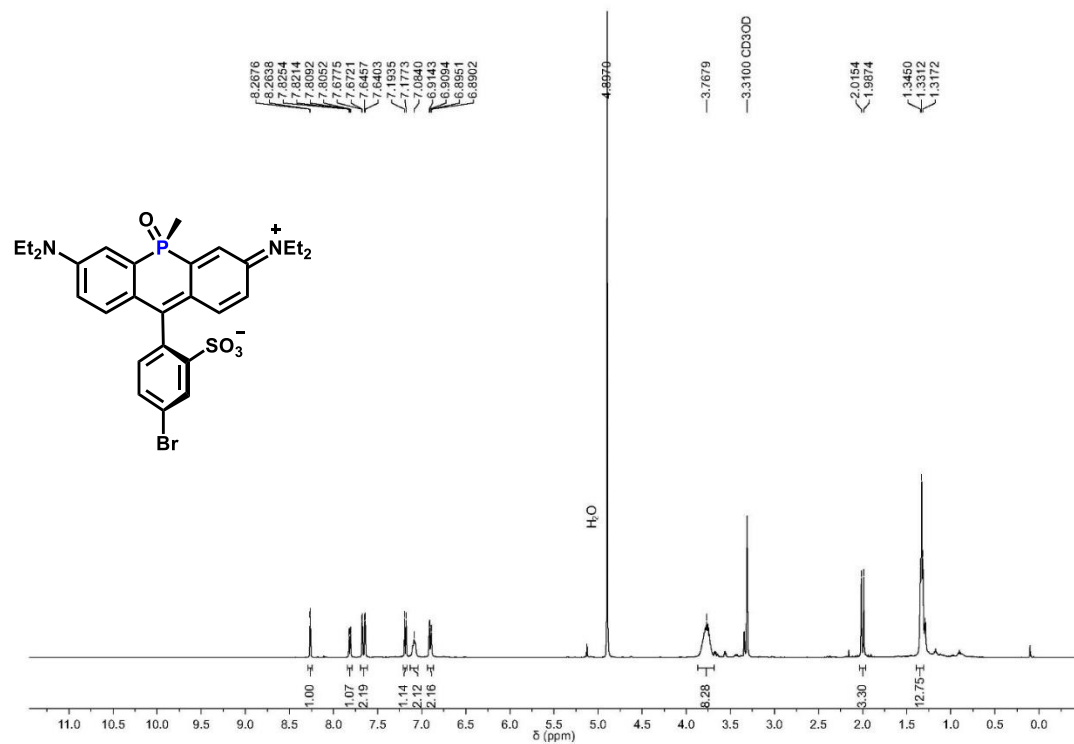
Spectrum S9. ³¹P NMR *m*-bromosulfo-phosphine oxide rhodamine (*trans*), **8**



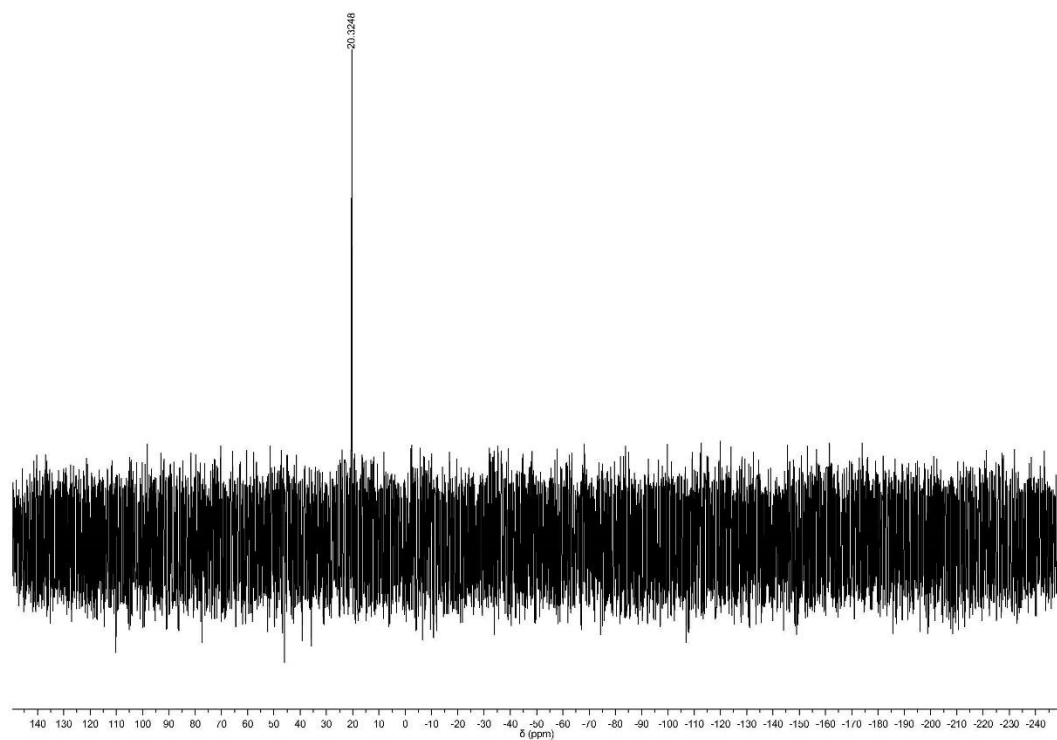
Spectrum S10. LC/MS traces m-bromosulfo-phosphine oxide rhodamine (trans), 8



Spectrum S11. ¹H NMR *p*-bromosulfo-phosphine oxide rhodamine (*cis*), **9**

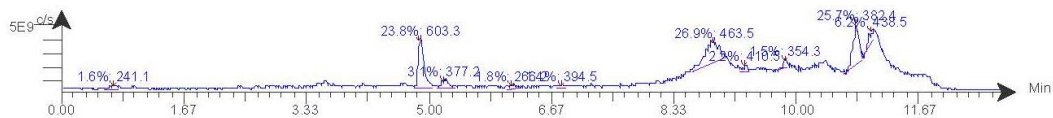


Spectrum S12. ³¹P NMR *p*-bromosulfo-phosphine oxide rhodamine (*cis*), **9**

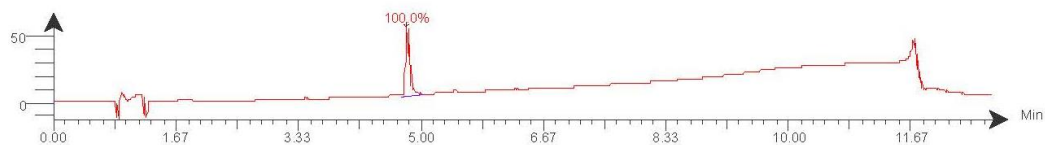


Spectrum S13. LC/MS traces *p*-bromosulfo-phosphine oxide rhodamine (cis), 9

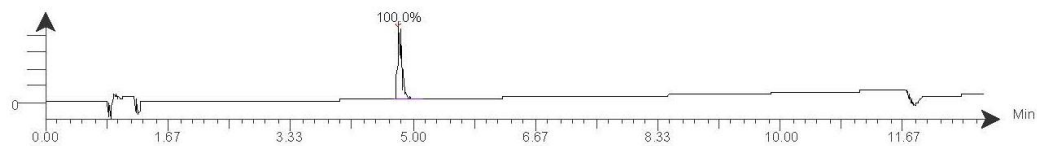
TIC
pBrTEPR_trans_datx 2017.05.16 12:52:14 ;
Intensity
ESI +



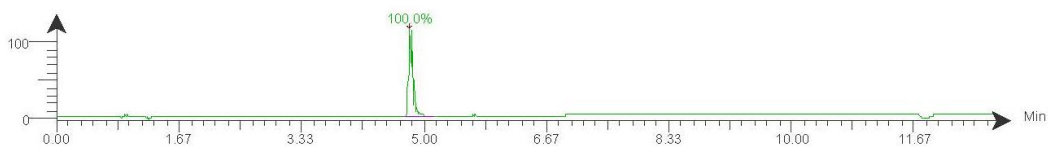
DAD: Signal B, 254 nm/Bw:4 nm
pBrTEPR_trans_datx 2017.05.16 12:52:14 ;
Intensity



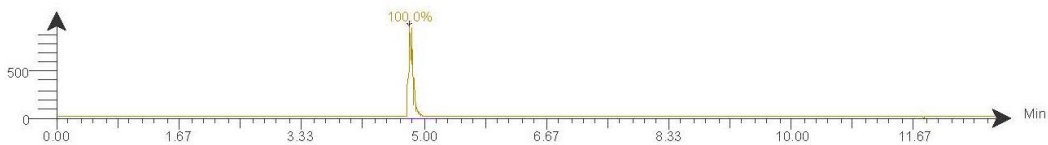
DAD: Signal C, 280 nm/Bw:4 nm
pBrTEPR_trans_datx 2017.05.16 12:52:14 ;
Intensity



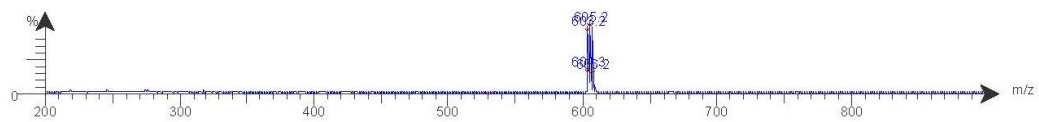
DAD: Signal D, 350 nm/Bw:4 nm
pBrTEPR_trans_datx 2017.05.16 12:52:14 ;
Intensity



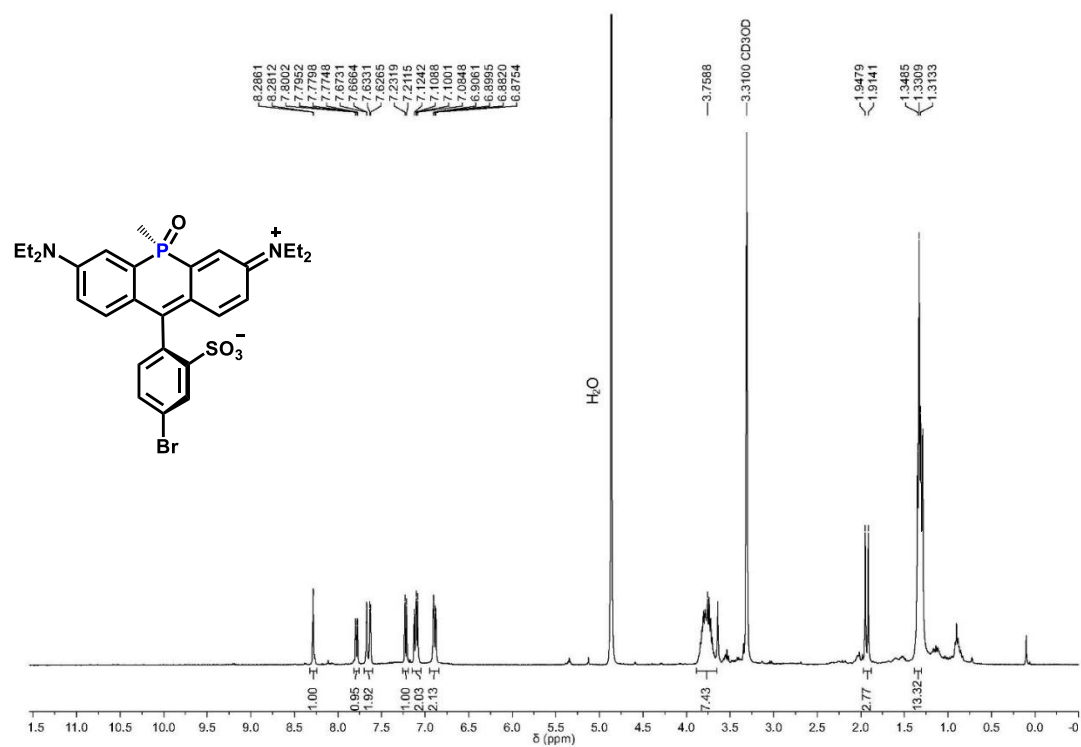
DAD: Signal E, 690 nm/Bw:4 nm
pBrTEPR_trans_datx 2017.05.16 12:52:14 ;
Intensity



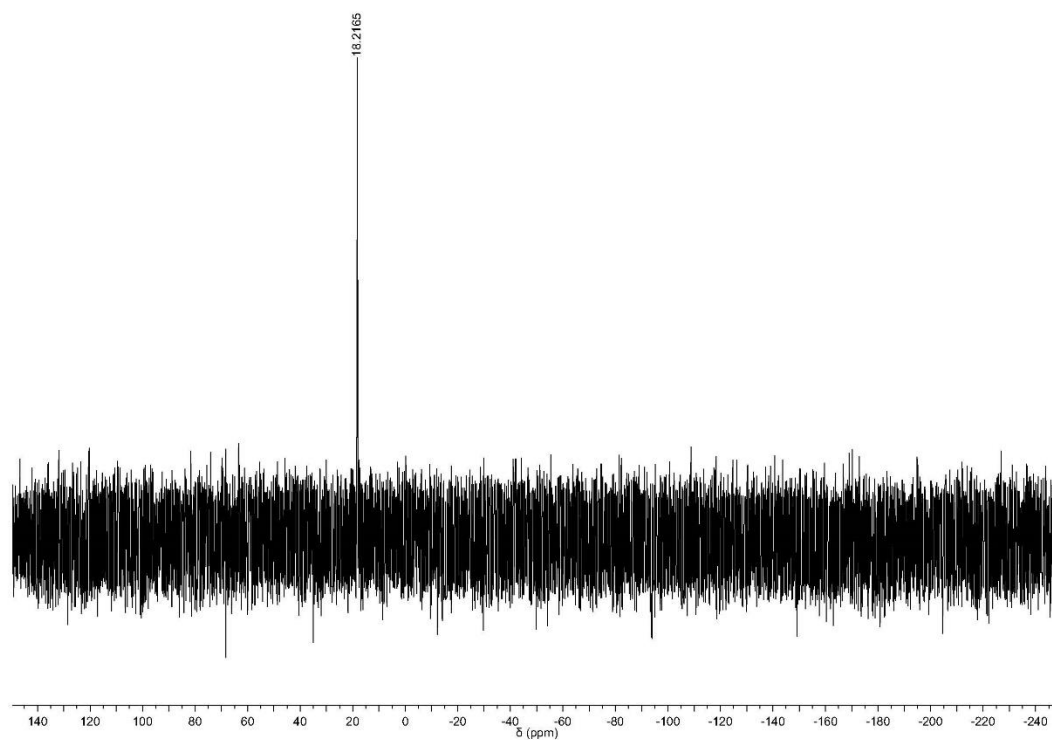
Spectrum RT 4.71 - 5.13 (72 scans)
pBrTEPR_trans_dabx 2017.05.16 12.52.14;
ESI + Max: 1.7E7



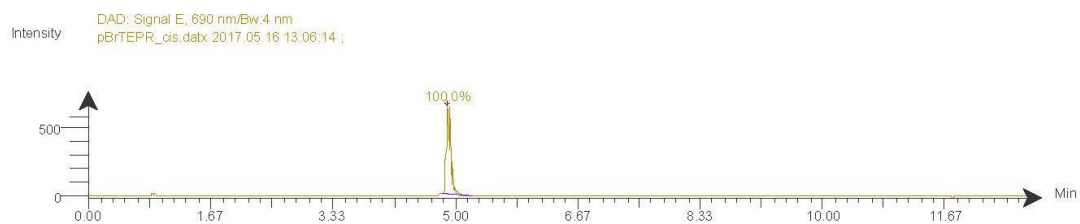
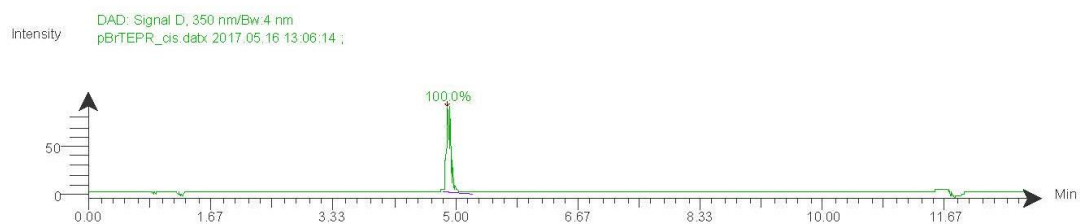
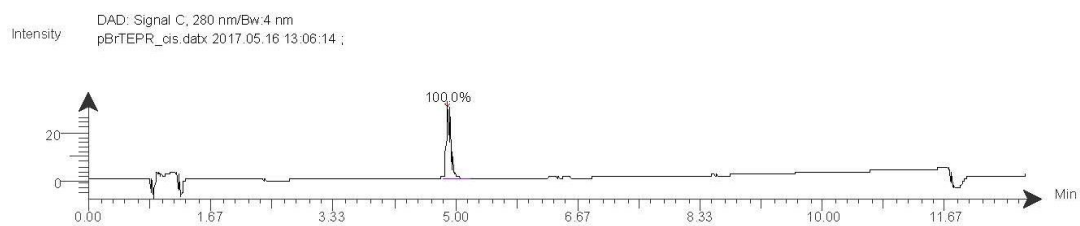
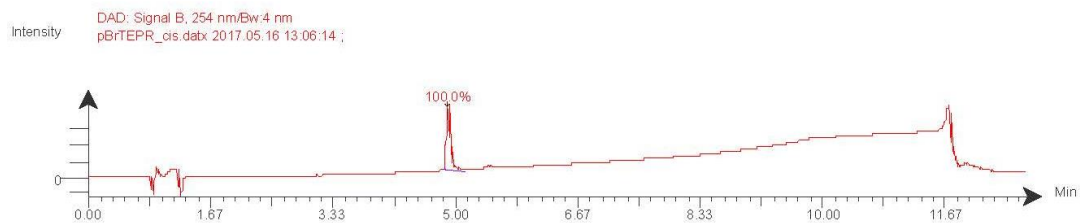
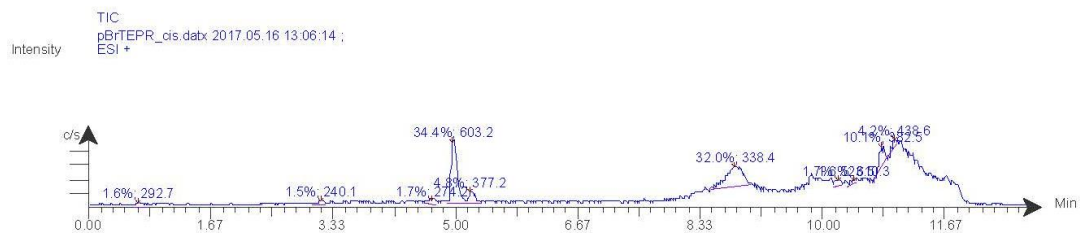
Spectrum S14. ¹H NMR *p*-bromosulfo-phosphine oxide rhodamine (*trans*), **9**



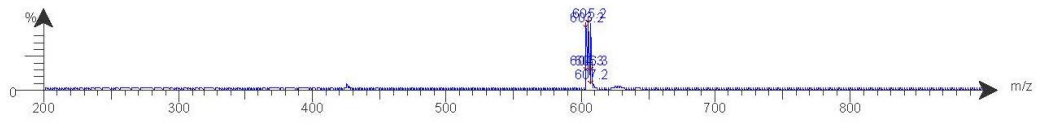
Spectrum S15. ³¹P NMR *p*-bromosulfo-phosphine oxide rhodamine (*trans*), **9**



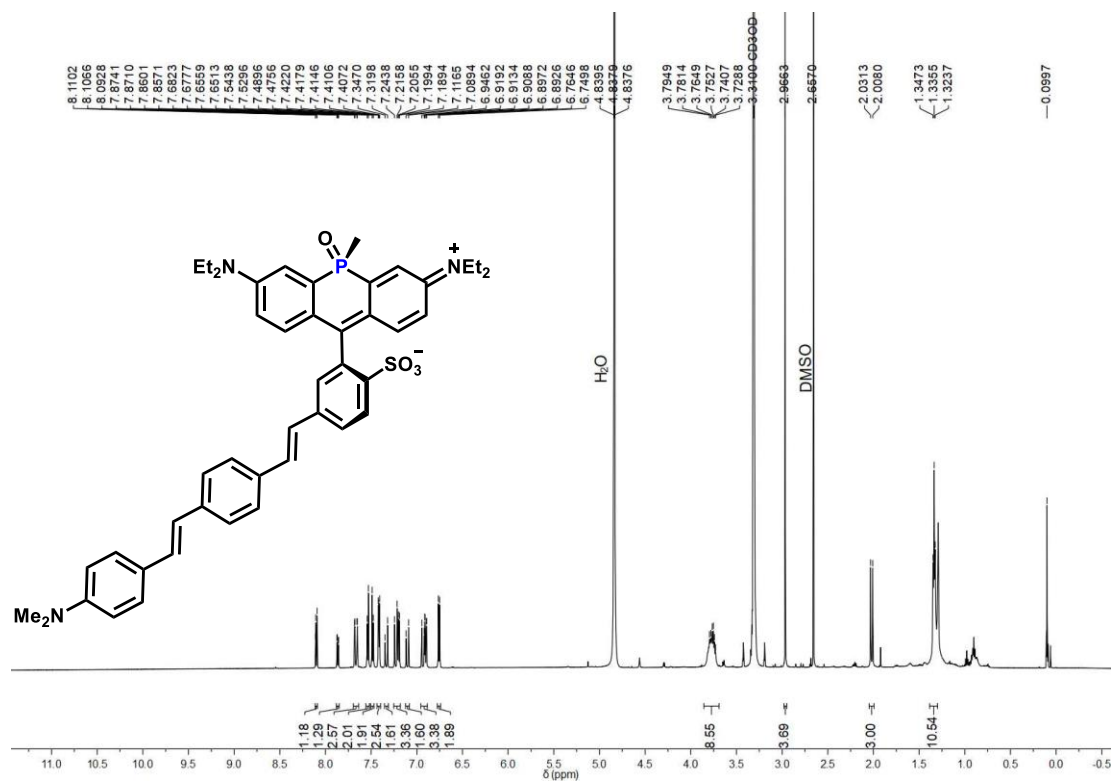
Spectrum S16. LC/MS traces *p*-bromosulfo-phosphine oxide rhodamine (trans), 9



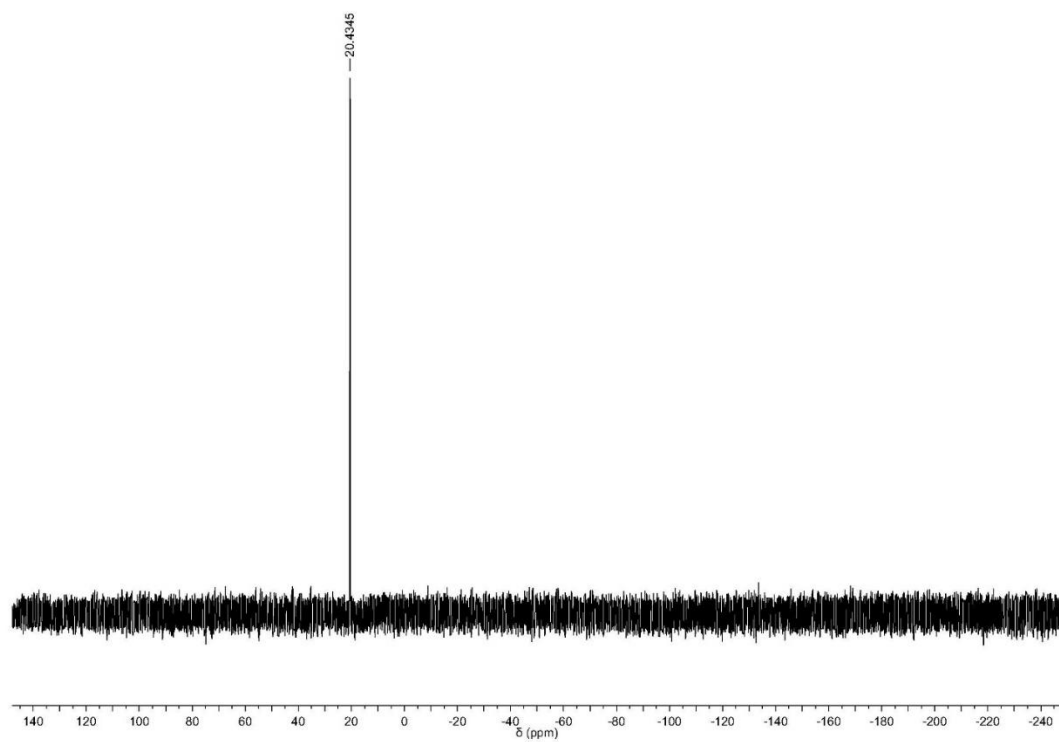
Spectrum RT 4.75 - 5.17 (73 scans)
pBrTEPR_cis.dabx 2017.05.16 13.06:14 ;
ESI + Max: 2.2E7



Spectrum S17. ¹H NMR poRhoVR (cis), **12**



Spectrum S18. ³¹P NMR poRhoVR (cis), **12**

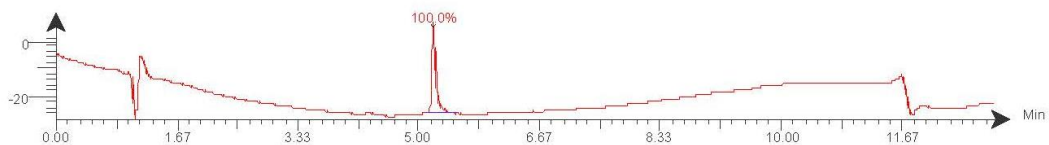


Spectrum S19. LC/MS traces poRhoVR (cis), 12

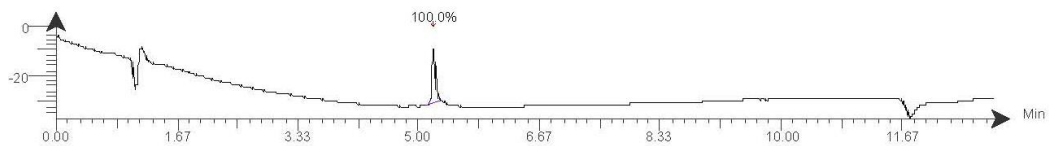
TIC
mNorAiPTLC2_1.dabx 2019.07.10 15:01:27;
ESI +



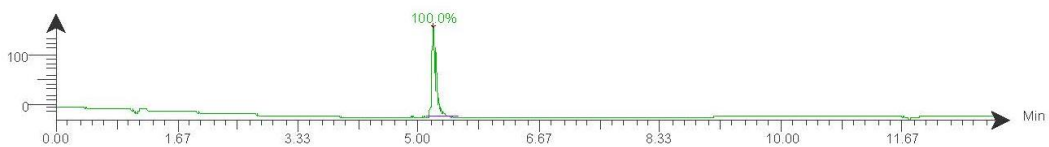
DAD: Signal B, 254 nm/Bw:4 nm
mNorAiPTLC2_1.dabx 2019.07.10 15:01:27;



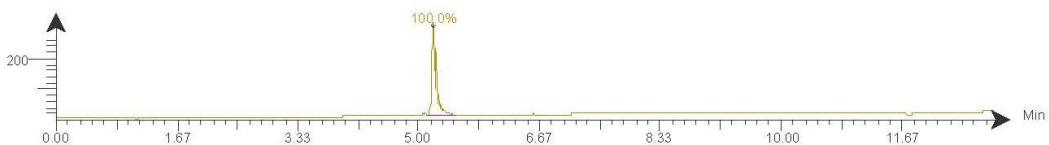
DAD: Signal C, 280 nm/Bw:4 nm
mNorAiPTLC2_1.dabx 2019.07.10 15:01:27;



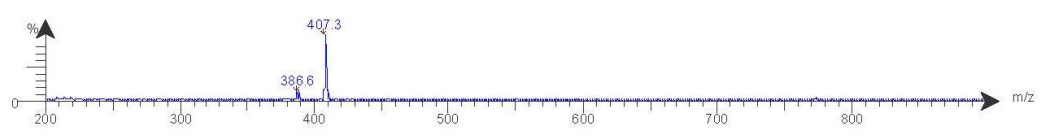
DAD: Signal D, 350 nm/Bw:4 nm
mNorAiPTLC2_1.dabx 2019.07.10 15:01:27;



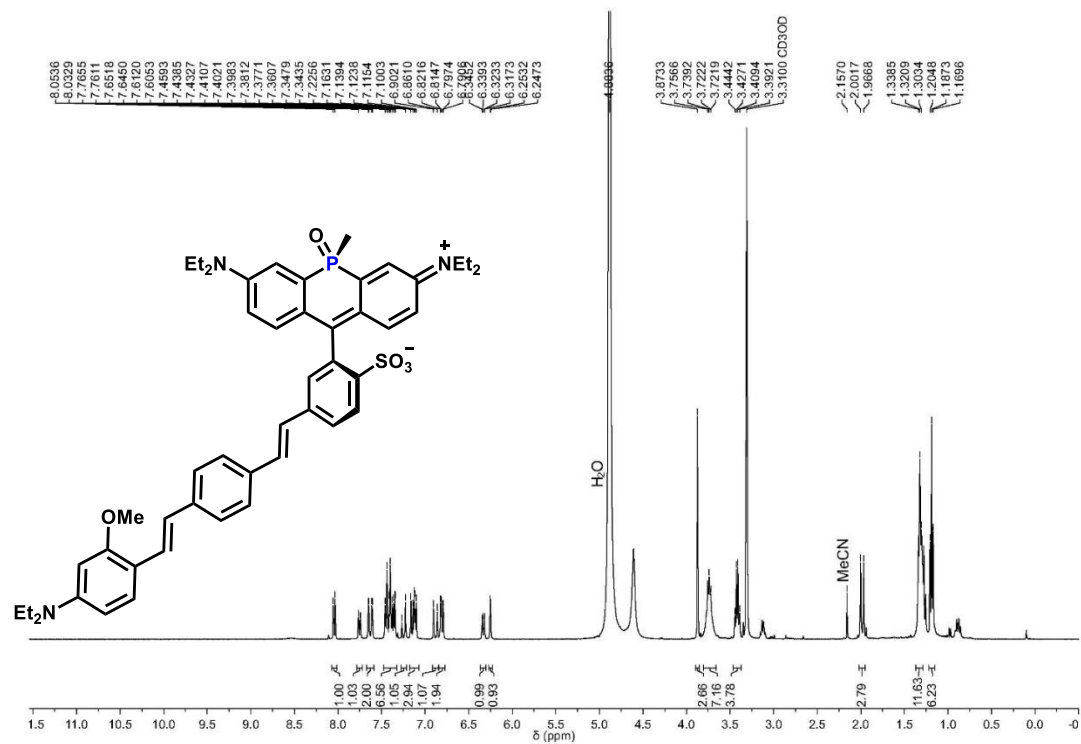
DAD: Signal E, 690 nm/Bw:4 nm
mNorAiPTLC2_1.dabx 2019.07.10 15:01:27;



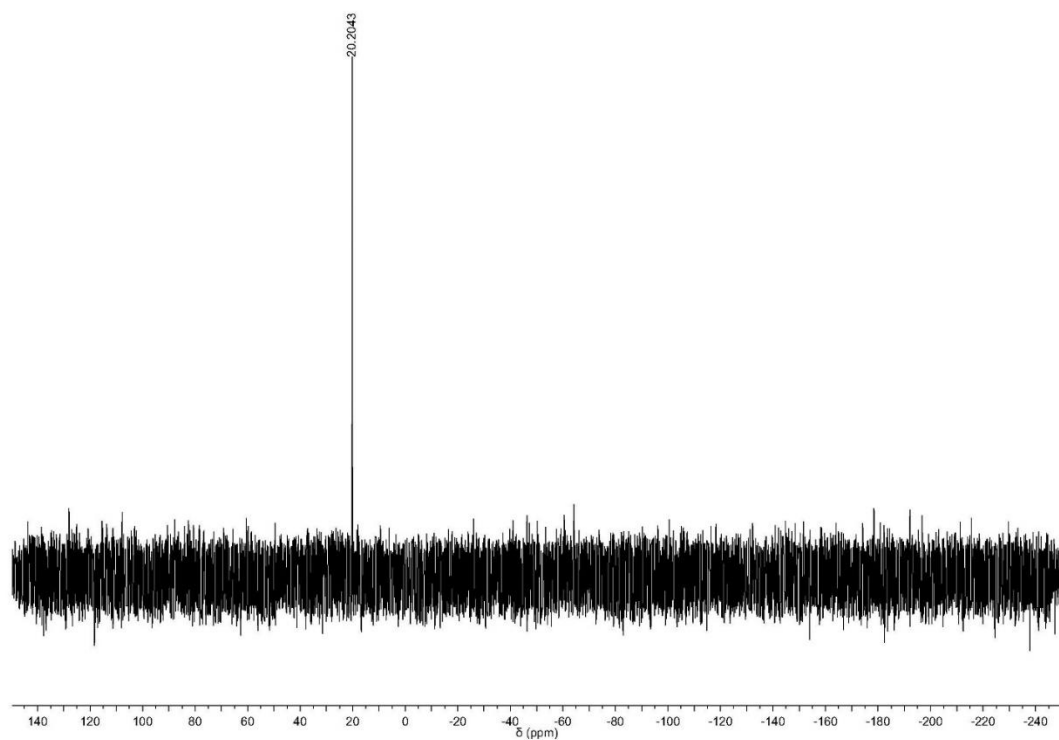
Spectrum RT 5.12 - 5.54 (73 scans)
mNorAPTL C2_1.dabx 2019.07.10 15:01:27 ;
ESI + Max: 8.8E6



Spectrum S20. ¹H NMR poRhoVR (cis), **13**

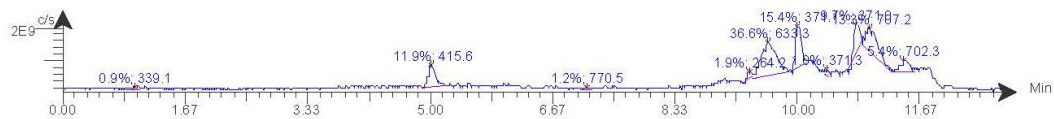


Spectrum S21. ³¹P NMR poRhoVR (cis), **13**

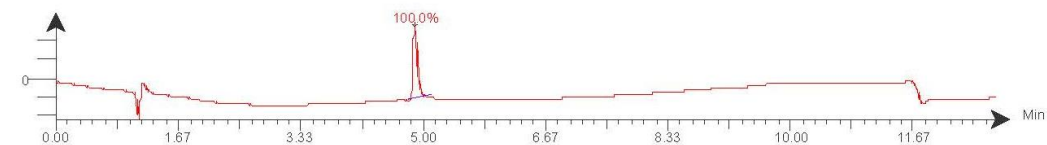


Spectrum S22. LC/MS traces poRhoVR (cis), 13

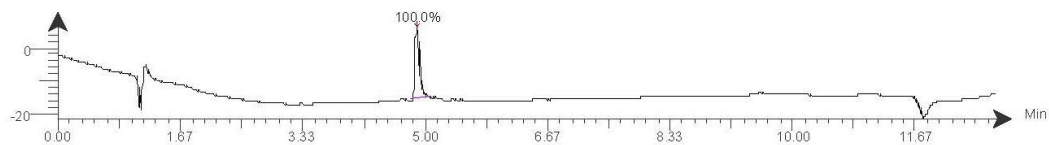
TIC
mOMe_prepped_Frac_1.datx 2019.07.06 17:40:32 ;
ESI +



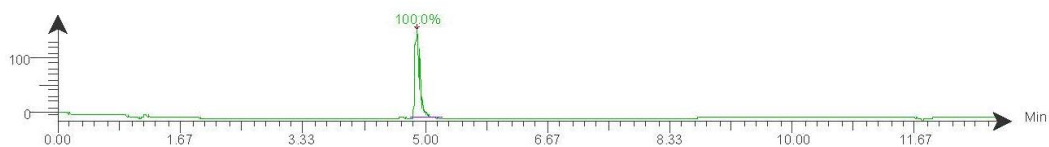
DAD: Signal B, 254 nm/Bw:4 nm
mOMe_prepped_Frac_1.datx 2019.07.06 17:40:32 ;



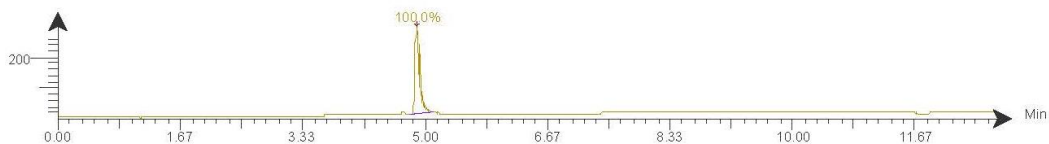
DAD: Signal C, 280 nm/Bw:4 nm
mOMe_prepped_Frac_1.datx 2019.07.06 17:40:32 ;



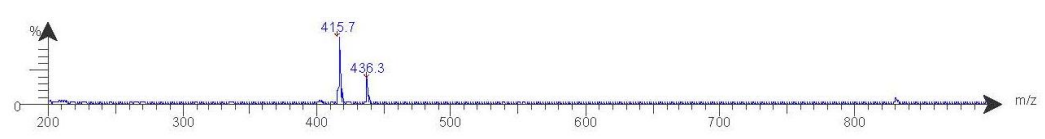
DAD: Signal D, 350 nm/Bw:4 nm
mOMe_prepped_Frac_1.datx 2019.07.06 17:40:32 ;



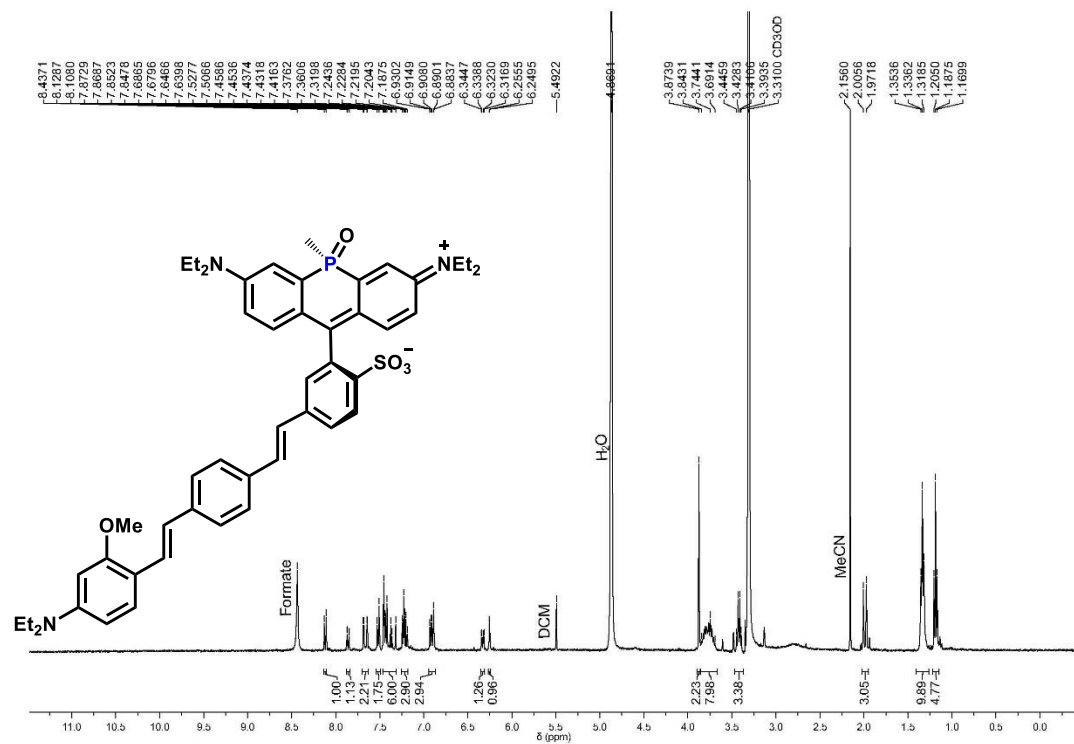
DAD: Signal E, 690 nm/Bw:4 nm
mOMe_prepped_Frac_1.datx 2019.07.06 17:40:32 ;



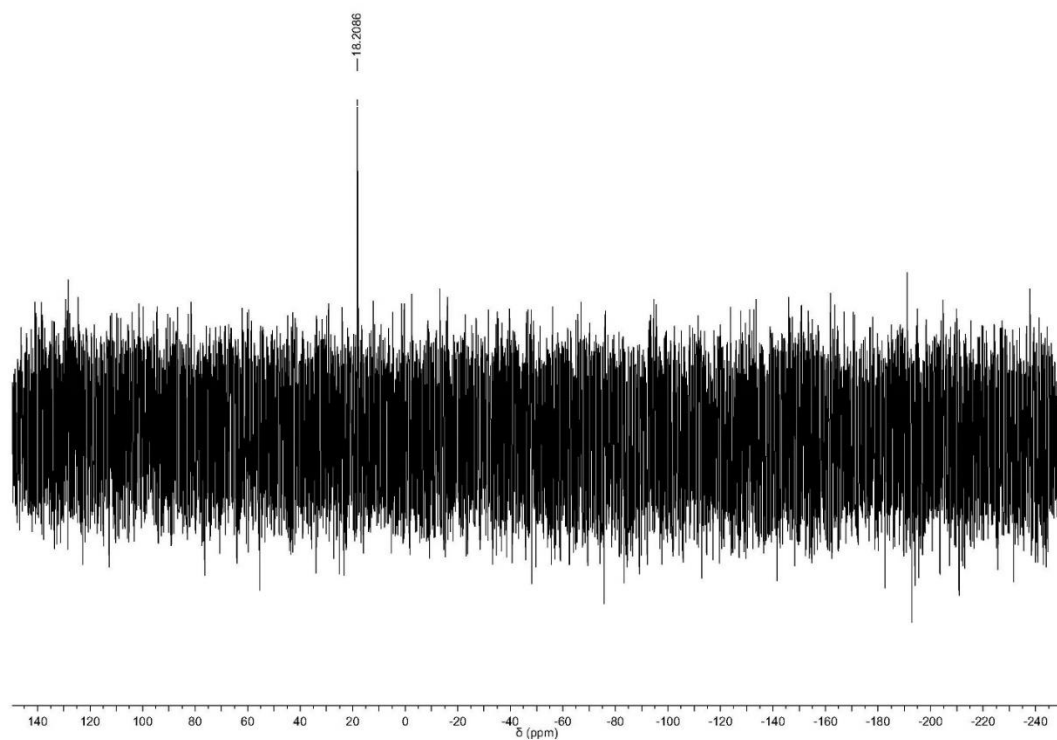
Spectrum RT 4.82 - 5.16 (59 scans)
mOMe_prepped_Frac_1.dlx 2019.07.06 17:40:32 ;
ESI + Max: 6.1E6



Spectrum S23. ¹H NMR poRhoVR (trans), **13**



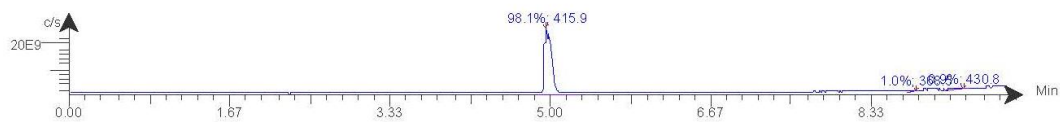
Spectrum S24. ³¹P NMR poRhoVR (trans), **13**



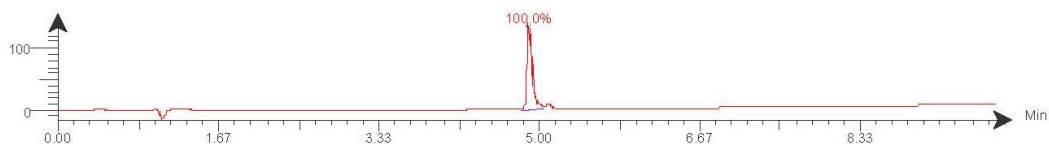
Spectrum

Spectrum S25. LC/MS traces poRhoVR (trans), 13

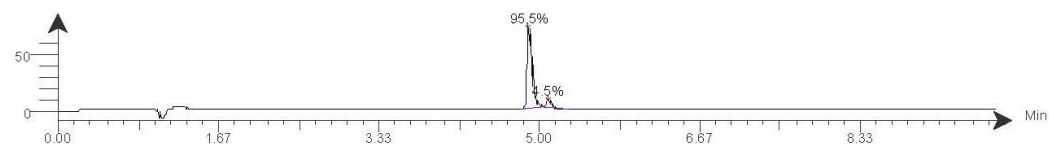
TIC
mOMe_iso3_green.datx 2016.11.14 19:45:42 ;
Intensity ESI +



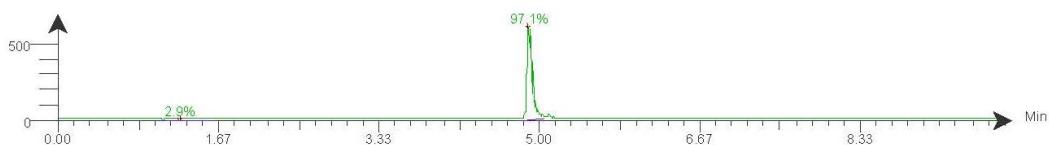
DAD: Signal B, 254 nm/Bw:4 nm
mOMe_iso3_green.datx 2016.11.14 19:45:42 ;
Intensity



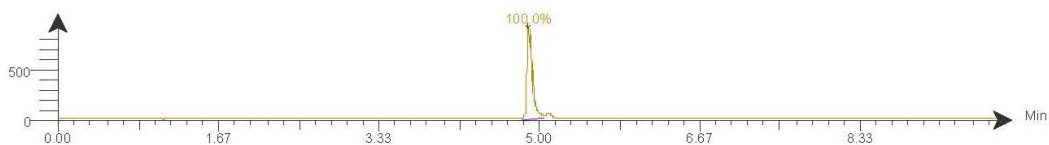
DAD: Signal C, 280 nm/Bw:4 nm
mOMe_iso3_green.datx 2016.11.14 19:45:42 ;
Intensity



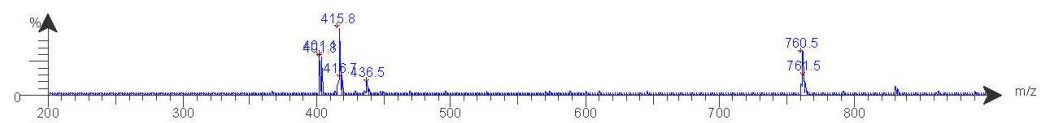
DAD: Signal D, 350 nm/Bw:4 nm
mOMe_iso3_green.datx 2016.11.14 19:45:42 ;
Intensity



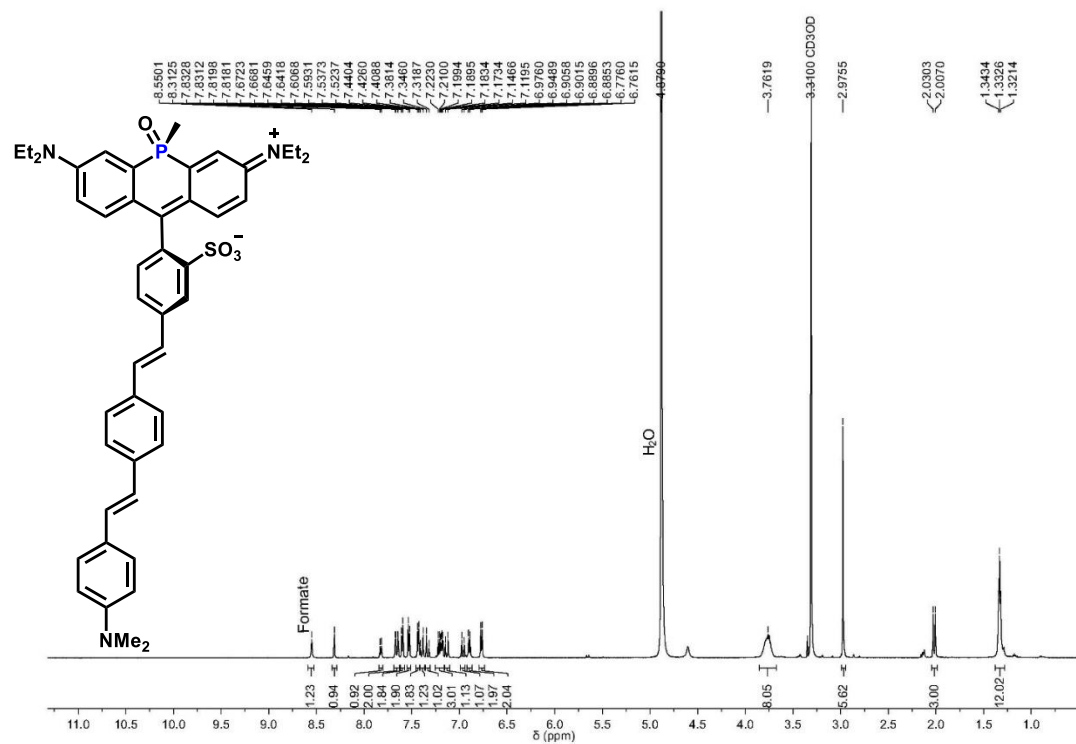
DAD: Signal E, 690 nm/Bw:4 nm
mOMe_iso3_green.datx 2016.11.14 19:45:42 ;
Intensity



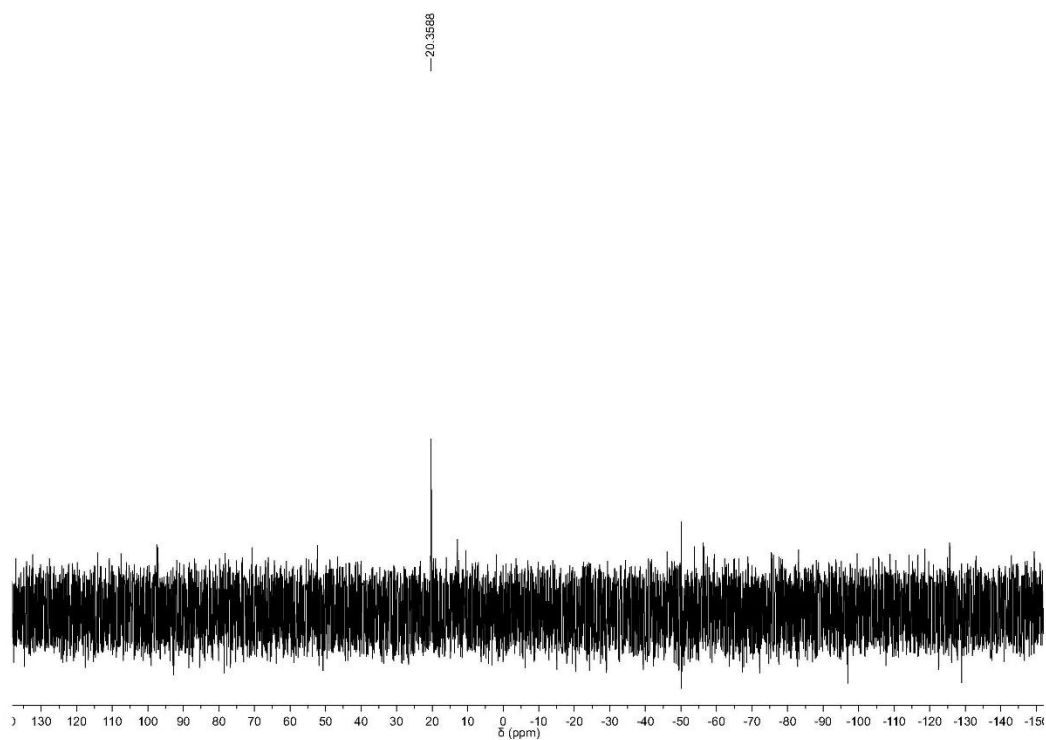
Spectrum RT 5.06 - 5.16 (19 scans)
mOMe_iso3_green.datx 2016.11.14 19:45:42 ;
ESI + Max: 9.3E6



Spectrum S26. ^1H NMR *poRhoVR* (cis), **14**

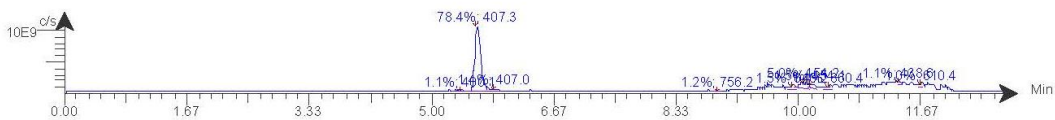


Spectrum S27. ^{31}P NMR *poRhoVR* (cis), **14**

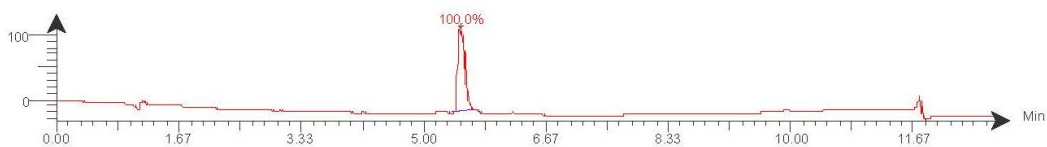


Spectrum S28. LC/MS traces poRhoVR (cis), 14

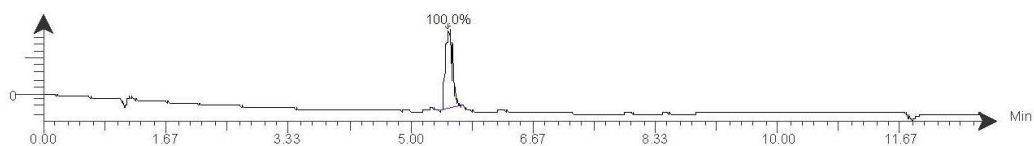
TIC
pnr_major.dabx 2018.05.30 17:09:30 ;
ESI +



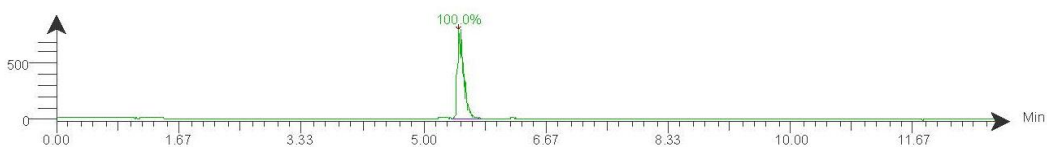
DAD: Signal B, 254 nm/Bw 4 nm
pnr_major.dabx 2018.05.30 17:09:30 ;



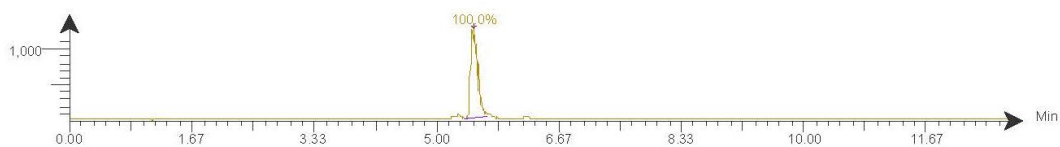
DAD: Signal C, 280 nm/Bw 4 nm
pnr_major.dabx 2018.05.30 17:09:30 ;



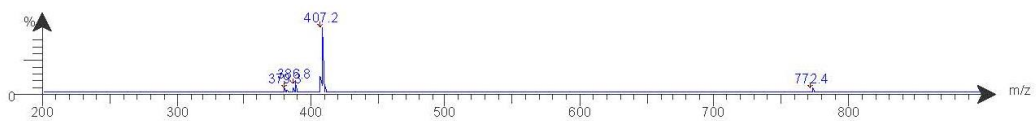
DAD: Signal D, 350 nm/Bw 4 nm
pnr_major.dabx 2018.05.30 17:09:30 ;



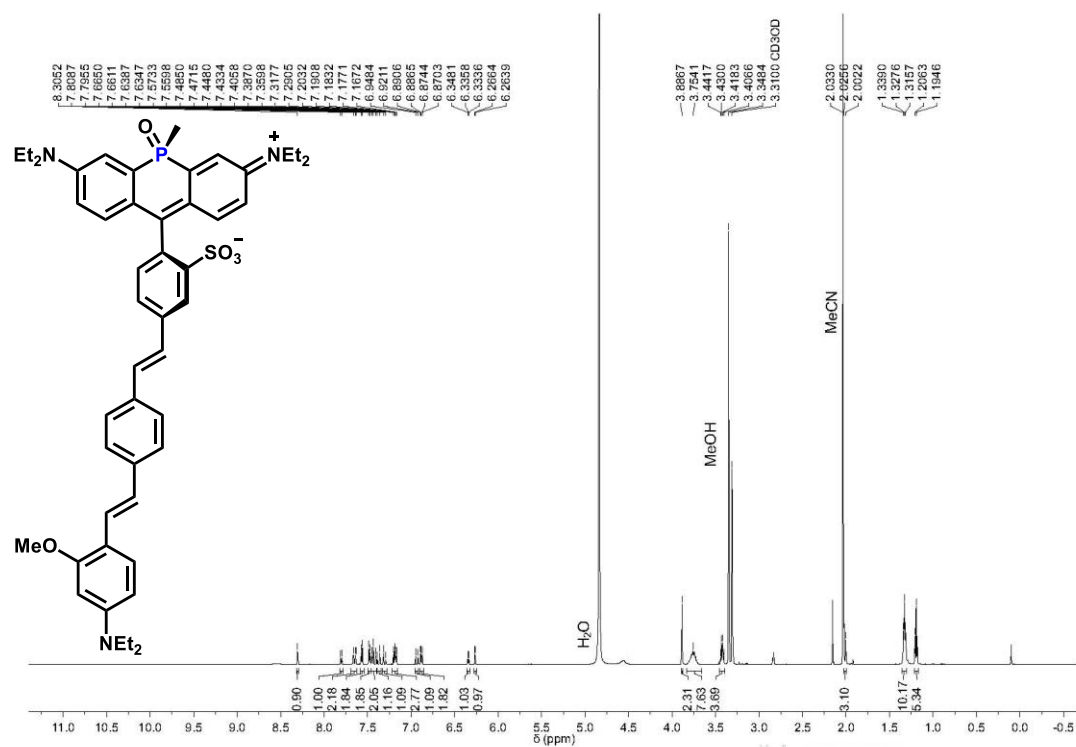
DAD: Signal E, 690 nm/Bw 4 nm
pnr_major.dabx 2018.05.30 17:09:30 ;



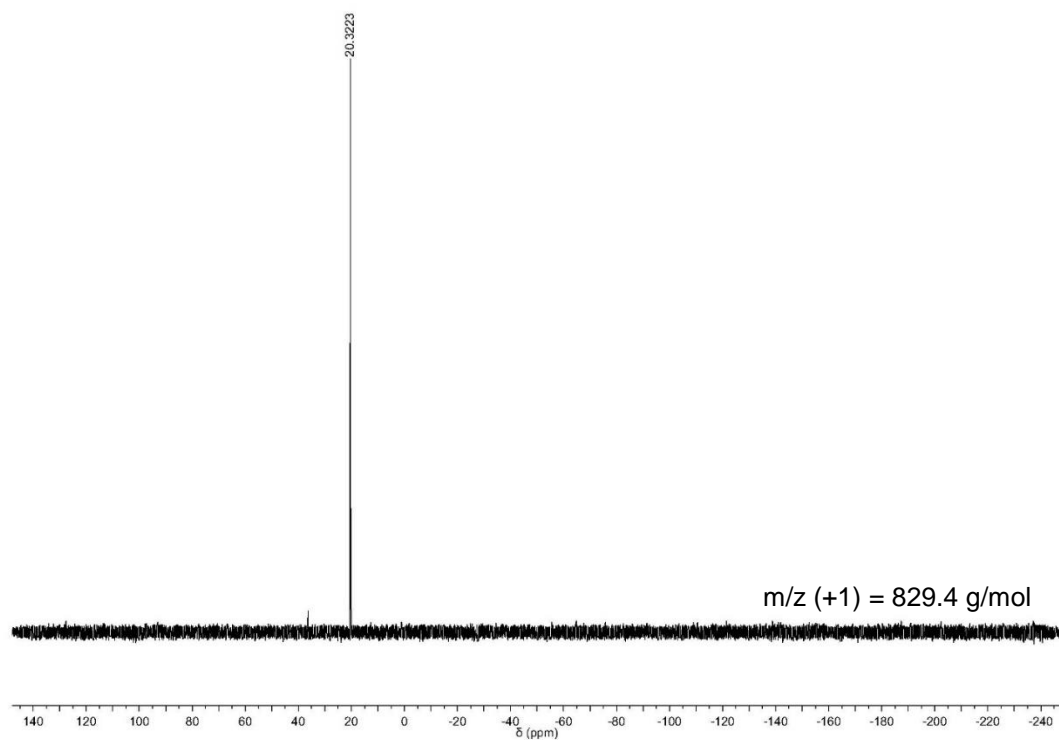
Spectrum RT 5.41 - 5.73 (54 scans)
pnr_major.dab_2018.05.30 17:09:30 ;
ESI + Max: 9.6E7



Spectrum S29. ¹H NMR poRhoVR (cis), **15**

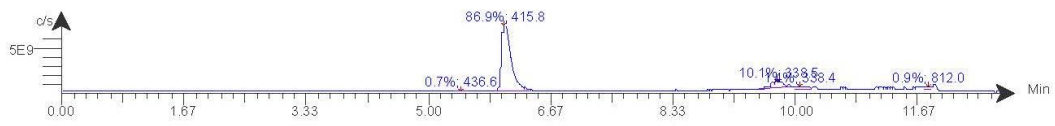


Spectrum S30. ³¹P NMR poRhoVR (cis), **15**

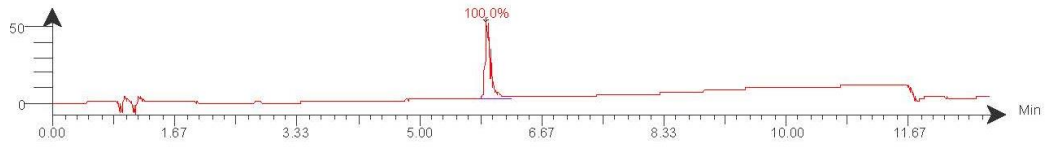


Spectrum S31. LC/MS traces poRhoVR (cis), **15**

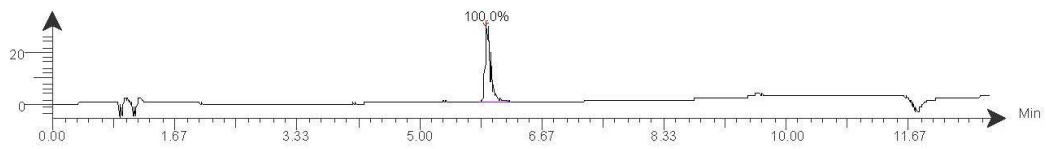
TIC
pOMe2ndC18_R2F6.dabx 2019.07.13 18:49:55 ;
ESI +



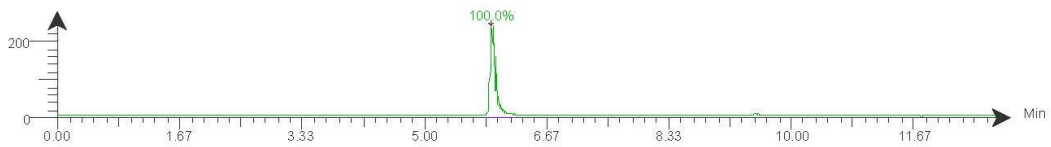
DAD: Signal B, 254 nm/Bw:4 nm
pOMe2ndC18_R2F6.dabx 2019.07.13 18:49:55 ;



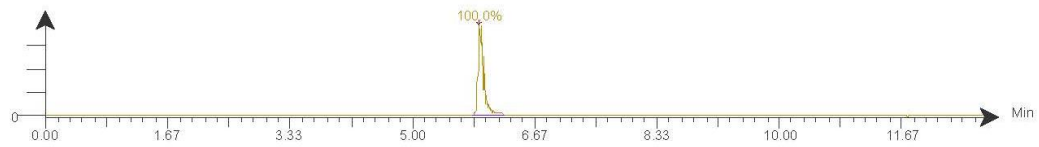
DAD: Signal C, 280 nm/Bw:4 nm
pOMe2ndC18_R2F6.dabx 2019.07.13 18:49:55 ;



DAD: Signal D, 350 nm/Bw:4 nm
pOMe2ndC18_R2F6.dabx 2019.07.13 18:49:55 ;



DAD: Signal E, 690 nm/Bw:4 nm
pOMe2ndC18_R2F6.dabx 2019.07.13 18:49:55 ;



Spectrum RT 6.07 (1 scans)
pOMe2ndC18_R2F6.dabx 2019.07.13 18:49:55 ;
ESI + Max: 1.8E8

